NAVAL POSTGRADUATE SCHOOL

MONTEREY, CALIFORNIA

THESIS

VERIFICATION OF CLOUD ANALYSES USED TO SUPPORT OVERHEAD IMAGERY COLLECTION

by

Robert J. Cleary

March 2012

Thesis Advisor: Tom Murphree
Second Reader: Karl D. Pfeiffer

Approved for public release; distribution is unlimited

THIS PAGE INTENTIONALLY LEFT BLANK

REPORT DOCUMENTATION PAGE		*Form Approved OMB No. 0704-0188*

Public reporting burden for this collection of information is estimated to average 1 hour per response, including the time for reviewing instruction, searching existing data sources, gathering and maintaining the data needed, and completing and reviewing the collection of information. Send comments regarding this burden estimate or any other aspect of this collection of information, including suggestions for reducing this burden, to Washington headquarters Services, Directorate for Information Operations and Reports, 1215 Jefferson Davis Highway, Suite 1204, Arlington, VA 22202-4302, and to the Office of Management and Budget, Paperwork Reduction Project (0704-0188) Washington DC 20503.

1. AGENCY USE ONLY *(Leave blank)*	**2. REPORT DATE** March 2012	**3. REPORT TYPE AND DATES COVERED** Master's Thesis
4. TITLE AND SUBTITLE Verification of Cloud Analyses used to Support Overhead Imagery Collection		**5. FUNDING NUMBERS**
6. AUTHOR(S) Robert J. Cleary		
7. PERFORMING ORGANIZATION NAME(S) AND ADDRESS(ES) Naval Postgraduate School Monterey, CA 93943-5000		**8. PERFORMING ORGANIZATION REPORT NUMBER**
9. SPONSORING /MONITORING AGENCY NAME(S) AND ADDRESS(ES) AS&T, NRO 14675 Lee Road, Chantilly, VA 20150-1715		**10. SPONSORING/MONITORING AGENCY REPORT NUMBER**

11. SUPPLEMENTARY NOTES The views expressed in this thesis are those of the author and do not reflect the official policy or position of the Department of Defense or the U.S. Government. I.R.B. Protocol number N/A.

12a. DISTRIBUTION / AVAILABILITY STATEMENT Approved for public release; distribution is unlimited	**12b. DISTRIBUTION CODE** A

13. ABSTRACT (maximum 200 words)

We verified the USAF World Wide Merged Cloud Analysis (WWMCA) against observations from the Cloudsat atmospheric sounder. We analyzed WWMCA data for 2010 for two regions that are of high interest to the national intelligence community and that differ in their meteorological characteristics. The two regions covered were: (a) much of southwest Asia; and (b) much of western Russia and the Barents Sea. We analyzed WWMCA performance according to four criteria: (1) type of cloud event (Definite-Cloud, Probable-Cloud, and No-Cloud); (2) geographic region; (3) time of day; and (4) time of year. We measured WWMCA performance using contingency table metrics and found marked differences in performance for the four criteria. In particular, WWMCA tended to perform better in analyzing: (a) No-Cloud and Definite-Cloud events than Probable-Cloud events; (b) the lower latitude region than the higher latitude region; and (c) persistent cloud events than variable cloud events. Our Heidke skill scores indicated that WWMCA performance was, in general, moderately better than that of a random set of analyses. Overall, WWMCA performance was problematic, given that WWMCA is a near real-time analysis product and is designed to initiate short lead time cloud forecasts used by the intelligence community.

14. SUBJECT TERMS Worldwide Merged Cloud Analysis, WWMCA, Cloud Depiction Forecast Systems II, CDFS II, cloud analysis, Cloudsat, 2B-Geoporf, National Reconnaissance Office, NRO			**15. NUMBER OF PAGES** 131
			16. PRICE CODE
17. SECURITY CLASSIFICATION OF REPORT Unclassified	**18. SECURITY CLASSIFICATION OF THIS PAGE** Unclassified	**19. SECURITY CLASSIFICATION OF ABSTRACT** Unclassified	**20. LIMITATION OF ABSTRACT** UU

THIS PAGE INTENTIONALLY LEFT BLANK

VERIFICATION OF CLOUD ANALYSES USED TO SUPPORT OF OVERHEAD IMAGERY COLLECTION

Robert J. Cleary
Lieutenant Commander, United States Navy
B.S., University of California at Santa Cruz, 2002

Submitted in partial fulfillment of the
requirements for the degree of

**MASTER OF SCIENCE IN
METEOROLOGY AND PHYSICAL OCEANOGRAPHY**

from the

**NAVAL POSTGRADUATE SCHOOL
March 2012**

Author: Robert J. Cleary

Approved by: Tom Murphree
                     Thesis Advisor

                     Karl D. Pfeiffer
                     Second Reader

                     Wendell Nuss
                     Chair, Department of Meteorology

iii

THIS PAGE INTENTIONALLY LEFT BLANK

ABSTRACT

We verified the USAF World Wide Merged Cloud Analysis (WWMCA) against observations from the Cloudsat atmospheric sounder. We analyzed WWMCA data for 2010 for two regions that are of high interest to the national intelligence community and that differ in their meteorological characteristics. The two regions covered were: (a) much of southwest Asia; and (b) much of western Russia and the Barents Sea. We analyzed WWMCA performance according to four criteria: (1) type of cloud event (Definite-Cloud, Probable-Cloud, and No-Cloud); (2) geographic region; (3) time of day; and (4) time of year. We measured WWMCA performance using contingency table metrics and found marked differences in performance for the four criteria. In particular, WWMCA tended to perform better in analyzing: (a) No-Cloud and Definite-Cloud events than Probable-Cloud events; (b) the lower latitude region than the higher latitude region; and (c) persistent cloud events than variable cloud events. Our Heidke skill scores indicated that WWMCA performance was, in general, moderately better than that of a random set of analyses. Overall, WWMCA performance was problematic, given that WWMCA is a near real-time analysis product and is designed to initiate short lead time cloud forecasts used by the intelligence community.

THIS PAGE INTENTIONALLY LEFT BLANK

TABLE OF CONTENTS

LIST OF FIGURES

xi

xiii

LIST OF TABLES

LIST OF ACRONYMS AND ABBREVIATIONS

AER	Atmospheric Environmental Research, Inc.
AFWA	Air Force Weather Agency
AFRL	Air Force Research Laboratory
AVDCLD	Advect Cloud Model
AVHRR	Advanced Very High Resolution Radiometer
B	Bias
CALIPSO	Cloud-Aerosol Lidar and Infrared Pathfinder Satellite Observation
CDFS	Cloud Depiction Forecast System
CDR	Cloud Data Records
CFM	Cloud Forecast Model
CPR	Cloud Profiling Radar
CSI	Critical Success Index
CSV	Comma Separated Value
DCF	Diagnostic Cloud Forecast Model
DMSP	Defense Meteorological Satellite Program
EO	Electro-optical
ESSP	Earth Systems Science Pathfinder
FAR	False Alarm Ratio
FOV	Field of View
GeoProf	Geometrical Profiling
H	Hit Rate
HDF	Hierarchical Data Format
HSS	Heidke Skill Score
IFOV	Instantaneous Field of View
IR	Infrared
GDR	Gridded Data Records
GFS	Global Forecast System
GOES	Geostationary Operational Environmental Satellite
LWIR	Longwave Infrared
METEOSAT	European Space Agency's Meteorological Satellite

METAR	Meteorological Aerodrome Report
MODIS	Moderate Resolution Imaging Spectroradiometer
MSL	Mean Sea Level
NASA	National Aeronautics and Space Administration
NCEP	Nation Centers for Environmental Prediction
NGIS	Northrop Grumman Information Systems
NOAA	National Oceanic Atmospheric Administration
NOGAPS	Navy Operational Global Atmospheric Prediction System
NPS	Naval Postgraduate School
NRO	National Reconnaissance Office
NWP	Numerical Weather Prediction
OCO	Orbiting Carbon Observatory
OI	Optimum Interpolation
OLS	Operational Line Scanner
PARASOL	Polarization and Anisotropy of Reflectances for Atmospheric Sciences coupled with Observations from a Lidar
PC	Proportion Correct
POD	Probability of Detection
POES	Polar Orbiting Environmental Satellites
RRV	Range Resolution Volume
RTNEPH	Real Time Nephanalysis
SCFM	Stochastic Cloud Forecast Model
SDR	Sensor Data Records
SERCAA	Support of Environmental Requirements for Cloud Analysis and Archive
SYNOPIC	Surface Synoptic Observations
TS	Threat Score
UCAR	University Corporation for Atmospheric Research
USAF	United States Air Force
WWMCA	Worldwide Merged Cloud Analysis

ACKNOWLEDGMENTS

THIS PAGE INTENTIONALLY LEFT BLANK

I. INTRODUCTION

A. IMPORTANCE OF CLOUD ANALYSES AND FORECASTS

Cloud analysis and forecasts are essential to the overhead imagery mission. Imagery satellites play a vital role in the national intelligence mission. They are low density/high demand assets that are quite sensitive to cloud masking of targets. Cloud cover impacts satellite imagery collection by obscuring sensors operating in the visual and infrared (IR) channels. Accurate cloud forecasts assist in target selection, the asset scheduling, and help reduce the need to reshoot targets. To improve cloud forecasts, a firm verification of the cloud analyses that go into cloud forecasts, and of the forecasts themselves, is needed.

Cloud analysis verification is very difficult, because: (1) clouds can form and dissipate in a relatively short period; and (2) clouds reside at various levels in the atmosphere and are advected by winds via nonlinear processes. Satellites observations can provide constant coverage over much of Earth and their images can be merged into a single, two-dimensional mosaic depicting, for example, cloud top height for a given area. However, this does not provide the three-dimensional (cloud thickness) analysis of clouds necessary to meet operational requirements for creating accurate cloud forecasts.

Currently, the Air Force Weather Agency (AFWA) is using the Cloud Depiction Forecast System (CDFS) II to merge satellite imagery and conventional (surface and upper air soundings) observations into a global cloud analysis product called Worldwide Merged Cloud Analysis (WWMCA). WWMCA initiates the cloud forecast models that provides cloud forecasts to the national intelligence community for overhead imagery collection planning. To date, there has not been an extensive study to verify operational CDFS II products against independent observations (the studies that have been done are described later in this chapter). The WWMCA component of CDFS II is difficult to verify because there are few independent instruments designed to detect clouds that have global coverage that are not used in developing WWMCA products (i.e., few satellite observations that are not ingested into CDFS II).

Our goal in this study was to begin the testing of CDFS II by verifying the operational cloud analysis products generated by WWMCA. Our main research questions were:

1. How should WWMCA products be verified?

2. How well does WWMCA perform according to the type of cloud condition, or cloud event?

3. How well does WWMCA perform according to the time of day and the time of year?

4. How well does WWMCA perform according to geographic location or region?

B.   SCOPE OF THIS RESEARCH

The purpose of this research was to develop, test, and apply a method to verify WWMCA products against cloud information from a space-based radar system, Cloudsat. Additionally, we wanted to develop initial verification results for use in evaluating the impacts of CDFS II products on the operational planning and operational outcomes of the IC users of CDFS II products—that is, to develop information that can be used to answer the questions "How do cloud analysis and forecast products affect satellite imagery collection? Figure 1 provides an overview of the approach being used in research at the Naval Postgraduate School (NPS) to address these operational impacts. The upper left portion of this figure summarizes the approach used in this study—comparing cloud analyses to cloud observations to verify the analyses. In future studies, we will compare cloud forecasts to cloud observations to verify the forecasts. The upper right portion of Figure 1 summarizes the approach being used in a companion study at NPS that is verifying the impacts of overhead imagery mission planning on mission outcomes through the use of a mission planning and outcomes model. The bottom portion of Figure 1 indicates how the results from the two types of verification studies will be merged to quantitatively assess the impacts of cloud analyses, cloud forecasts, and actual clouds on operational planning and operational outcomes.

Analyzing Cloud Analysis and Forecast Impacts on Imagery Collection
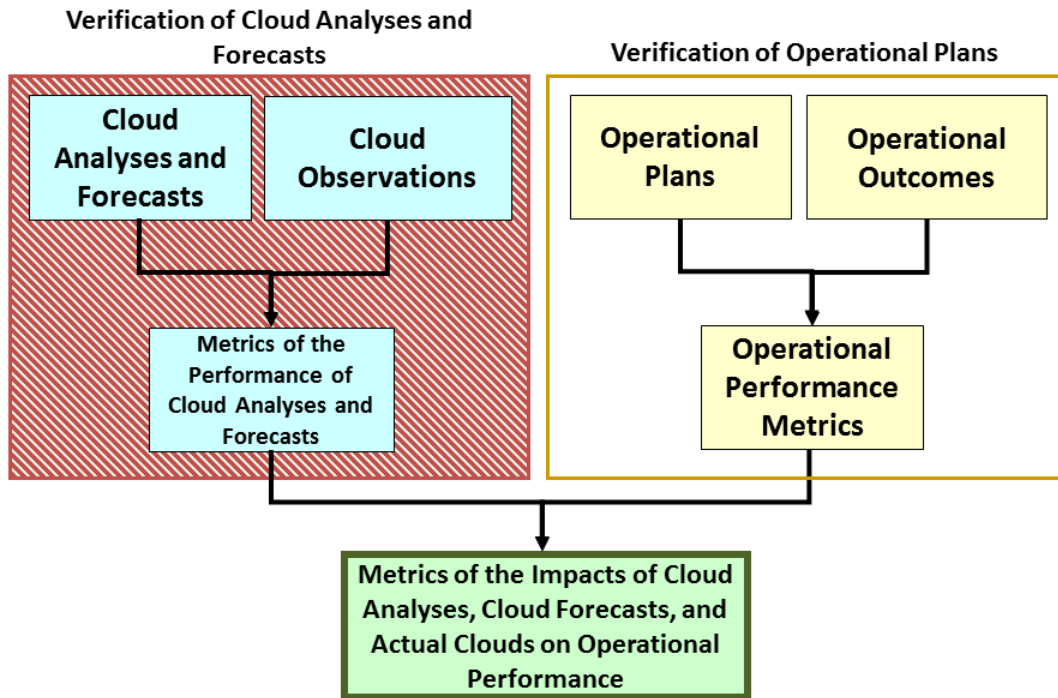
Figure 1.   A schematic illustration of the approach being used at NPS to quantitatively assess the impacts of cloud analyses, cloud forecasts, and actual clouds on operational planning and operational outcomes. The upper left portion of the figure summarizes the approach being used in this study to verify WWMCA cloud analyses. The upper right portion of the figure summarizes the approach being used in a companion NPS study to verify operational planning. The bottom portion of the figure represents the merger of information from the two verification studies.

C.   PRIOR RESEARCH

The most relevant prior studies for our research were conducted by the University Corporation for Atmospheric Research (UCAR), Atmospheric Environmental Research, Inc. (AER), and the U.S. Air Force 16th Weather Squadron. The first was a WWMCA verification study in which WWMCA output was compared against Cloudsat data (UCAR 2008), and the second was a small follow up effort performed in 2010 (AER 2010). Details of these studies are available to the United States government personnel

and contractors but were never captured in a technical report or paper and are only briefly summarized in a verification and validation paper by Northrop Grumman Information Systems (NGIS 2011). The studies covered two periods spanning approximately three months: 01 April—29 June 2008 (Northern Hemisphere only) and 28 March—31 May 2010 (Northern and Southern Hemispheres). These studies concluded that WWMCA detected clouds when Cloudsat said there was cloud 64% of the time in the Northern Hemisphere and more than 80% of the time in the Southern Hemisphere. NGIS (2011) reported that WWMCA tended to under analyze cloud, as opposed to falsely assigning cloudy conditions to no-clouds conditions.

The study by the 16th Weather Squadron (Selin 2011, personal communication), was a continuation of the UCAR study but used Cloudsat data to assess WWMCA performance in identifying clouds at low, middle, and high levels in the Northern Hemisphere. Two three month periods were evaluated: 01 April—29 June 2008 and 28 March—31 May 2010. The study concluded that WWMCA does an adequate job of classifying low and middle clouds correctly, if it is able to detect them. WWMCA had the hardest time detecting low and middle clouds. Selin suggests that problems in the detection of low and middle level clouds is probably the biggest obstacle when it comes to using WWMCA for cloud level and cloud profile information.

Ruggiero (2000) describes a study conducted by the Air Force Research Laboratory (AFRL) to examine processes for using cloud analysis products to initialize numerical weather prediction (NWP) models. The study focused on eastern Massachusetts in September 1995 and used surface observations and rawinsonde data in the verification process. The study concluded that the cloud detection algorithms used in WWMCA at the time of the study were able to detect clouds when clouds were present 81% of the time and agreed with the observed cloud fraction 73% of the time (NGIS 2011).

Horsman (2007) verified WWMCA against real-time surface weather observations at ten different Air Force bases within the continental United States for

16 days. This study found that WWMCA performance varied by climate region. Overall, the study found that overall, WWMCA performed poorly with a "verification of 27% and a miss rate of 32%" (Horsman 2007).

Norquist (2007) verified WWMCA against field measurements collected from cloud profiling radar (CPR) and a portable lidar during two efforts at Hanscom Air Force Base, MA. From 36 days of data, a total of 117 hours were selected in which both instrumental observations and WWMCA were available (by design, cloud cover was present in all observations). "Of these 117 hours, WWMCA detected clouds in 91 giving WWMCA an overall cloud detection rate of 78%" (NGIS 2011).

Gustafson et al. (2011) compared Moderate Resolution Imaging Spectroradiometer (MODIS) derived cloud mask data from Aqua and Terra to WWMCA cloud cover data for June and September of 2010. Cloud fractions for both MODIS cloud masks and WWMCA were calculated and classified as either clear (<20%), partly-cloud (20—80%), and cloudy (>80%). Table 1 displays the comparison results from Terra for June 2010 (Aqua results were very similar). Overall, the cloud fractions of WWMCA and MODIS were in agreement 65% of the time. WWMCA performed less well in polar regions and relatively well in oceanic glint regions and over bright backgrounds, such as deserts. Gustafson concluded that MODIS cloud mask data is less than ideal as an independent source of cloud truth.

Table 1.   The results of cloud fraction binning from WWMCA/MODIS (Terra) comparison from June 2010. Table based on NGIS (2011).

Cloud Fractions	Percentage (%)
Clear matched	25
Partly cloudy matched	6
Cloudy matched	34

Bartlett (2009) evaluated several methods for verifying WWMCA cloud distributions. These methods include comparisons with MODIS imagery and cloud-

related information from the Navy Operational Global Atmospheric Prediction System (NOGAPS). The study concluded that quantitative verification of cloud distributions can be achieved and that more reference distributions based on satellite imagery be developed.

In 2004 and 2011, the 14th Weather Squadron and AER, looked at the long-term mean behavior of WWMCA (NGIS 2011). Their study concluded that the merging processes used to develop WWMCA products can introduce errors that are artifacts of the merging processes. Most of the artifacts were found at the higher latitudes where observations are provided primarily by polar orbiting satellites (NGIS 2011). The study also concluded that some of WWMCA's performance problems arise from physical inconsistencies in the merging processes.

It is difficult to summarize the results of these prior studies, since: (a) they are based on different periods, locations, and analysis methods; and (b) most are not well documented. However, these studies seem to indicate that: (1) the WWMCA probability of detection (POD) for clouds may be, overall, in the range of 65-85%; (2) WWMCA seems to under analyze clouds, especially highly optically thin cirrus (in part by design) and low clouds over oceans; and (3) verification of WWMCA is problematic due to the relative lack of independent and comprehensive verifying data. These prior studies assessed WWMCA products from a wide range of years. However, CDFS II has undergone many changes since it was first implemented in 2002. There have been multiple science level changes and the tunable parameters have been continuously altered to improve the baseline performance. Thus, the results from the prior studies are useful but may be out of date, or soon may become out of date.

The prior studies have provided useful results, but they have a number of important shortcomings that indicate further studies are needed. These shortcomings include:

1. The data sets, methods, and results for these studies have not been well documented.

2. The studies covered relatively short periods.

3. Most of the studies only looked at small regions.

4. The studies that investigated large regions provided their results at relatively coarse spatial resolutions.

5. The studies suffered from a lack of comprehensive, independent observational data against which to verify WWMCA.

6. The studies apparently used and/or reported only limited verification metrics (e.g., POD was reported but not FAR, bias, Heidke skill score, or other metrics needed to develop a full verification).

7. The studies provided little information on how WWMCA performance has changed over time, as upgrades to CDFS II have been made.

To address these shortcomings we designed our study to achieve the following objectives.

1. Design and develop a method to do routine, near real-time verification of WWMCA based on Cloudsat observations.

2. Test the method for a range of cloud events, locations, and periods.

3. Develop initial verification results using a range of metrics.

4. Develop initial verification results for use in evaluating the impacts of cloud analyses, cloud forecasts, and actual clouds on the planning and outcomes of satellite imagery collection operations. That is, provide initial information for answering the question: "How do cloud analysis and cloud forecast performance, and actual clouds themselves, affect the planning and outcomes of satellite imagery collection operations?"

D.   ORGANIZATION OF THESIS

Chapter II gives background information on CDFS II, WWMCA, and Cloudsat, and also discusses the methodology used to verify and compare WWMCA data using Cloudsat. Chapter III discusses the results of the WWMCA verification. Chapter IV provides a study summary, conclusions, and recommendations for future research.

THIS PAGE INTENTIONALLY LEFT BLANK

II. DATA AND METHODS

A. OVERVIEW

This chapter provides background information on CDFS II, WWMCA, Cloudsat, and Cloudsat's data product 2B-GeoProf. The datasets used for this study and the methodology for processing and matching WWMCA and Cloudsat data are discussed.

B. CDFS II AND WWMCA DESCRIPTION

1. Cloud Depiction Forecast System (CDFS) II

The Cloud Depiction Forecast System (CDFS) II is a computer processing system designed and operated by the Air Force Weather Agency (AFWA) that produces an hourly, global, cloud analysis from individual satellites and merges them with conventional observations (e.g., surface observations and upper air soundings) into a Worldwide Merged Cloud Analysis (WWMCA) that reports the following parameters (HQ AFWA/DNXM 2011):

- total cloud percentage

- layered cloud percentage

- layered cloud type

- layered cloud top heights

- layered cloud base heights

- pixel mean time in Julian minutes

Figure 2 illustrates the different CDFS II components, including WWMCA, how they are related to each other, and the process for generating cloud analyses and forecasts. Both polar orbiting and geostationary satellites provide observations to CDFS II. The polar-orbiters are those in the Defense Meteorological Satellite Program (DMSP) and National Oceanic and Atmospheric Administration (NOAA) Polar Orbiting Environmental Satellites (POES) program. The geostationary satellites include those in the

Geostationary Operational Environmental Satellite (GOES) and the European Space Agency's Meteorological Satellite (METEOSAT) programs. The satellite and conventional observations undergo a four level process to be merged into a global cloud analysis. Level one is data calibration, level two classifies each pixel into cloudy or clear, level three applies cloud layering and typing, and level four consists of merging the separate analyses into one global analysis, called WWMCA. WWMCA is used to initiate a suite of cloud forecast models (HQ AFWA/DNXM 2011). Refer to Appendix A for a detailed description of the four processing levels.

Met Sats
DMSP[1]
POES[2]
GOES[3]
METOSAT[4]

Observations
Surface
Upper Air

Specialized Global Analysis
Surface Temps
Snow Depth

Cloud Analysis
WWMCA[5]

FITL[6]

ADVCLD[7]

SCFM[8]

DCF[9]

FITL

Inputs   Analysis   Output   Forecast

[1] Defense Meteorological Satellite Program
[2] Polar Operational Environment Satellite
[3] Geostationary Operational Environment Satellite
[4] Meteorological Satellites operated by European Space Agency
[5] Worldwide Merge Cloud Analysis

[6] Forecaster in the loop
[7] Advect Cloud
[8] Stochastic Cloud Forecast Model (Global)
[9] Diagnostic Cloud Forecast (Regional)

Figure 2.   Schematic overview of the Cloud Depiction Forecast System II. Observational data are received from meteorological satellites, conventional observations, and global analyses from various models. These data are merged into one global cloud analysis, called WWMCA, which is used to initiate cloud forecast models. Quality control is performed on the cloud analysis and model output products by a forecaster. Figure from HQ AFWA/DNXM (2011).

WWMCA is known to have some deficiencies (HQ AFWA/DNXM 2011). First, WWMCA often places high cirrus clouds at too low an altitude due to surface radiation emission contamination in the brightness temperatures. Second, CDFS II tends to under analyze low clouds. A correction is required because low cloud top

temperatures may be very close or exceed that of the underlying surface temperatures, thus producing a false colored pixel (HQ AFWA/DNXM 2011).

2. Worldwide Merge Cloud Analysis (WWMCA)

WWMCA provides information for a global grid of square cells that each covers an area of 24 km by 24 km (true at 60° latitude). For each cell, the following information is provided:

- **i** and **j** spatial coordinates

- total cloud percentage

- layered cloud percentage

- layered cloud type

- layered cloud top heights

- layered cloud base heights

- mean pixel time in Julian minutes

Figure 3 shows the data format of a WWMCA file. The total cloud amount is the percentage of cloud-filled pixels divided by the by the total number of pixels per cell. Layered cloud amount uses the same calculation as total cloud amount, except that the calculation uses the coldest (top) layer pixels. Cloud base height is calculated using the RTNEPH (Real Time Nephanalysis) technique (Kiess and Cox 1988). Cloud top height is calculated by interpolation of the Naval Operational Global Atmosphere Prediction System (NOGAPS) atmospheric temperature and height profiles to the mean cloud top temperatures for each grid cell. The highest percentage of cloud type in the final analysis decides cloud type for the cell (HQ AFWA/DNXM 2011). WWMCA is used to initialize three cloud forecast models:

1. Advect Cloud (ADVCLD)

2. Stochastic Cloud Forecast (SCFM)

3. Diagnostic Cloud Forecast (DCF)

WWMCA File Format

```
20040101000773 0641 S 1 050 7 02978 04778 1 005 5 02723 03923 000 0 00000 00000 000 0 00000 00000 999 100
20040101000774 0641 S 1 008 8 07594 09394 0 547 0 46770 6477 1 005 0 32930 4493 000 0 00000 00000 000 0 00000 00000 999 100
20040101000775 0641 S 1 082 9 08772 09672 1 009 0 70780 7978 000 0 00000 00000 000 0 00000 00000 000 0 00000 00000 999 100
20040101000776 0641 S 1 033 8 07079 88879 1 008 6 17807 978 000 0 00000 00000 000 0 00000 00000 000 0 00000 00000 999 100
20040101000777 0641 S 1 058 9 08601 09501 1 009 0 66300 7530 000 0 00000 00000 000 0 00000 00000 000 0 00000 00000 999 100
20040101000778 0641 S 1 064 9 08470 09370 1 008 0 61250 7925 000 0 00000 00000 000 0 00000 00000 000 0 00000 00000 999 100
20040101000779 0641 S 1 042 8 05730 07530 1 008 0 51590 6959 000 0 00000 00000 000 0 00000 00000 000 0 00000 00000 999 100
20040101000780 0641 S 1 083 8 05587 07387 1 005 0 54740 6674 000 0 00000 00000 000 0 00000 00000 000 0 00000 00000 999 100
20040101000781 0641 S 1 100 9 07099 07999 000 0 00000 00000 000 0 00000 00000 000 0 00000 00000 999 100
```

I   J
Layer 1   Layer 2   Layer 3   Layer 4

Year
Month
Day
Hour

Hemisphere

Within each layer:
Percent coverage at that layer
Cloud type (1-9)
Height of base (meters)
Height of top (meters)

Total cloud amount from all layers (percent)

Cloud Type Table					
1	Cb	4	Cu	7	Ac
2	St	5	As	8	Cs
3	Sc	6	Ns	9	Ci

Figure 3.   Worldwide Merge Cloud Analysis file format. Figure from HQ AFWA/DNXM (2011).

C.   CLOUDSAT

1.   Description of Cloudsat

Cloudsat is a National Aeronautics and Space Administration (NASA) operated satellite launched on April 28, 2006. It carries a W-band (94 GHz) cloud profiling radar (CPR) for sensing condensed cloud particles and detecting precipitation, and is part of the Earth Systems Science Pathfinder (ESSP) mission. The original Cloudsat program was funded for 22 months and has been extended to September 2011. Ground operations are performed by the United States Air Force (USAF) at Kirkland Air Force Base in Albuquerque, New Mexico. The CPR has been providing continuous, global time series of vertical cloud structure and properties at a vertical resolution of 485 m since June 2, 2006 (Stephens et al. 2008).

Cloudsat was designed to help fulfill four mission objectives: "(1) quantify the representation of clouds and cloud processes in global atmospheric circulation models, (2) quantify the relationships between vertical profiles of cloud liquid water and ice and radiative heating of the atmosphere and surface; (3) evaluate cloud properties retrieved

12

from other satellites system (e.g., Aqua); and (4) contribute to improving the understanding of the indirect effect of aerosols on clouds by investigating the effect of aerosols on cloud and precipitation formation" (Stephens et al. 2008), which is critical to the understanding of climate change.

The Cloudsat satellite flies in a constellation of satellites referred to as an "A-Train," which consists of the Cloud-Aerosol Lidar and Infrared Pathfinder Satellite Observation (CALIPSO) satellite, followed by other NASA satellites (Figure 4). CALIPSO has a two-wavelength, polarization-sensitive backscattering lidar that provides high resolution vertical profiles of clouds (NASA Facts–Cloudsat 2003). Cloudsat uses near-nadir pointing millimeter-wavelength radar capable of probing the vertical structure of a cloud (Cloudsat Data Products Handbook 2011). The combination of data from theses satellites provides a valuable source of cloud information. The other satellites that makeup the "A-Train" are Aura, Polarization and Anisotropy of Reflectances for Atmospheric Sciences coupled with Observations from a Lidar (PARASOL), Aqua, and Orbiting Carbon Observatory (OCO).
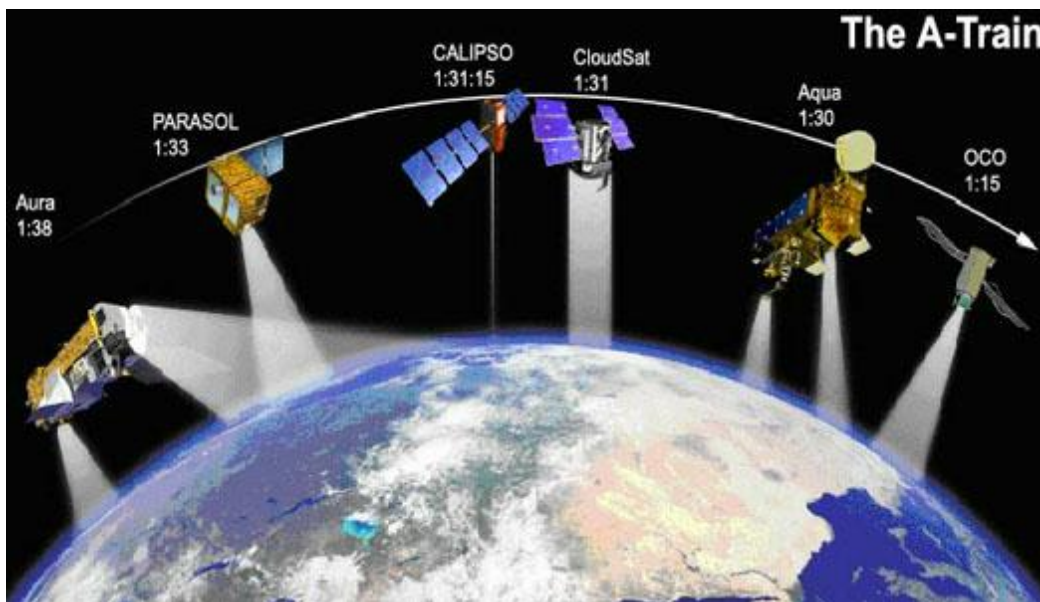
Figure 4.   Depiction of the satellites that make up the "A-train". Each satellite has its name and time of equator crossing listed. Note that CALIPSO trails Cloudsat by 15 seconds to allow for synergy between Aqua, Cloudsat, and CALIPSO. From NASA Facts–A-Train 2003.

The constellation flies in a Sun-synchronous orbit with a mean equatorial altitude of 705–730 km and an inclination of 98.2°. This orbit is fixed, so that there are no changes in the orbital elements over long time periods. The revisit time is 16 days. This means that Cloudsat repeats ground track every 16 days, or 233 revolutions (Cloudsat—Education: FAQ 2011).

Clouds are weak scatters of microwave radiation, in contrast to the stronger reflections from Earth's surface. To detect these weak cloud signals, the CPR was designed for a minimum detectable signal, Z_{min}, of -28 dBZ (Stephens et al. 2008). Table 2 summarizes the defining parameters of the radar confirmed by measurements before and after launch. The CPR emits a 3.3 microsecond pulse resulting in a vertical resolution of 485 m. The back scattered signal is oversampled to produce a range gate spacing of 240 m. From the altitude of 705 km, the instantaneous field of view (IFOV), at mean sea level, is 1.7 km along and 1.3 km across track (Figure 5), and 688 pulses are averaged to produce a nominal footprint of 2.5 km along track. The volume defined by the along track footprint and 240 m range is referred to as a range resolution volume (RRV) (Mace et al. 2007).

Table 2.   Cloud profiling radar (CPR) parameters and their respective performances. From Stephens et al. 2008.

Parameter	Performance
Frequency	94.05 GHz
Altitude	705-730 km
Range resolution (6 dB)	485 m
Cross-track resolution	1.4 km
Along-track resolution	1.8 km
Pulse width	3.3 μs
Peak power (measured)	32.6 dB
PRF	3700-4300- Hz
Antenna diameter	1.85 m
Antenna gain	63.1 dBi
Antenna side lobes	-50 dB @ $\theta > 7°$
Integration time (single-beam)	0.16 s
Data window	30 km
Minimum detected reflectivity (measured)	-30 dBZ
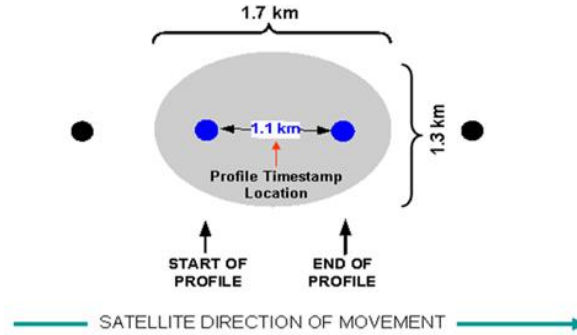
Figure 5.   The instantaneous field of view (IFOV) for the Cloudsat cloud profiling radar (CPR). From Cloudsat Product Handbook (2011).

Due to the radiometric differences between cold scenes (e.g., clear skies over a cold surface at night) and hot scenes (e.g., clear skies over a warm surface during daytime), the single-beam Z_{min} varies by $\pm$ 1 dB. Cloudsat's calibration as of 2008 of Z_{min} is 29.9 to 30.9 dBZ (Stephens et al. 2008).

Cloudsat has problems detecting some low level strata, cumulus, non-drizzling stratocumulus, warm altocumulus composed of small water droplets, and optically thin, high cirrus (Mace et al. 2007). Since the CPR vertical resolution is 485 m and surface reflectivity is up to five times greater than cloud reflectivity, measurements in the lowest two RRVs of the profile are dominated by surface back scatter.   This surface contamination can extend up to 1 km, and the signal usually returns to maximum sensitivity by the 5th RRV. However, on average, clouds that reflect above 10 dBZ in the 3rd and 4th RRVs (i.e., 480 to 960 m above surface) are detected above surface contamination (Mace et al. 2007).   Sassen and Khvorostyanov (2007) explain how the radiative and backscattering properties of mixed-phase clouds effect their detection.

2.   Description of 2B Cloud Geometrical Profiling (GeoProf) Product

The 2B Cloud Geometrical Profiling Product (GeoProf) identifies the levels in the vertical column sampled by Cloudsat that contain significant radar echo from hydrometeors and provides an estimate of the radar reflectivity factor for each of these volumes. Details on the Geoprof algorithms are provided in the Level 2 GEOPROF

Product Process Description and Interface Control Document (2007). The 2B GeoProf product uses an algorithm that reads the Cloudsat 1B-CPR granule, which measures the backscatter power as a function of distance from the radar, and the corresponding MODIS-AUX and ECMWF-AUX granules to produce the cloud mask (Cloudsat Standard Data Products Handbook 2008). MODIS' cloud fraction from the visible 250 m MOD35 product is integrated over the Cloudsat footprint (CloudSat 2B GEOPROF Quality 2007).

The cloud mask data is stored in the 2B-GeoProf data product and contains a value between 0 and 40 for each range bin, with values greater than 5 indicating the likelihood of hydrometeors (Stephens et al. 2008). Larger values indicate a higher likelihood of hydrometeors and a lower likelihood of false detections (Table 3). A Cloudsat data file contains one granule, where a granule is the data collected during one orbit. Granules are broken into 31 segments that allow for a visual view of the data (Figure 6).

Table 3.   Description of Cloudsat cloud mask values, false detection rates, and false detections. The percentage of false detection is 100 times the number of false detections divided by the total number of detections for the specific cloud mask value. From Stephens et al. (2008).

Mask Value	Meaning	% false detections goal	Estimated % false detection via CALIIPSO comparison
-9	Bad or missing radar data		
5	Significant return power but likely surface clutter		
6-10	Very weak echo (detected using along-track averaging)	<50%	44%
20	Weak echo (detection may be artifact of spatial correlation)	<16%	5%
30	Good echo	<21%	4.3%
40	Strong echo	<0.2%	0.6%

MODIS 11 um channel (CloudSat ground track subject to parallax error)
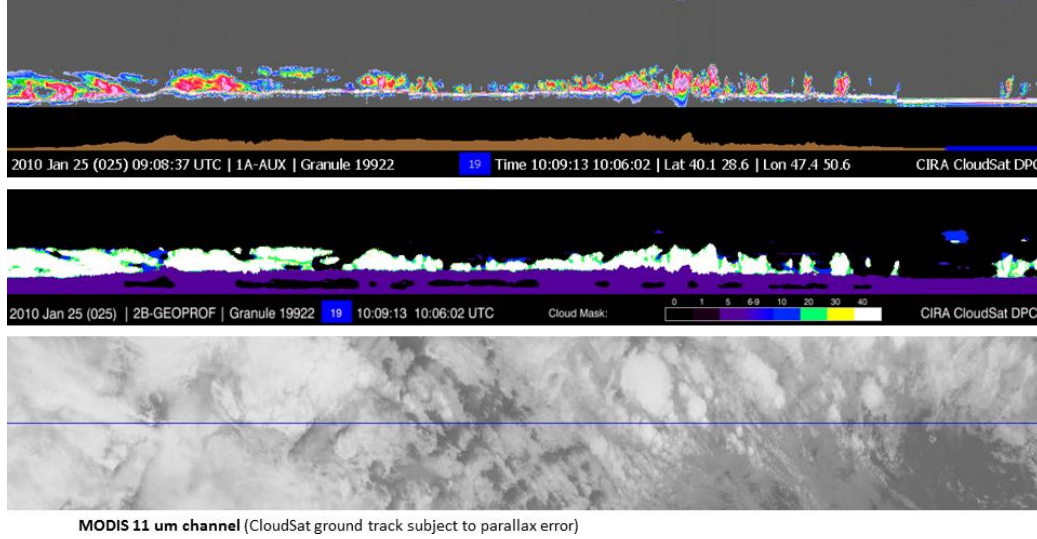
Figure 6.   A visualization of Cloudsat data for one segment of a granule. The top pane is
the 1A Aux data and contains the date and start time of the granule, and the
starting/ending latitude-longitude and times of that segment. The middle panel
is the 2B-GeoProf cloud masking, which is color coded for masking values.
The bottom panel is an Aqua MODIS image (11 μm) of the granule, which
was taken one minute prior to the data collection of the granule. From
Cloudsat Data Processing Center (2011).

D.   STUDY REGIONS AND PERIODS

We selected two regions for this study based on open source information about
where the U.S. national intelligence community has a high interest in electro-optical (EO)
imagery. We selected WWMCA Box 22 (Figure 7) because it encompasses much or all
of Iraq, Iran, Afghanistan, and Pakistan, all of which are important in U.S. national
security. WWMCA Box 22 contains mountains, deserts, ocean, and coastal regions and
mostly resides in the mid-latitudes, extending south to 18°N and north to 50° N, and
within the field of view (FOV) for geostationary satellites. The diversity of climates,
terrains, and the availability of geostationary satellite information for use in developing
WMCA products, makes Box 22 a good case for testing the mid-latitude performance of
WWMCA. We also selected WWMCA Box 29 (Figure 7) because it too covers areas of
interest to the IC. Box 29 encompasses much of western Russian and the Barents Sea in
the Arctic, a region of increasing interest due to decreases in Arctic sea ice and the
potential for increased Arctic maritime activity. Box 29 extends between 50° N and

90° N, so WWMCA products for this box rely on polar orbiting satellites. Thus, Box 29 is a good case for assessing the high latitude performance of WWMCA.

The period of the study was January, April, July, and October 2010. These months were chose to represent the four main seasons of the year. We limited our study to just two WWMCA boxes, and four months of one year due to time constraints. However, the methods developed in our study can be readily applied to assess the performance of many other boxes, months, and years. They can also be readily applied to look at regions smaller or larger than one WWMCA box, and to periods less than or greater than one month. See Chapter IV for more information on applications of methods and extensions of our study.
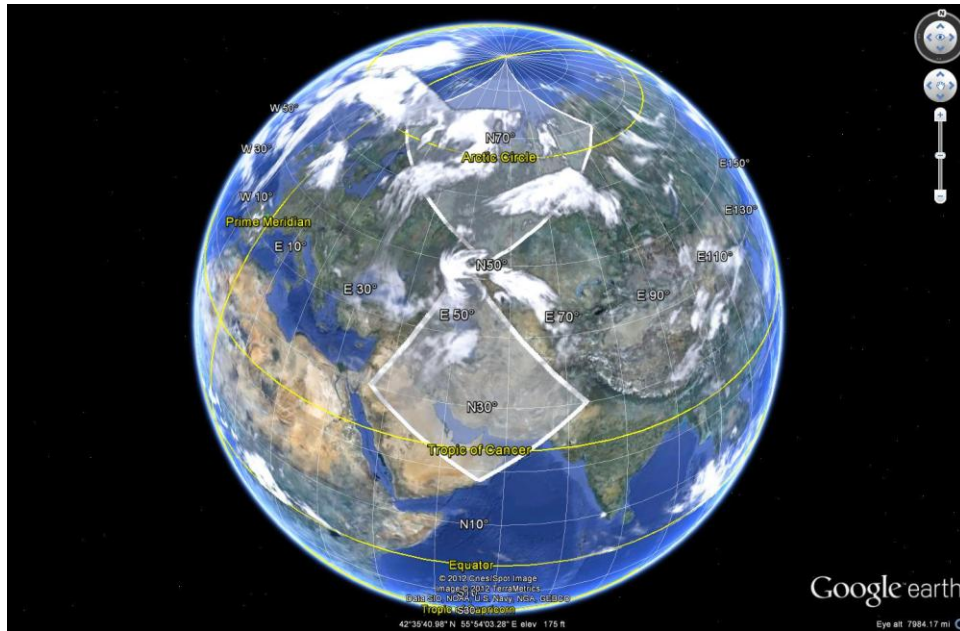
Figure 7.   Location of WWMCA boxes 22 and 29, shown by the white southern and northern boxes, respectively. These boxes appear skewed in the image due to the map projection. Box 22 includes much or all of Iraq, Iran, Afghanistan, and Pakistan. Box 29 includes much of western Russia and the Barents Sea. Base image from Google Earth (2011).

E. DATA SETS

1. WWMCA

The WWMCA data set used for this study was provided by the 16th Weather Squadron and consisted of global, hourly cloud analyses for all of 2010 in an ASCII format. The file name convention is: the prefix CLD, year, month, and WWMCA box number. For example, the data files for WWMCA Box 22 for March and October 2010 are CLD201003022 and CLD201010022, respectively. The data files contain all the hourly cloud analyses for a WWMCA box for an entire month and have about 1.5 million lines of data per file. One zipped WWMCA data file is about 100 MB and has an unzipped-to-zip ration of 10:1.

2. Cloudsat–2B-Geoprof

The Cloudsat 2B-GeoProf data was downloaded from the Cloudsat Data Processing Center and are in a Hierarchical Data Format (HDF). Each file has 37,100 lines of data and the name convention is: the Julian date and granule start time (hour, minute, second), granule number, type of sensor (Cloudsat = CS), data product type, and the suffix 'GRANULE_P_R04E03.hdf.' For example, granule 19893 is named 2010023092101 _19893_CS_2B-GEOPROF _GRANULE_ P_R04_E03.hdf. One zipped Cloudsat data file is about 13 MB and has an unzipped-to-zip 3:1.

F. METHODS

The Cloudsat and WWMCA data sets are on different temporal and spatial grids that have different resolutions, and differ in the variables they use to describe clouds. So the data needed to be processed and put on a common footing before it could be analyzed. This section describes the programming requirements and associated tasks necessary to compare and analyze the two sets of data in a spreadsheet program (e.g., Microsoft Excel). The major challenge was getting the Cloudsat data: (a) onto the same time and space grid as the WWMCA data; and (b) into the same units as the WWMCA data. This consisted of matching Cloudsat data to the WWMCA cells, converting Cloudsat cloud mask measurements into total cloud amount percentages for a given

WWMCA cell, and binning both WWMCA and Cloudsat data into common cloud cover events. The WWMCA variable of interest for this research project was total cloud amount.

The WWMCA data is organized into 128 square boxes (64 boxes per hemisphere) with each box containing 128 cells (Figure 8). The cells have unique **i-j** coordinates that describe the latitude and longitude of the cell. The cells are 24 x 24 km, true at 60° latitude (HQ AFWA/DNXM 2011).
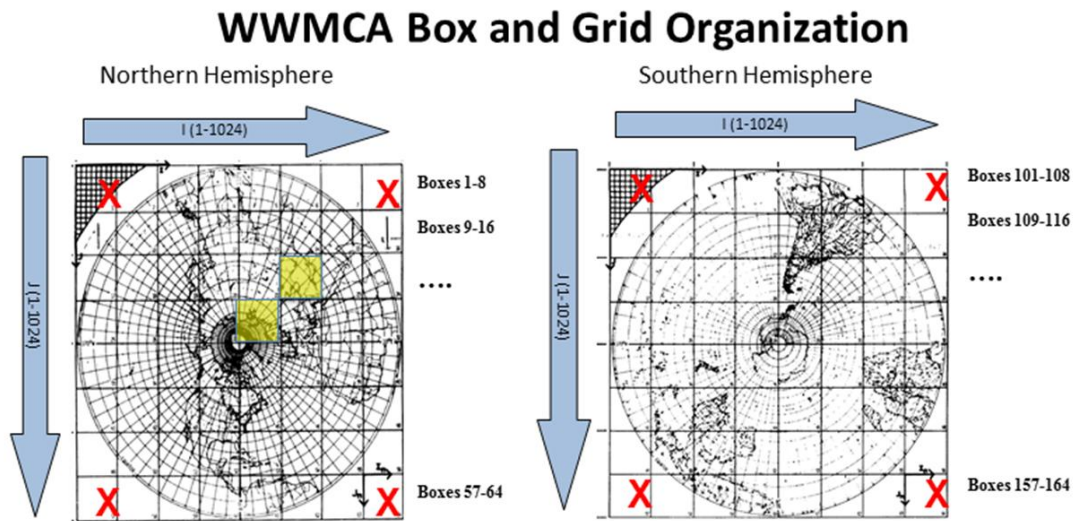
Figure 8. The WWMCA grid is organized into 128 square boxes (64 boxes per hemisphere) with each box containing 128 cells. The cells have unique i-j coordinates that describe the latitude and longitude of the cell. The cells are 24 km long on a side (true at 60° latitude). The yellow shaded boxes are the two WWMCA boxes that we focused on in this study. The northern box is WWMCA Box 29 and the southern one is Box 22. Base figures from 16th Weather Squadron (2011).

Each Cloudsat granule is 40,786 km in length and contains 37,088 profiles. Each profile represents a vertical sounding from the satellite through the atmosphere to the surface. The horizontal surface area represented by each profile is the Cloudsat pixel area (or IFOV). Each Cloudsat pixel (Figure 5) is about 1.3 km wide (across the track) and 1.7 km long (along the track). The main Cloudsat data of interest for this study was the Cloudsat cloud mask data in the 2B-Geoprof product, which provided information

about the presence or absence of clouds, along with corresponding date-time and latitude-longitude data. This data was available for each profile and for each of 125 vertical levels within the profile (Figure 9). The cloud mask values indicate the likelihood of cloud detection and are described in Table 3. The Cloudsat dataset also includes a variable that describes the height of the Cloudsat levels above mean sea level (MSL) that we used to filter out the backscatter from the surface (see next section).
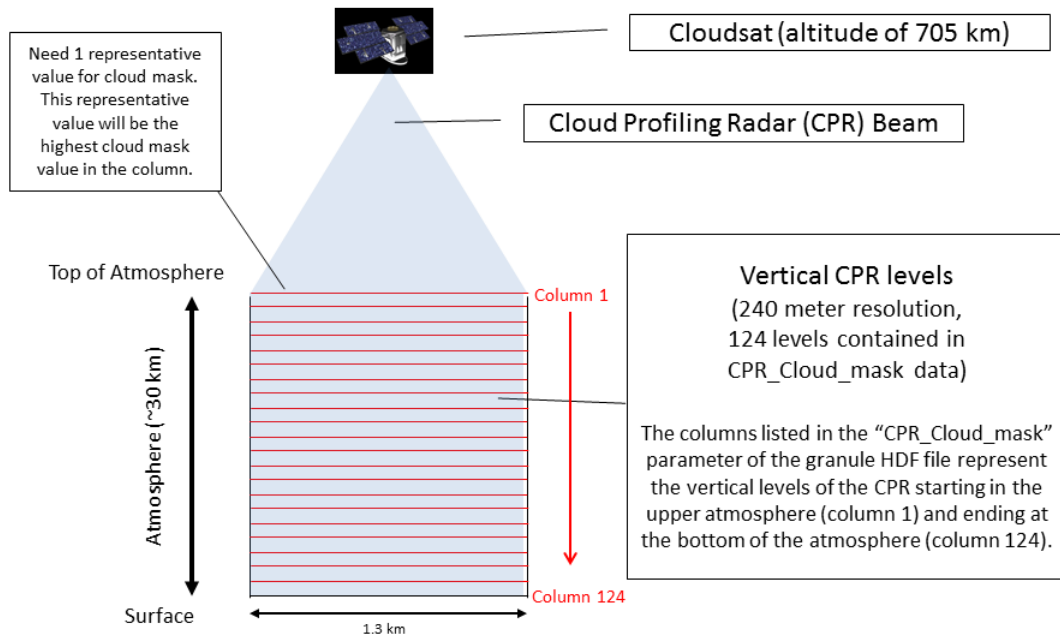
Figure 9.   Vertical levels in Cloudsat.

Figure 10 illustrates the processing of the WWMCA and Cloudsat data that we did to prepare the data for analysis, as well as the analysis of the processed data.
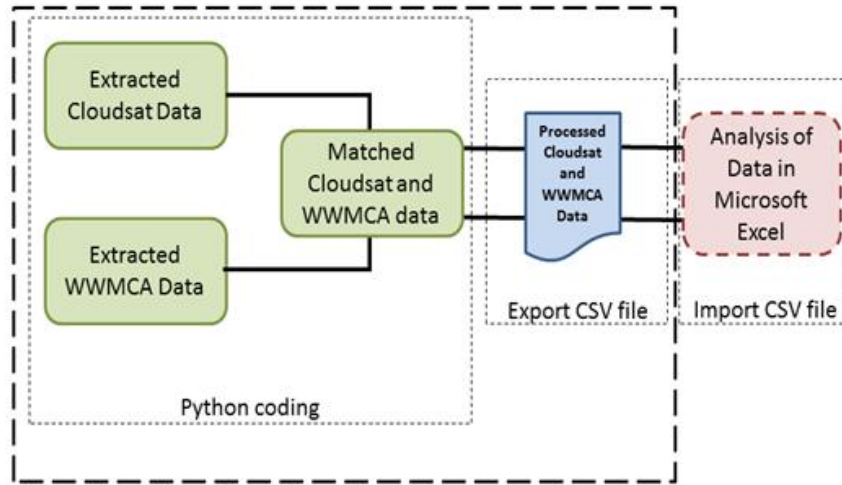
Figure 10.   Overview of data processing conducted to prepare WWMCA and Cloudsat datasets for analysis.

1.   Cloudsat Data Preparation

Cloudsat data was prepared for verifying the WWMCA data by running a set of Python programs that extracted the required data from a data base containing the 2010 Cloudsat data files that intersected WWMCA Boxes 22 and 29. The required data were:

- profile time

- UTC start time

- latitude

- longitude

- height

- CPR cloud masking

The data for these variables were extracted and matched to the appropriate WWMCA verification time and cell. The Cloudsat observations were matched to WWMCA verification times that best represented the atmospheric cloud state for that time, using a similar to that used by CDFS II to match satellite observations to the cloud analysis. Cloudsat observations that fall within the first (second) half of an hour were matched to WWMCA data of that (the following) hour. For example, if a Cloudsat observation was from 0817Z, it was matched to the 0800 WWMCA verification time. If the observation was from 0831Z, it was matched to the 0900 verification time. Next, the Cloudsat data was mapped, or converted, to the WWMCA grid and matched to the corresponding WWMCA cells within the WWMCA box of interest, either Box 22 or Box 29.

We used the height variable to remove from the data processing effort any Cloudsat observations with heights less than 1 km, to eliminate backscatter from the ground. We also identified the WWMCA cells that contained six or more Cloudsat pixels, so that we could focus our analyses on the cells and times for which there was at least 25% coverage by Cloudsat (six Cloudsat pixels cover 25% coverage of a WWMCA).

Cloudsat cloud masking data are available at 125 vertical levels for each profile (Figure 9). For comparison to the WWMCA total cloud amount data, we reduced the 125 values to a single representative cloud mask value for each profile. We used the highest cloud mask value from the 125 levels as the representative cloud mask value (after deleting the values from the lowest 1 km, as described above). There are pros and cons to this selection of the cloud mask value. In particular, this selection minimizes the risk of overstating the cloud masking, but it may underestimate the actual cloud masking. Recall that the cloud masking values represent the likelihood of occurrence of hydrometeors in a profile. So a summation, or an average, of values from more than one of the 125 levels might well overstate the likelihood clouds. Thus, we chose to use the highest cloud mask value to represent the full profile.

We assigned a cloud occurrence value to each pixel by using the Cloudsat cloud mask value for each Cloudsat pixel to determine if cloud or no-cloud conditions had occurred. If the cloud mask value was less than 30, we assigned a cloud occurrence value of 0 to indicate a no-cloud condition. If the cloud mask value was 30 or greater, we assigned a cloud occurrence value of 1 to indicate the presence of cloud, or cloud conditions. It is important to note that prior studies used a Cloudsat cloud mask value of 20 as the cloud/no-cloud threshold, rather than the value of 30 that we used. The Cloudsat Standard Data Products Handbook (2008) states that values of 30 or greater are associated with the greatest confidence in cloud detection. Based on this, we decided to use a cloud mask value of 30 as the threshold for determining whether clouds were or were not present in a profile. However; to test the sensitivity of our analysis results to this threshold selection, we also used a threshold value of.

Next, we converted the set of Cloudsat cloud and no-cloud condition values for all the pixels in a WWMCA cell to a single total cloud amount for the cell using the following calculation:

$$\frac{Number\ of\ Cloudsat\ cloudy\ points}{Total\ number\ of\ Cloudsat\ points} * 100 = Total\ cloud\ amount\ (\%)$$

That is, we divided the number of Cloudsat pixels that indicated the presence of clouds within a WWMCA cell by the total number of Cloudsat pixels in the cell, and then multiplied by 100, to derive a total cloud amount percentage for the cell. For example, if 12 out of 19 Cloudsat pixels in a WWMCA cell showed cloud conditions, then the total cloud amount for the cell was calculated to be 63% (Figure 11).

One WWMCA Cell

24 km

12 of 19 points are cloud. The total
cloud amount is 63%
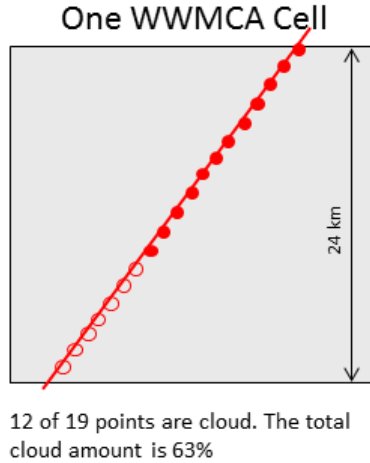
Figure 11.   Schematic illustration of the overlap of a Cloudsat swath (red line) and a
WWMCA cell (gray box). The red circles indicate the Cloudsat
representation of cloud conditions (solid red circles) and no-cloud conditions
(open red circles). The total cloud amount for the cell, as indicated by
Cloudsat, is the number of cloud conditions divided by the number of cloud
and no-cloud conditions, all multiplied by 100. For this case, 12 of the 19
circles indicate cloud conditions, so the total cloud amount is 63%.

The resulting Cloudsat total cloud amount data was then binned into one of three cloud
cover events (Table 4). Cells that had a total cloud amount value $\geq$ 80% were assigned to
the Definite-Cloud event bin. Cells that had a total cloud amount value $\leq$ 20% were
assigned to the No-Cloud event bin. Cells with in between total cloud amount values
were assigned to the Probable-Cloud event bin.

Table 4.   Method used to determine cloud cover event status for a WWMCA cell based
on the Cloudsat-based total cloud amount (%) for the cell.

Cloud Event Number	Total Cloud Amount	Event Name
1	$\leq$ 20 %	No-Cloud
2	21—79 %	Probable-Cloud
3	$\geq$ 80 %	Definite-Cloud

2.   WWMCA Data Preparation

We needed to match up the WWMCA total cloud amount data to the Cloudsat
data in the CSV file that was generated during the Cloudsat data preparation stage by

25

inserting WWMCA data in the appropriate rows. The rows represent the time and location of the data. So inserting the WWMCA data into the correct rows meant that we did a temporal and spatial match of the Cloudsat and WWMCA data.

We extracted WWMCA data and wrote it to a CSV file for the period and location of the Cloudsat data that was already in the CSV file. However, since the WWMCA data has a lower temporal and spatial resolution than the Cloudsat data, there are rows that contain Cloudsat data and duplicate WWMCA data from adjacent rows. All of the WWMCA information contained in a data line (Figure 3), including the mean pixel age was written to the CSV file containing the Cloudsat data.

We then binned WWMCA total cloud amount into the same three cloud cover events as Cloudsat total cloud amount (Table 4).

In summary, there are significant differences in the spatial and temporal resolutions of WWMCA and Cloudsat data. WWMCA data is contained in 1024 x 1024 cells per hemisphere with a horizontal resolution of 24 km. Cloudsat data has a 1.3 x 1.7 km footprint and is referenced to latitude and longitudes. CDFS II outputs a new WWMCA product every hour, and Cloudsat flies over a WWMCA cell for three minutes, twice daily. This indicates three significant challenges in verifying WWMCA against Cloudsat (and many other observational data sets): (1) accurately matching the two data sets in space; (2) accurately matching the two data sets in time; and (3) obtaining a sufficient amount of independent observational data to use in verifying WWMCA (finding an adequate amount of independent observations that fall within a WWMCA cell to confidently verify the WWMCA analysis for that cell). Cloudsat and many other global observational data sets are readily available on regular latitude-longitude grids. Verification of WWMCA would be a much more straightforward process if WWMCA data was also readily available on a regular latitude-longitude grid.

3.   Analyzing Data in Microsoft Excel

Verification of the WWMCA cloud analysis to Cloudsat data was accomplished with Microsoft Excel. Refer to Appendix B for the format and formulas used to analyze the data. The CSV file containing the processed WWMCA and Cloudsat data for a given

month was imported into Excel and data lines with values of "-1" and "less than 6 points" were filtered out of the analysis process, since these points represented missing data and WWMCA cells with less 25% area covered by Cloudsat observations, respectively.

Next we tallied the hits, false alarms, misses, and correction rejections for the three cloud cover events for Cloudsat cloud thresholds values 20 and 30. The tallies were generated for use in entering data into the contingency tables we used to verify the performance of WWMCA. Table 5 explains the logic for determining whether a given WWMCA-Cloudsat data pair would be counted as a hit, false alarm, miss, and correction rejection. In this table, the upper portion describes the logic for verifying the performance of WWMCA in analyzing Definite-Cloud events (cloud event 3), the middle portion does the same for Probable-Cloud events (cloud event 2), and the bottom portion does the same for No-Cloud events (cloud event 1). The cell letters (A, B, C, D) refer to the four cells in the two by two contingency tables that we used (see next section and Wilks 2006). For example, the third row of Table 5 shows that if WWMCA analyzed cloud event 3 and Cloudsat observed cloud event 3, then a tally would be entered in cell A of the contingency table, which is the Hit cell.

Table 5.   Logic for tallying hits, false alarms (False), misses (Miss) and correct rejections (Reject) when comparing a WWMCA cloud cover analysis to the corresponding Cloudsat cloud cover observation.

Tallying Logic for Verifying WWMCA Performance in Analyzing Cloud Cover Events			
3	**Cell**	**WWMCA**	**Cloudsat**
Hit	A	3	3
False	B	3	1 or 2
Miss	C	1 or 2	3
Reject	D	1 or 2	1 or 2
2	**Cell**	**WWMCA**	**Cloudsat**
Hit	A	2	2
False	B	2	1 or 3
Miss	C	1 or 3	2
Reject	D	1 or 3	1 or 3
1	**Cell**	**WWMCA**	**Cloudsat**
Hit	A	1	1
False	B	1	2 or 3
Miss	C	2 or 3	1
Reject	D	2 or 3	2 or 3

Next, we took the tallied categories for cloud cover events and then flagged the data as either day or night. This was done by using the monthly mean sunset and sunrise times for a reference point within a WWMCA box that we assumed to be representative to the entire box (Table 6). The reference point we used for Box 22 was Tehran, Iran. The reference point for Box 29 was Orenburg, Russia. In Box 29, data lines that fell within the Arctic Circle (Cloudsat latitudes $\geq 70°N$) were flagged as either day or night depending on the time of year. January and April were assumed to be polar night conditions, and July and October were assumed to be polar day conditions. We then created separate tallies for the day and night hit, false alarm, miss, and correction rejection categories. This allowed us to separately assess the performance of WWMCA for all hours of the day, for daylight hours, and for nighttime hours.

Table 6.   Mean times of sunrise and sunsets for reference points within WWMCA Box 22 and Box 29. We assumed that the reference point times were representative of the entire WWMCA box. The daylight times were used to flag WWMCA and Cloudsat data as either day or night data.

Box 22 Reference: Tehran, Iran   **Daylight Range**

Box 22	Sunrise (Local)	Sunset (Local)	Sunrise (Local)	Sunset (Local)	GMT +6 hrs	GMT +6 hrs	Sunrise (Z)	Sunset (Z)	Sunrise (Z)	Sunset (Z)	Filter Type
Jan	9:30	17:30	0.3958	0.7292	3:30	0.1458	0.5417	0.8750	13:00	21:00	Day
Apr	7:30	21:00	0.3125	0.8750	3:30	0.1458	0.4583	1.0208	11:00	0:30	Night
Jul	6:00	22:30	0.2500	0.9375	3:30	0.1458	0.3958	1.0833	9:30	2:00	Night
Oct	8:30	19:30	0.3542	0.8125	3:30	0.1458	0.5000	0.9583	12:00	23:00	Day

Box 29 Reference: Orenburg, Russia   **Daylight Range**

Box 29	Sunrise (Local)	Sunset (Local)	Sunrise (Local)	Sunset (Local)	GMT +6 hrs	GMT +6 hrs	Sunrise (Z)	Sunset (Z)	Sunrise (Z)	Sunset (Z)	Filter Type
Jan	9:00	18:00	0.3750	0.7500	6:00	0.2500	0.6250	1.0000	15:00	0:00	Day
Apr	7:00	21:00	0.2917	0.8750	6:00	0.2500	0.5417	1.1250	13:00	3:00	Night
Jul	6:30	22:30	0.2708	0.9375	6:00	0.2500	0.5208	1.1875	12:30	4:30	Night
Oct	8:30	19:30	0.3542	0.8125	6:00	0.2500	0.6042	1.0625	14:30	1:30	Night

4.   Contingency Table Analysis

The performance of WWMCA was verified using 2 x 2 contingency table methods (Table 7; Wilks 2006). Even though WWMCA is an analysis we are treated it as an hourly forecast so that we could assess its performance using standard performance metrics. We calculated a number of performance metrics based on Table 7.

Table 7.   The format of the 2 x 2 contingency table analysis used to verify WWMCA cloud analyses. Based on Wilks (2006).

		Observations (Cloudsat)			
		Cloud	No-cloud		
Analysis (WWMCA)	Cloud	A Hits (A / N)	B False Alarms (B / N)	A + B (A + B) / N	Marginal Totals for Analysis & Marginal Distributions for Analysis
	No-cloud	C Misses (C / N)	D Correct Rejections (D / N)	C + D (C + D) / N	
		A + C (A + C) / N	B + D (B + D) / N	N = A + B + C + D 1.00	
		Marginal Totals for Observations & Marginal Distributions for Observations		Sample Size & Total Probability	

We calculated a number of WWMCA performance metrics based on Table 7. The probability of detection (POD), also called hit rate (H), is the ratio of correct analyses of an event to the number of times the event occurred. In our case, the events of interest were Definite-Cloud, Probable-Cloud, and No-Cloud events, which we analyzed separately. The H or POD was calculated by:

$$H = POD = \frac{Hits}{(Hits + Misses)}$$

Proportion correct (PC), which Wilks (2006) states is the most straightforward and sensitive measure of the accuracy of nonprobabilistic forecasts for discrete events, credits correct cloud and no-cloud analyses equally, and is the ratio of the number of

correct analyses to the total number of samples. However, PC does not distinguish between correct event and no-event analyses. We calculated the proportion of occasions when the analysis was correct by:

$$PC = \frac{(Hits + Correct\ Rejections)}{Number\ of\ Samples}$$

We also calculated the threat score (TS), or critical success index (CSI), which eliminates from consideration correct rejections. The best possible threat score is one and the worst is a zero (Wilks 2006) and was calculated by:

$$TS = CSI = \frac{Hits}{(Hits + False\ Alarms + Misses)}$$

The bias (B) is the total number of analyses of an event divided the total number of observations of the event. Unbiased analyses would have a bias value of 1. Bias values greater than one indicate that the event occurred more often than it was observed (the event was over analyzed) and bias values less than one indicate the event occurred less often than observed (the event was under analyzed). We calculated bias by:

$$B = \frac{Total\ for\ Analysis}{Total\ for\ Observations} = \frac{(Hits + False\ Alarms)}{(Hits + Misses)}$$

The false alarm ratio (FAR) is the ratio of false alarms for an event to the total number of analyses of the event, or the fraction of analyses that were wrong (Wilks 2006). Thus, FAR is the number of false alarms divided by the sum of the hits and false alarms, all for the event of interest. The best value for FAR is zero and worst value is one. The false alarm ratio was calculated by:

$$FAR = \frac{False\ Alarms}{Total\ for\ Analysis}$$

The skill of the analysis was tested with the Heidke skill score (HSS). The Heidke skill score is based on the portion correct as the basic accuracy measure. Perfect analyses would yield a score of one; a score of zero would indicate that the analyses are equivalent to random reference analyses; and a negative score would indicate that the analyses were worse than random analyses. Wilks (2006) explains that the reference measure for the Heidke skill score is the portion that is correct from a random analysis statistically independent of observations. We calculated the Heidke skill score as:

$$HSS = \frac{2(Hits * Correct\ Rejections - False\ Alarms * Misses)}{(Hits + Misses)(Misses + Correct\ Rejections) + (Hits + False\ Alarms)(False\ Alarms + Correct\ Rejections)}$$

A description of our WWMCA performance results is provided in Chapter IV.

5. Summary of Assumptions

In order to verify WWMCA against Cloudsat, we made a number of important assumptions. In particular, we assumed that:

1. Cloudsat is the 'truth' for describing the actual clouds in the atmosphere.
2. The Cloudsat level with the high cloud mask value is representative of all 125 levels and provides a good measure of the total cloud mask.
3. Cloudsat observations that cover ≥25% of a WWMCA cell are adequate to represent all the clouds in the cell and for verifying WWMCA for that cell.
4. The mean monthly sunrise/sunset times near the center latitude of a WWMCA box are representative of the whole box.
5. January, April, July, and October are representative of the major seasons.
6. Cloud cover can be adequately represented by the three cloud events described in Table 4.

7.   WWMCA performance can be adequately assessed using metrics based on 2 x 2 contingency tables.

We applied these assumptions for a variety of reasons—in particular to keep our analyses relatively straightforward. Assumption 1 is not easy to modify, since extensive independent cloud observations are scarce. Assumptions 2-7 can be modified and we recommend doing so in future studies. In addition, we recommend testing the sensitivity of the performance results to these assumptions (see Chapter IV).

THIS PAGE INTENTIONALLY LEFT BLANK

III. RESULTS

A. OVERVIEW

In this chapter, we present the results of WWMCA verification for WWMCA Boxes 22 and 29 using a Cloudsat cloud mask value of 30 for the cloud/no-cloud threshold. For comparison, WWMCA verification results from Cloudsat cloud mask value of 20 for cloud/no-cloud threshold are shown in Appendix C. The number of occurrences of hits, false alarms, misses, and correct rejections for the three cloud cover events—3: Definite-Cloud, 2: Probable-Cloud, and 1: No-Cloud—described in section 2.F.3, were used to characterize WWMCA performance through formulas stated in section 2.F.4. The performance results are provided for each of the three cloud cover events, for the daytime data, for nighttime data, and for combined daytime and nighttime data (referred to as "All Day" results). These results are presented for each of the four months we analyzed (January, April, July, and October) and for the two WWMCA boxes we analyzed (22 and 29). Note that in the figures in this chapter, *Definite-Cloud* events are sometimes referred to as *Cloud* events. Our emphasis in analyzing WWMCA was on its performance in analyzing Definite-Cloud and No-Cloud events, since these are of most interest to IC users of CDFS II products. However, we also present in the following sections the results for WWMCA performance in analyzing Probable-Cloud events, which, as shown in these sections, tends to be quite low.

B. WWMCA BOX 22

For WWMCA Box 22, Figures 12 and 13 show the number of occurrences of hits (A), false alarms (B), misses (C), and correct rejections (D) for each cloud cover event, and Figure 14 shows the marginal distribution of the cloud events, for the four months. Figures 12 and 13 show that the highest number of occurrences for each cloud event was in the correct rejections category. No-Cloud events had the largest number of hits in each month and Definite-Cloud events had the second highest. The marginal distributions of cloud events for both WWMCA and Cloudsat (Figure 14) show a general decline (increase) in Definite-Cloud (No-Cloud) events from January through October. The

information in Figures 12–14 is useful in assessing the number and percentage of opportunities that WWMCA had to correct analyze the three cloud events (Figure 14) and how well WWMCA did in analyzing those events (Figures 12–14). For example, Figure 14 shows that in July and October there were high percentages of No-Cloud events, but relatively low percentages of Definite-Cloud events. This in turn indicates that in July and October: (a) No-Cloud events were relatively common and therefore perhaps relatively easy to correctly analyze; and (b) Definite-Cloud events were relatively rare and therefore perhaps relatively difficult to correctly analyze.
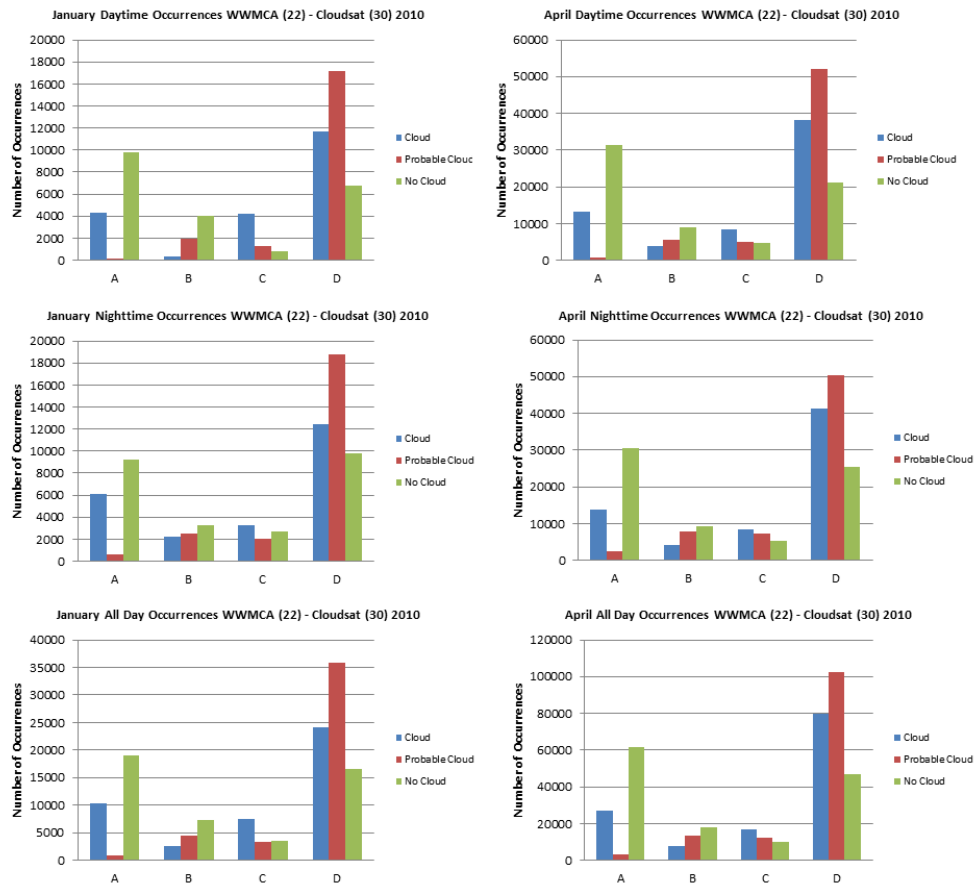
Figure 12. Number of 2 x 2 contingency table occurrences in January and April 2010 for WWMCA Box 22 for all three cloud cover events: Definite-Cloud (blue), Probable-Cloud (red), and No-Cloud (green). On the horizontal axes: A indicates Hits, B indicates False Alarms, C indicates Misses, and D indicates Correct Rejections. The top panels shows the daytime occurrences, the middle panels shows the nighttime occurrences, and the bottom panels show the results for both daytime and nighttime occurrences. Results based on using a Cloudsat cloud mask value of 30 for the cloud/no-cloud threshold.

36

Figure 13.   Number of 2 x 2 contingency table occurrences in July and October 2010 for WWMCA Box 22 for all three cloud cover events: Definite-Cloud (blue), Probable-Cloud (red), and No-Cloud (green). On the horizontal axes: A indicates Hits, B indicates False Alarms, C indicates Misses, and D indicates Correct Rejections. The top panels shows the daytime occurrences, the middle panels shows the nighttime occurrences, and the bottom panels show the results for both daytime and nighttime occurrences. Results based on using a Cloudsat cloud mask value of 30 for the cloud/no-cloud threshold.
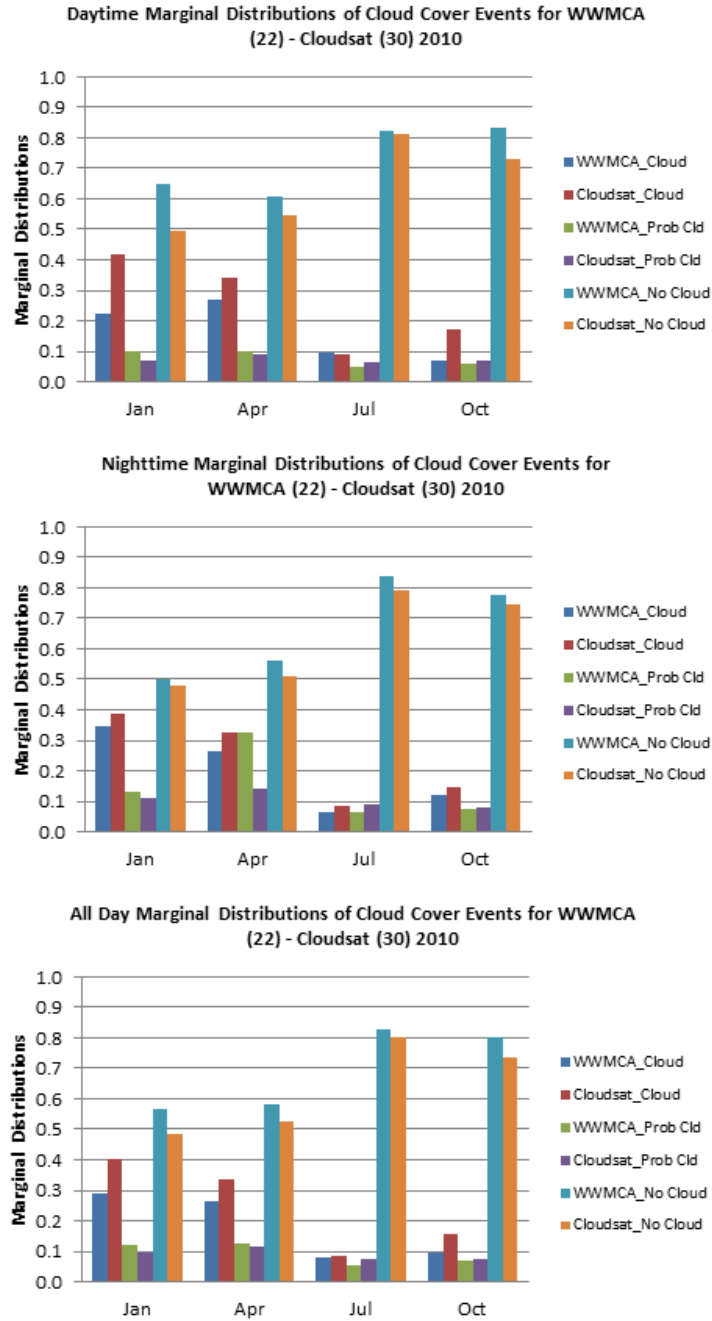
Figure 14.   Marginal distributions of cloud cover events for WWMCA and Cloudsat for WWMCA Box 22: Definite-Cloud, Probable-Cloud, and No-Cloud). The calculation of the marginal distributions is shown in Table 7. The top panel shows the results for daytime data, the middle panel for nighttime data, and the bottom panel for both daytime and nighttime data. Results based on using a Cloudsat cloud mask value of 30 for the cloud/no-cloud threshold.

The POD for the cloud cover events are shown in Figure 15. Overall, WWMCA did the best for No-Cloud events year round—especially during the daytime and in July and October, when No-Cloud events were relatively common (Figure 14). In particular, WWMCA analyses of No-Cloud events were correct 85—95% of the time. But WWMCA analyses of Definite-Cloud events were correct about 57—62% of the time for winter, spring, and summer, and 45% of the time in the fall. The mean Daytime No-Cloud POD was 95% and the mean nighttime No-Cloud POD was 88%. The mean POD of Definite-Cloud events were considerably less: daytime ranged 36—64% and nighttime 49—65%. The lowest Definite-Cloud POD occurred in fall daytime and summer nighttime. The POD for Definite-Cloud events are similar to but somewhat lower than those from UCAR (2008), which reported a POD for Cloud events of 64% (Chapter I, Section C). The relatively high (low) POD for No-Cloud (Definite-Cloud) events may be related to the abundance (scarcity) of No-Cloud (Definite-Cloud) events, especially in July and October (see prior discussion of Figure 14).
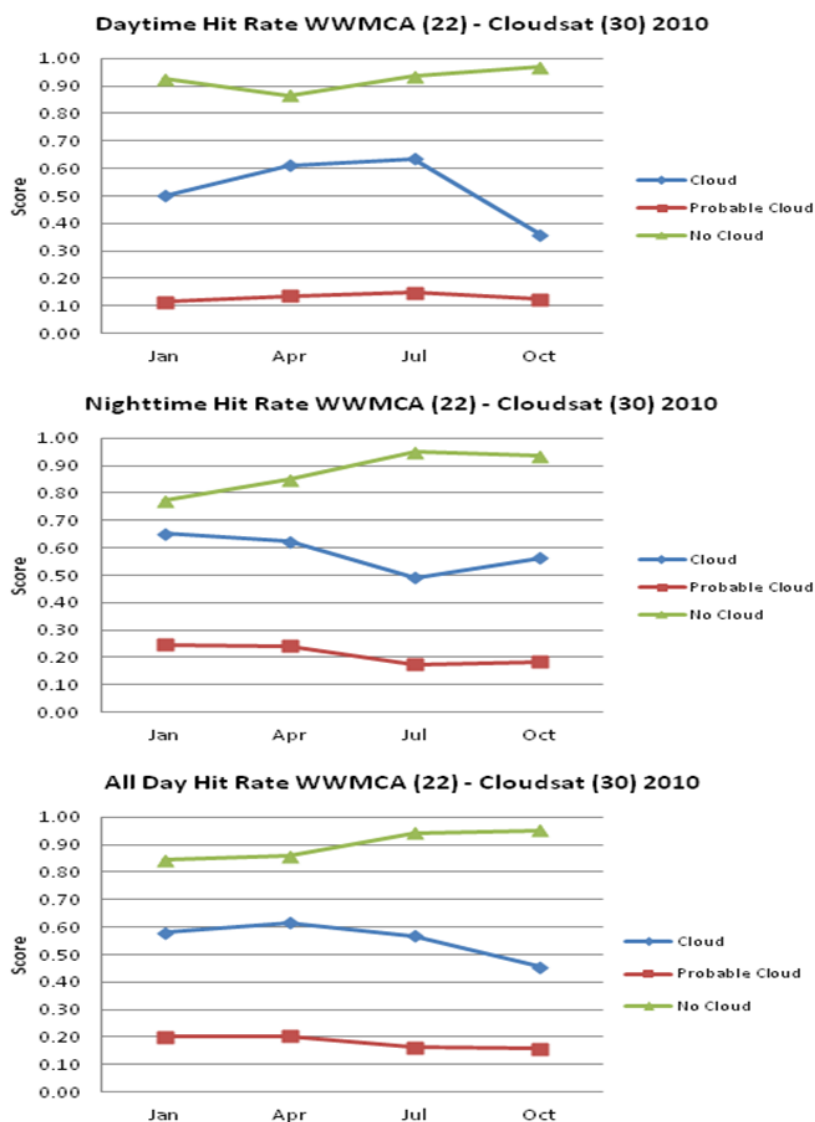
Figure 15.   WWMCA probability of detection (POD), or hit rate (H), for WWMCA Box
22 for all three cloud cover events: Definite-Cloud (blue), Probable-Cloud
(red), and No-Cloud (green). The top panel shows the results for daytime
data, the middle panel for nighttime data, and the bottom panel for both
daytime and nighttime data. Results based on using a Cloudsat cloud mask
value of 30 for the cloud/no-cloud threshold.

Figure 16 shows the WWMCA FAR for Box 22, which range from 5 to 40%. The FAR for Definite-Cloud was relatively low in winter and spring, but relatively high in summer and fall. The FAR for No-Cloud events showed the opposite evolution, from relatively high in winter and spring to relatively low in summer and fall. This is consistent with the occurrence and marginal distributions results (Figures 12–14), with the FAR for an event type being lower when the event type is common and higher when the event type is rare. The FAR results also correspond with the POD results, especially the low FAR for No-Cloud events in summer and fall that is associated with a high POD of 95%. The results shown in Figures 12–16 suggest that WWMCA did better in persistent, or common, cloud cover conditions—for example, better in analyzing Definite-Cloud events in winter and spring when those events were common, and better in analyzing No-Cloud events in summer and fall when those events were common.

Figure 16.   WWMCA false alarm ratios for WWMCA Box 22 for all three cloud cover events: Definite-Cloud (blue), Probable-Cloud (red), and No-Cloud (green). The top panel shows the results for daytime data, the middle panel for nighttime data, and the bottom panel for both daytime and nighttime data. Results based on using a Cloudsat cloud mask value of 30 for the cloud/no-cloud threshold.

The WWMCA PC results for Box 22 are shown in Figure 17. The three cloud cover events had similar performance, with better performance in the summer and fall than winter and spring. Day and nighttime PC were within approximately 15% of each

42

other throughout the year. Overall, the PC results for Definite-Cloud events were a little better than for No-Cloud events. The PC results are consistent with the POD and FAR results in indicating that WWMCA did well in persistent conditions.

Figure 17. WWMCA proportion correct (PC) for WWMCA Box 22 for all three cloud cover events: Definite-Cloud (blue), Probable-Cloud (red), and No-Cloud (green). The top panel shows the results for daytime data, the middle panel for nighttime data, and the bottom panel for both daytime and nighttime data. Results based on using a Cloudsat cloud mask value of 30 for the cloud/no-cloud threshold.

The PC performance metrics gives equal credit for hits and correct rejections (Chapter II, Section F.4; Wilks 2006). Thus, we also calculated the threat score (TS) to focus the performance analysis on the hits. The TS results for Box 22 are shown in Figure 18 and reveal uniformly better No-Cloud performance than Definite-Cloud performance, with the best performance being for No-Cloud in the summer and fall (about 85%). Daytime TS for no-cloud was about 68% in winter and spring and increased to about 85% in summer and fall; TS for definite cloud was about 50% in winter and spring and decreased to 45% in summer and 34% in fall. Nighttime TS for no-cloud was about 65% in winter and spring and increased to 87% in summer and fall; definite cloud was 52% in winter and spring and increased to about 42% in summer and fall. The high TS for No-Cloud during summer and fall is consistent with the POD of 95% (Figure 15) and the low FAR of 10% (Figure 16). The higher TS for Definite-Cloud events in winter and spring are related to Definite-Cloud events having been relatively common in those months (Figure 14). Taken together, these results support the idea that WWMCA performs:

1.   better when cloud conditions that are relatively persistent and/or common

2.   worse when analyzing cloud conditions that are relatively variable (spatially, temporally) and/or uncommon.

Figure 18. WWMCA threat scores (TS) for WWMCA Box 22 for all three cloud cover events: Definite-Cloud (blue), Probable-Cloud (red), and No-Cloud (green). The top panel shows the results for daytime data, the middle panel for nighttime data, and the bottom panel for both daytime and nighttime data. Results based on using a Cloudsat cloud mask value of 30 for the cloud/no-cloud threshold.

Figure 19 shows the bias (B) and indicates that No-Cloud events were over analyzed in winter, spring, and fall, and were mostly unbiased in summer. Definite-Cloud events were consistently under analyzed, especially in the fall, with the exception of summer when the analysis of Definite-Cloud events was mostly unbiased. These results are consistent with the findings of the UCAR (2008) and AER (2010) studies. There is a larger bias for daytime Definite-Cloud and No-Cloud events in winter and fall, as opposed to spring and summer, and there is a generally lower bias for Definite-Cloud events at night. These results are also consistent with the results shown in Figures 15–18 For example, the over (under) analysis of No-Cloud (Definite-Cloud) in October is consistent with the high (low) POD in that month.

Figure 19.   WWMCA bias (B) for WWMCA Box 22 for all three cloud cover events: Definite-Cloud (blue), Probable-Cloud (red), and No-Cloud (green). The top panel shows the results for daytime data, the middle panel for nighttime data, and the bottom panel for both daytime and nighttime data. The heavy dark line at B = 1 indicates an unbiased analysis. Values greater (less) than 1 indicate a cloud cover event that was over (under) analyzed. Results based on using a Cloudsat cloud mask value of 30 for the cloud/no-cloud threshold.

The Heidke skill scores are shown in Figure 20 and show relatively little difference between the months or between day and night. The highest skill scores were associated with No-Cloud, ranging from about 50% in January night to 65% in October night. The HSS results for Definite-Cloud events are similar to but somewhat less than those for No-Cloud events. As with the other performance metrics, the poorest performance for Definite-Cloud events is in October. The HSS for Probable-Cloud events are considerably lower than for the other two events, ranging from 8% to 13% throughout the year. The HSS results are consistent with the POD, FAR, PC, and TS results. However, it is interesting to note that HSS shows relatively small differences in July and October between No-Cloud and Definite-Cloud, unlike the case, in general, for POD, FAR, and TS. This may be because HSS gives more (less) credit for good performance in analyzing uncommon (common) events—and in July and October; Definite-Cloud (No-Cloud) events were uncommon (common) (see Figure 14).

Figure 20.   WWMCA Heidke skill score (HSS) for WWMCA Box 22 for all three cloud
              cover events: Definite-Cloud (blue), Probable-Cloud (red), and No-Cloud
              (green). The top panel shows the results for daytime data, the middle panel
              for nighttime data, and the bottom panel for both daytime and nighttime data.
                    The heavy dark line at the zero value indicates that the WWMCA is
              equivalent to reference analyses (random analyses statistically independent of
              observations). A perfect WWMCA cloud analysis would have a value of one.
              Negative values indicate WWMCA performs worse than reference analyses.
              Results based on using a Cloudsat cloud mask value of 30 for the cloud/no-
                                            cloud threshold.

C.   WWMCA BOX 29

For Box 29, we analyzed points north of 70° N as being in polar night during all of January and all of April, and in polar day during all of July and all of October. This is an incorrect way to analyze the April and October data that arose due to an error in the analysis coding. Thus, for the April and October results, readers should focus their attention on just the All Day results.

Figures 21 and 22 show the number of occurrences of hits (A), false alarms (B), misses (C), and correct rejections (D) for each cloud cover event, and Figure 23 shows the marginal distribution of the cloud events, for the four months. Note that there was a more even distribution of the three cloud event types for Box 29 (Figures 21 and 22) than for Box 22 (Figures 12 and 13). In particular, the marginal distribution of cloud events for WWMCA and Cloudsat (Figure 23) show that neither Definite-cloud nor No-Cloud events dominated in 2010 in Box 29 as opposed to Box 22. Thus, Box 29 in 2010 represented more mixed and variable cloud conditions than did Box 22 in 2010. Box 29 for 2010 may also have presented WWMCA with a more challenging analysis problem than did Box 22, since Box 29 showed less persistence of any one cloud event type. Note too that WWMCA understated the percentage of Definite-Cloud events, and overstated the number of No-Cloud events, except during July (Figure 23). WWMCA also overstated the percentage of Probable-Cloud events in all months.
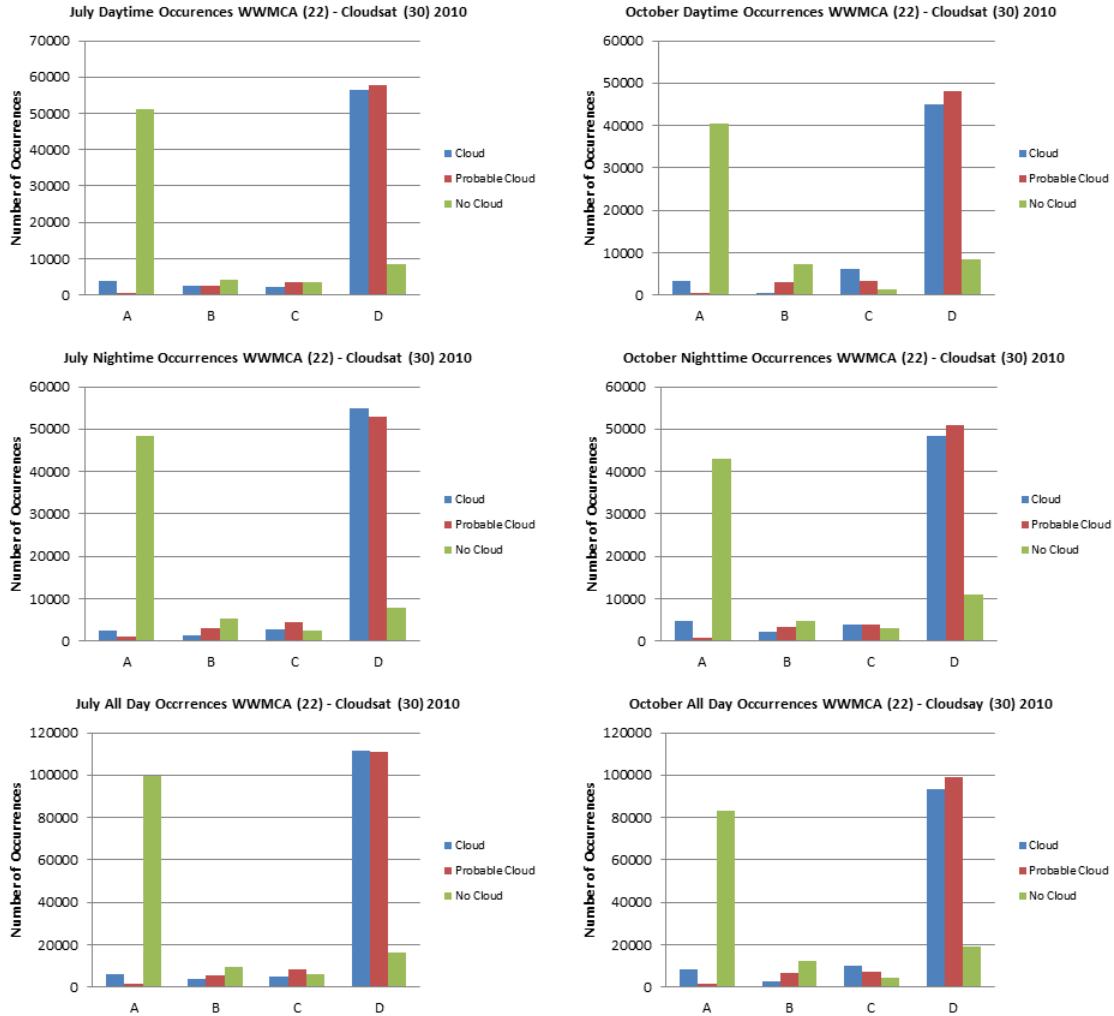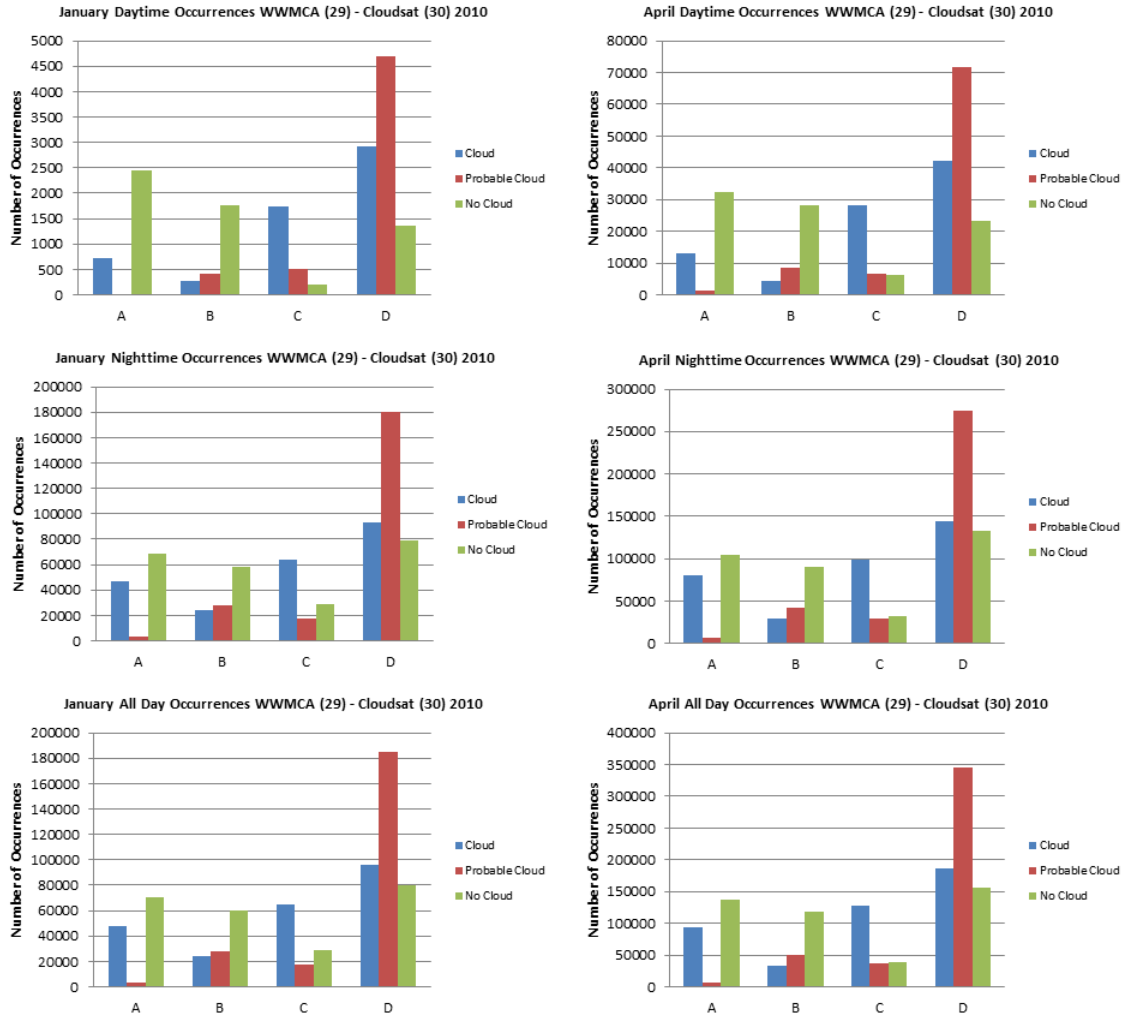
Figure 21.   Number of 2 x 2 contingency table occurrences in January and April 2010 for WWMCA Box 29 for all three cloud cover events: Definite-Cloud (blue), Probable-Cloud (red), and No-Cloud (green). On the horizontal axes: A indicates Hits, B indicates False Alarms, C indicates Misses, and D indicates Correct Rejections. The top panels shows the daytime occurrences, the middle panels shows the nighttime occurrences, and the bottom panels show the results for both daytime and nighttime occurrences. Results based on using a Cloudsat cloud mask value of 30 for the cloud/no-cloud threshold.

51
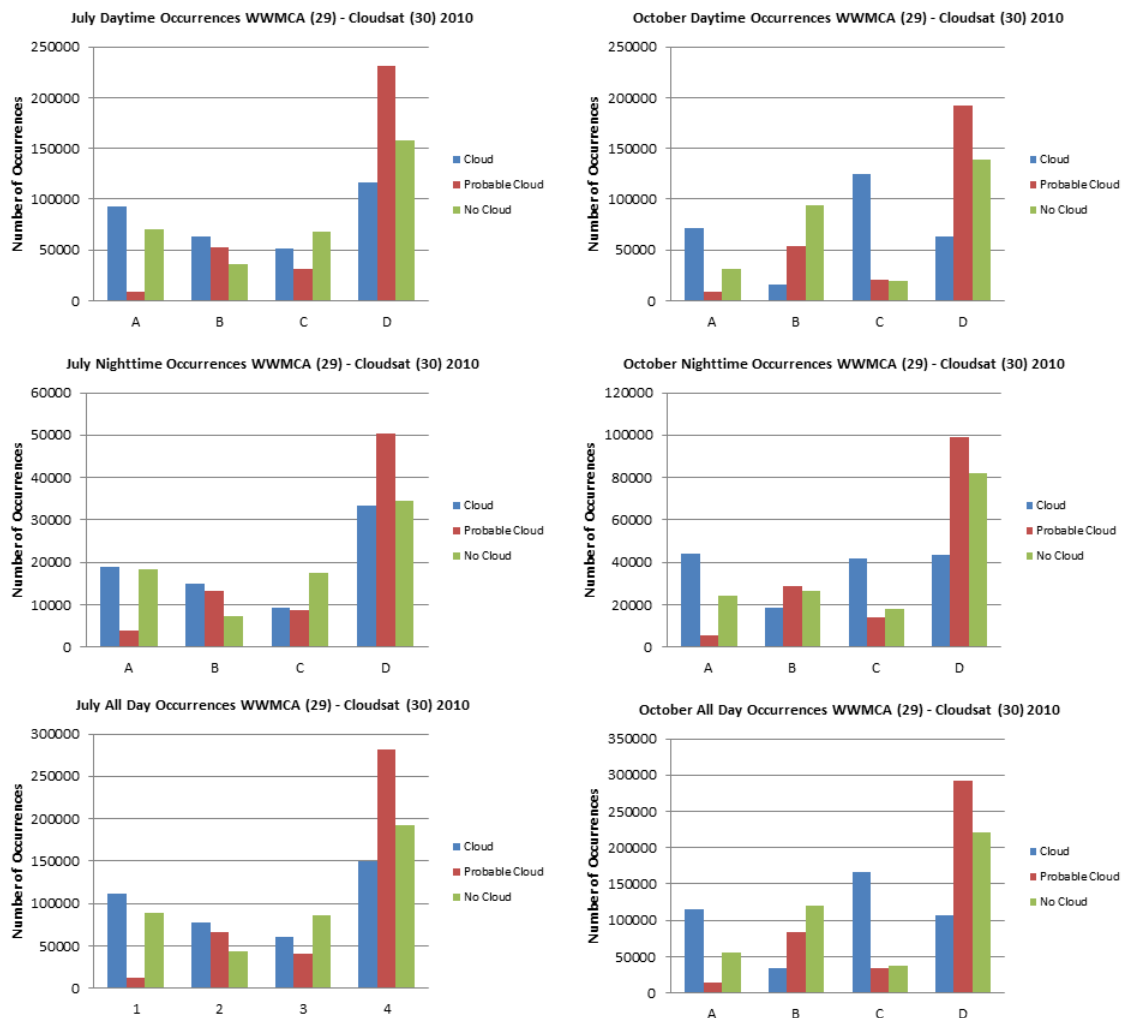
Figure 22.   Number of 2 x 2 contingency table occurrences in July and October 2010 for WWMCA Box 29 for all three cloud cover events: Definite-Cloud (blue), Probable-Cloud (red), and No-Cloud (green). On the horizontal axes: A indicates Hits, B indicates False Alarms, C indicates Misses, and D indicates Correct Rejections. The top panels shows the daytime occurrences, the middle panels shows the nighttime occurrences, and the bottom panels show the results for both daytime and nighttime occurrences. Results based on using a Cloudsat cloud mask value of 30 for the cloud/no-cloud threshold.
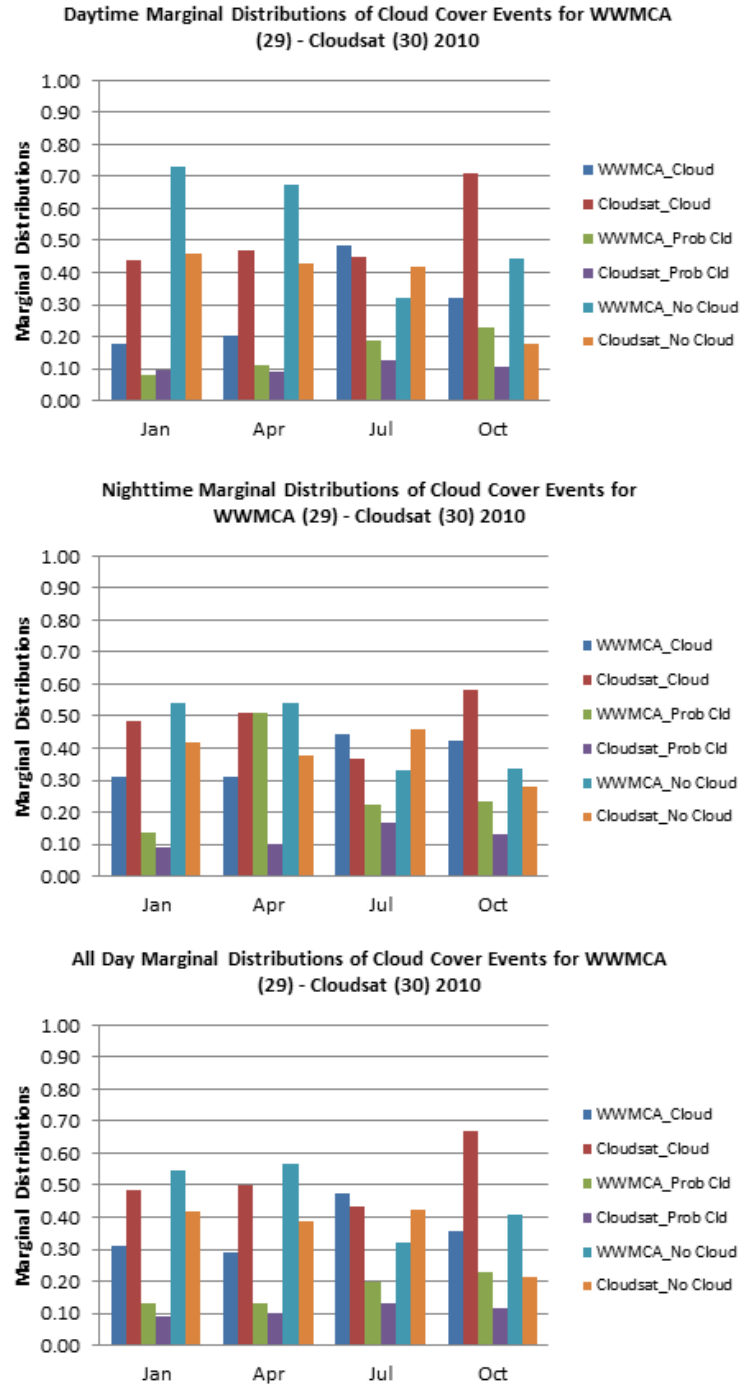
Figure 23.   Marginal distributions of cloud cover events for WWMCA and Cloudsat for WWMCA Box 29: Definite-Cloud, Probable-Cloud, and No-Cloud). The calculation of the marginal distributions is shown in Table 7. The top panel shows the results for daytime data, the middle panel for nighttime data, and the bottom panel for both daytime and nighttime data. Results based on using a Cloudsat cloud mask value of 30 for the cloud/no-cloud threshold.

The POD for the cloud cover events are shown in Figure 24. Note that the All Day results show PODs for: (1) No-Cloud events were 71–78% in winter and spring, but 51–60% in summer and fall; (2) Definite-Cloud events were 42% in winter and spring, 64% in summer, and 41% in fall; and (3) Probable-Cloud events were 15%–29%, with an increasing trend throughout the year. These POD results were considerably lower than those for Box 22 (Figure 15). The Definite-Cloud results are also lower than the 64% POD for cloud reported in UCAR (2008).
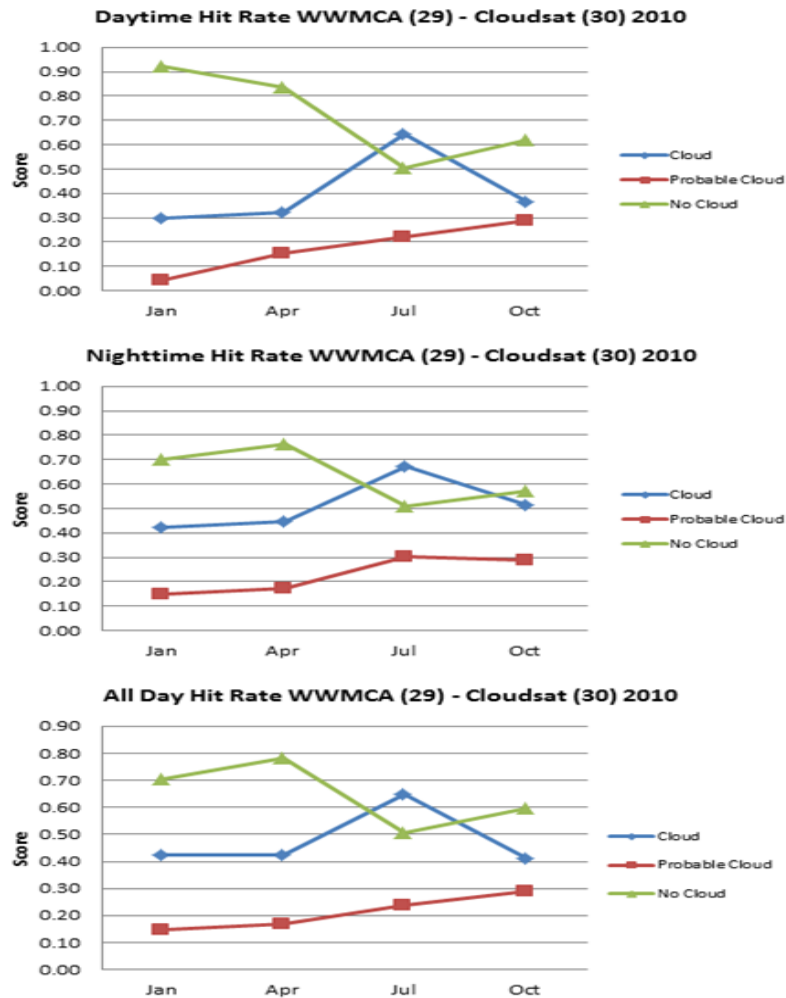
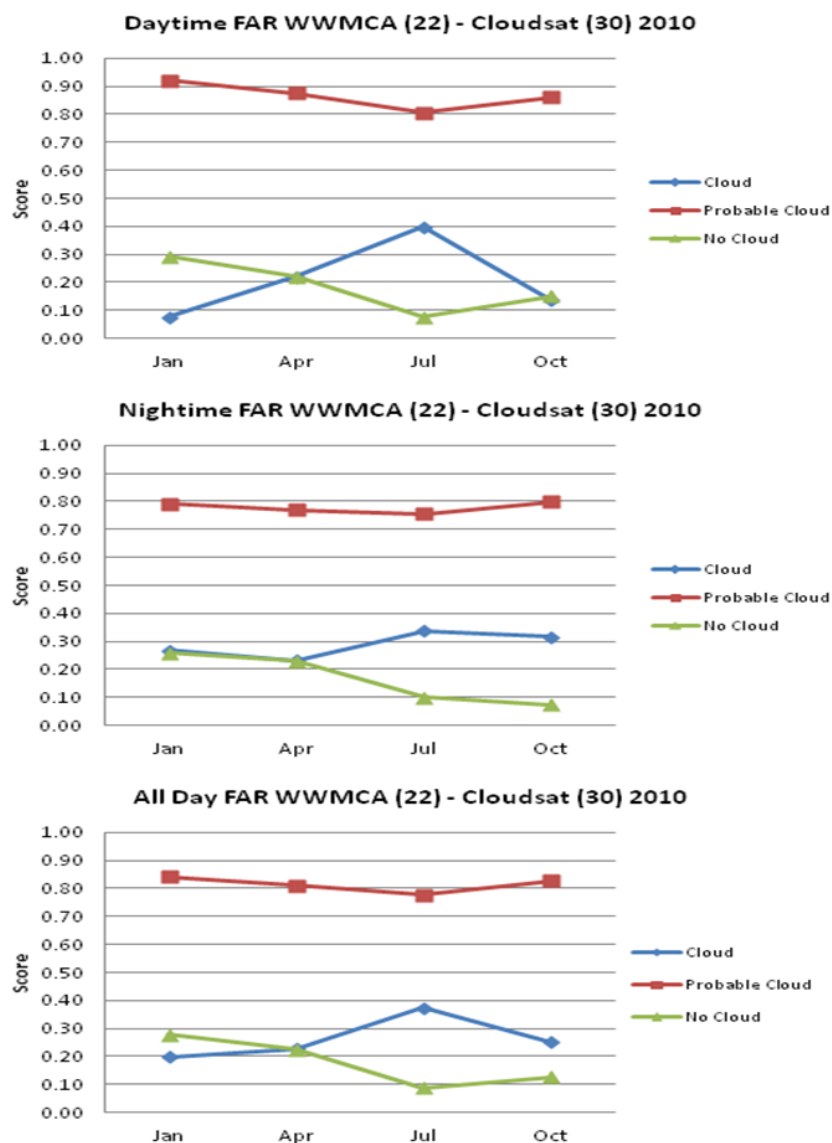Figure 24.   WWMCA probability of detection (POD), or hit rate (H), for WWMCA Box 29 for all three cloud cover events: Definite-Cloud (blue), Probable-Cloud (red), and No-Cloud (green). The top panel shows the results for daytime data, the middle panel for nighttime data, and the bottom panel for both daytime and nighttime data. Results based on using a Cloudsat cloud mask value of 30 for the cloud/no-cloud threshold.

Figure 25 show that Definite-Cloud events had an All Day FAR of about 22% to 34% throughout the year, except for summer when the FAR was 41%. This summer increase in FAR is consistent with Figure 23, which shows the marginal distribution of WWMCA exceeded the marginal distribution of Cloudsat in July. The All Day FAR for No-Cloud events ranged from 33% to 46% throughout the year, except in October when it increased to 69%. Note that Figure 23 shows that the WWMCA No-Cloud marginal distribution was double that of Cloudsat in October. Note that the FAR values for Box 29 were considerably higher than for Box 22 (Figure 16).
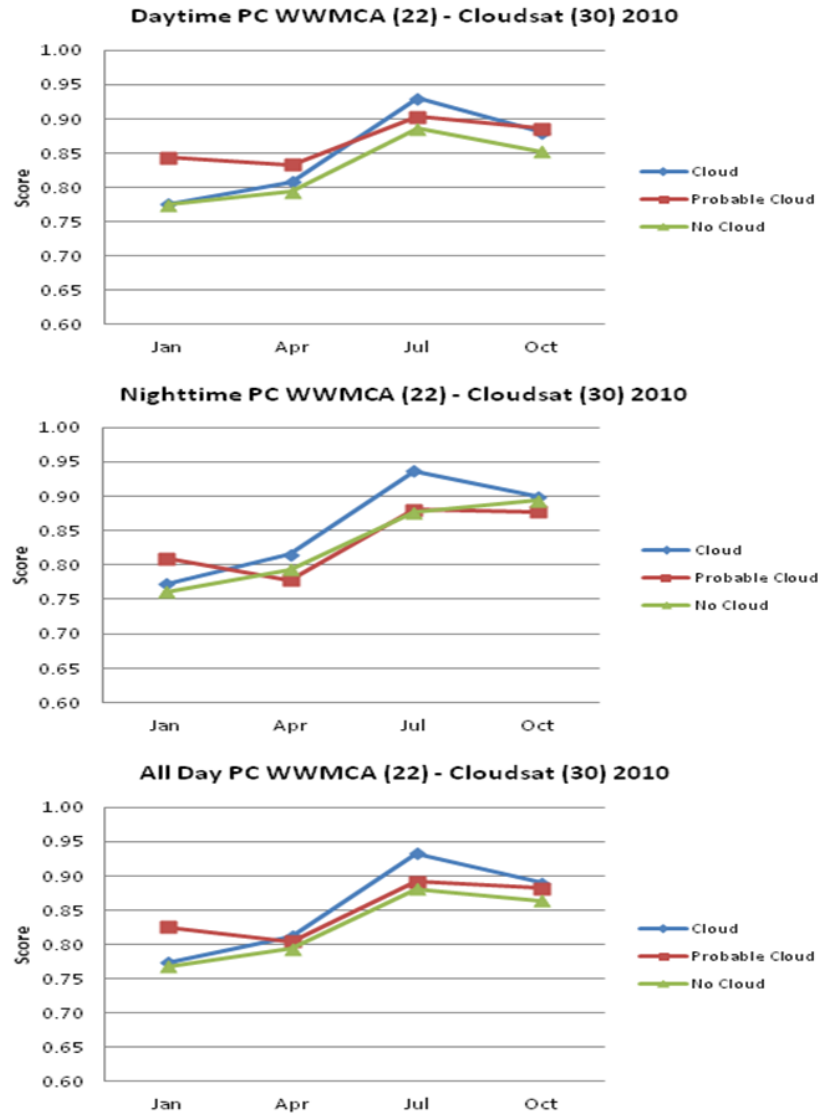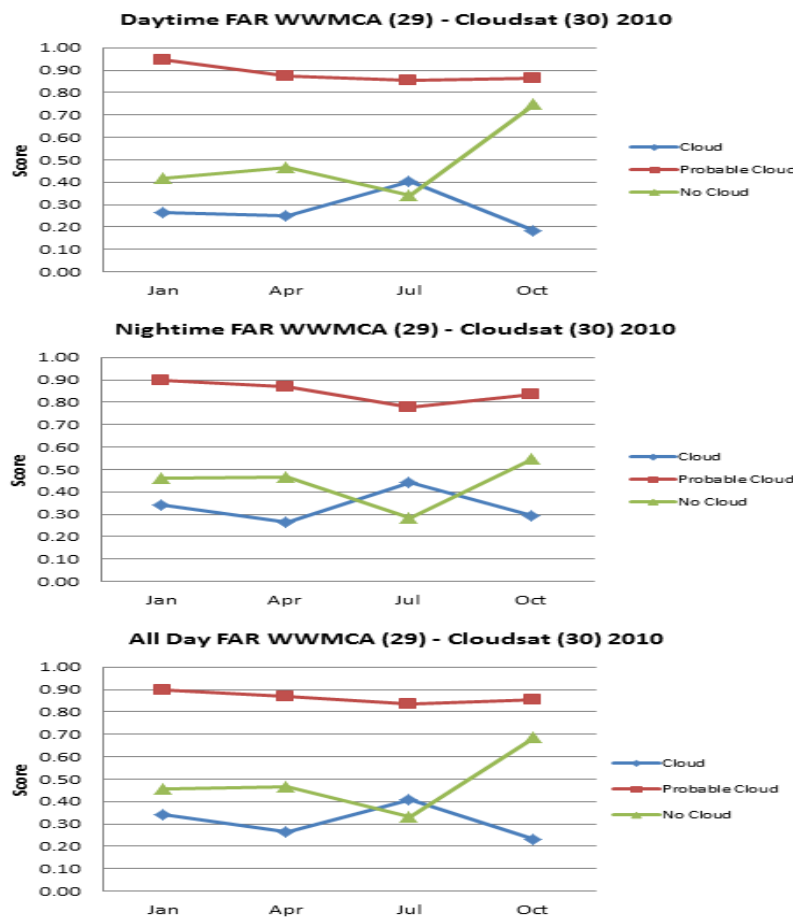

Figure 25.   WWMCA false alarm ratios for WWMCA Box 29 for all three cloud cover events: Definite-Cloud (blue), Probable-Cloud (red), and No-Cloud (green). The top panel shows the results for daytime data, the middle panel for nighttime data, and the bottom panel for both daytime and nighttime data. Results based on using a Cloudsat cloud mask value of 30 for the cloud/no-cloud threshold.

The WWMCA PC results for Box 29 are shown in Figure 26. The All Day Definite-Cloud and No-Cloud events had similar scores, about 64%, throughout the year, although Definite-Cloud decreased to 53% in fall. The lower PC for Definite-Cloud in October is consistent with the lower Definite-Cloud POD values in October (Figure 24).
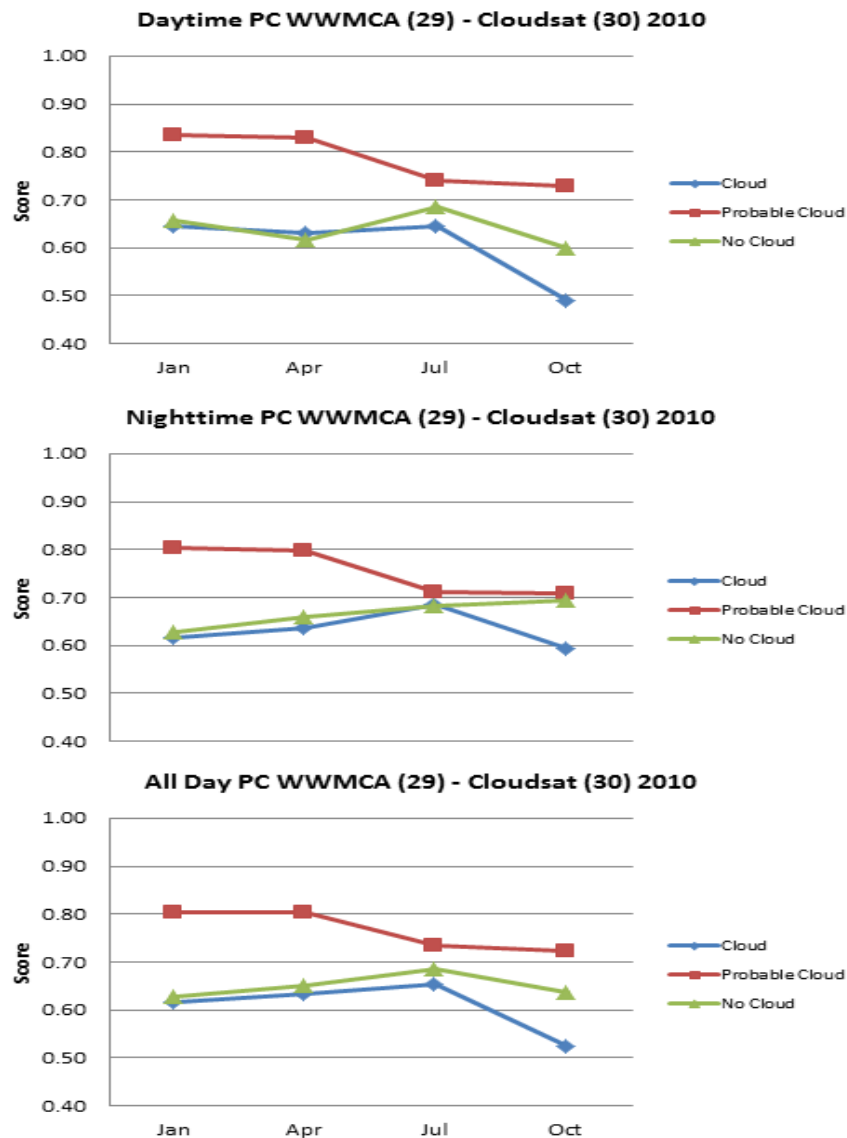
Figure 26.   WWMCA proportion correct (PC) for WWMCA Box 29 for all three cloud cover events: Definite-Cloud (blue), Probable-Cloud (red), and No-Cloud (green). The top panel shows the results for daytime data, the middle panel for nighttime data, and the bottom panel for both daytime and nighttime data. Results based on using a Cloudsat cloud mask value of 30 for the cloud/no-cloud threshold.

The TS results for Box 29 are shown in Figure 27 and reveal similar No-Cloud and Definite-Cloud performance. All Day No-Cloud TS was slightly better in winter spring and All Day Definite-Cloud TS was slightly better in summer and fall. Box 29 had considerably lower TS scores than Box 22 (Figure 18), which is consistent with the lower POD (Figure 24) and higher FAR (Figure 25) for Box 29. These results suggest that WWMCA performance is worse when there is relatively high variability and low persistence in the cloud event types (Figures 21–27 for Box 29) and better when there is relatively low variability or high persistence (Figures 12–20 for Box 22).
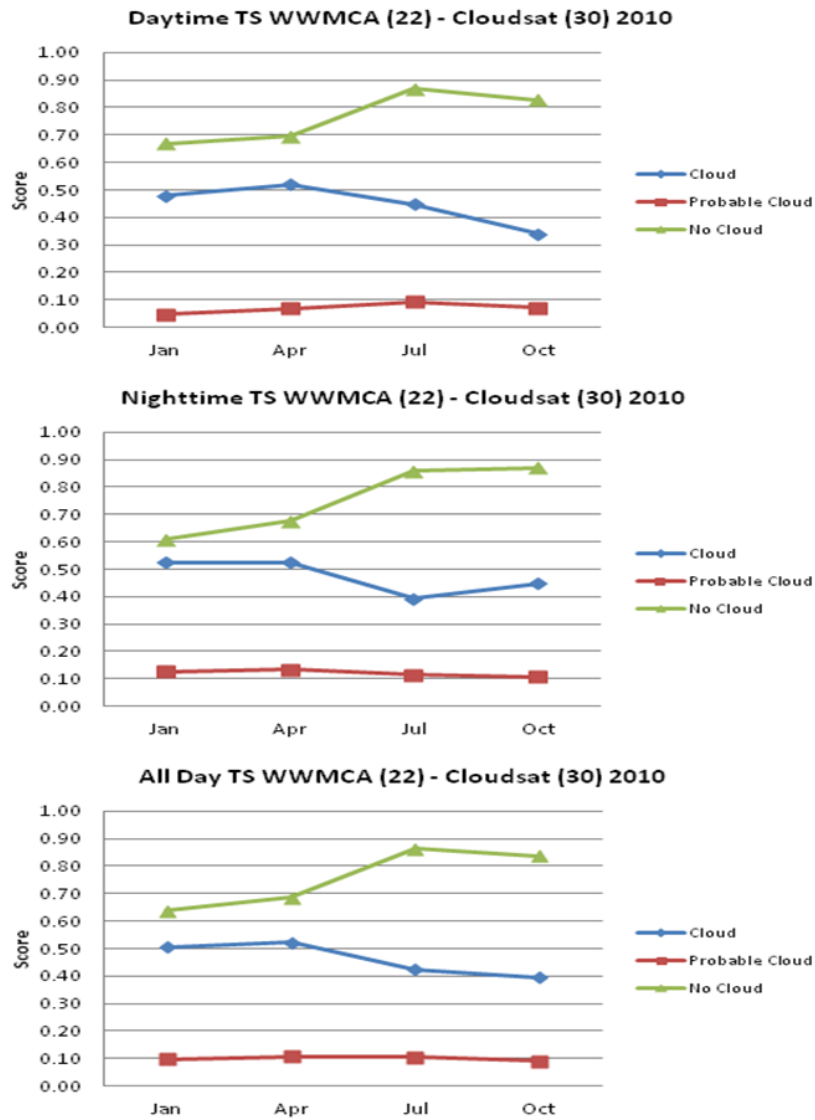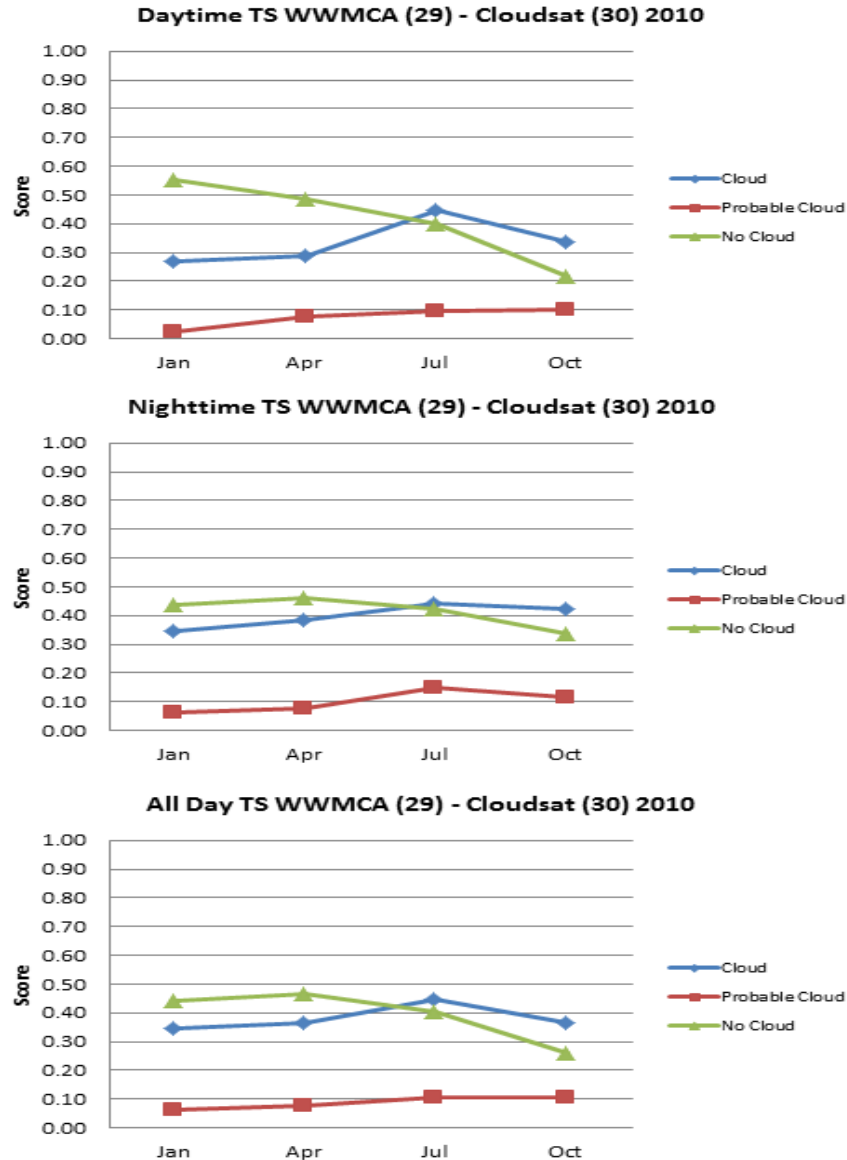
Figure 27. WWMCA threat scores (TS) for WWMCA Box 29 for all three cloud cover events: Definite-Cloud (blue), Probable-Cloud (red), and No-Cloud (green). The top panel shows the results for daytime data, the middle panel for nighttime data, and the bottom panel for both daytime and nighttime data. Results based on using a Cloudsat cloud mask value of 30 for the cloud/no-cloud threshold.

Figure 28 shows the bias (B) results for Box 29. Definite-Cloud (No-Cloud) events were substantially under-analyzed (over analyzed) in winter, spring and fall, consistent with the marginal distribution results (Figure 23). The four month average All

Day Definite-Cloud (No-Cloud) bias was approximately 1.5 (-0.6). The overall patterns in Figure 28 are similar to those for Box 22 (Figure 19) but with larger bias magnitudes than for Box 22.
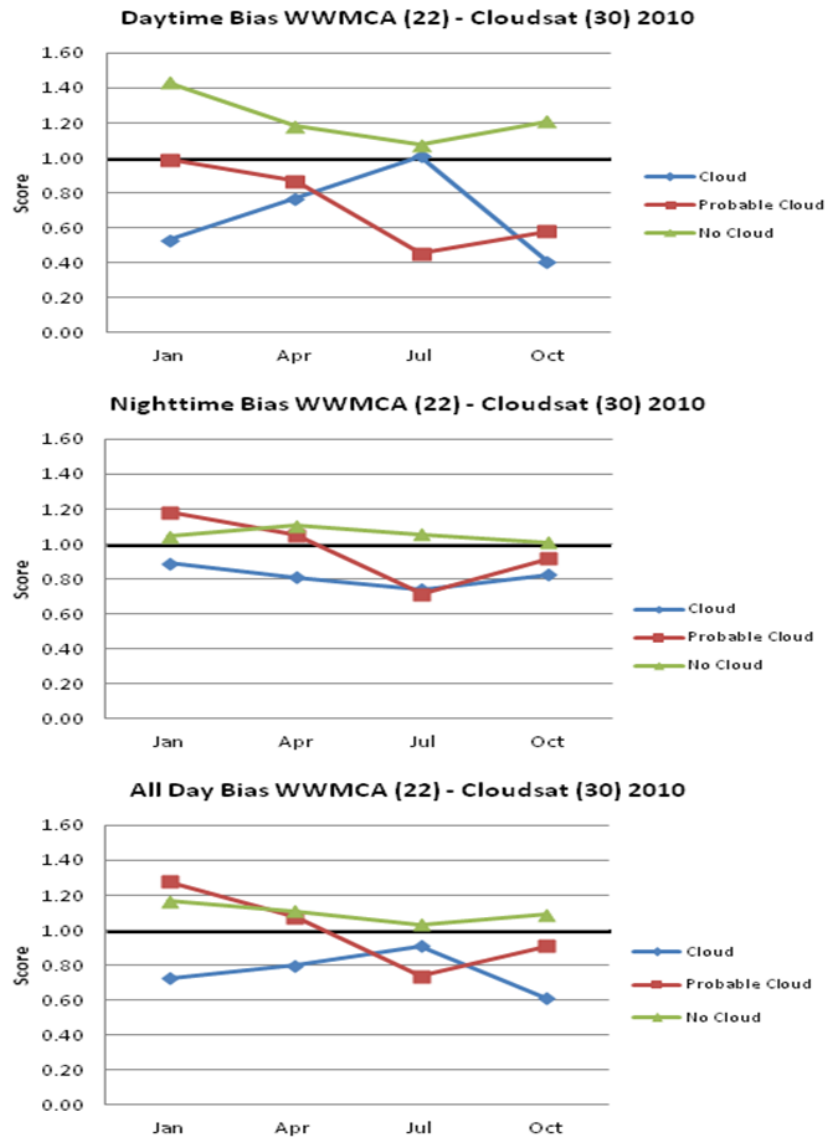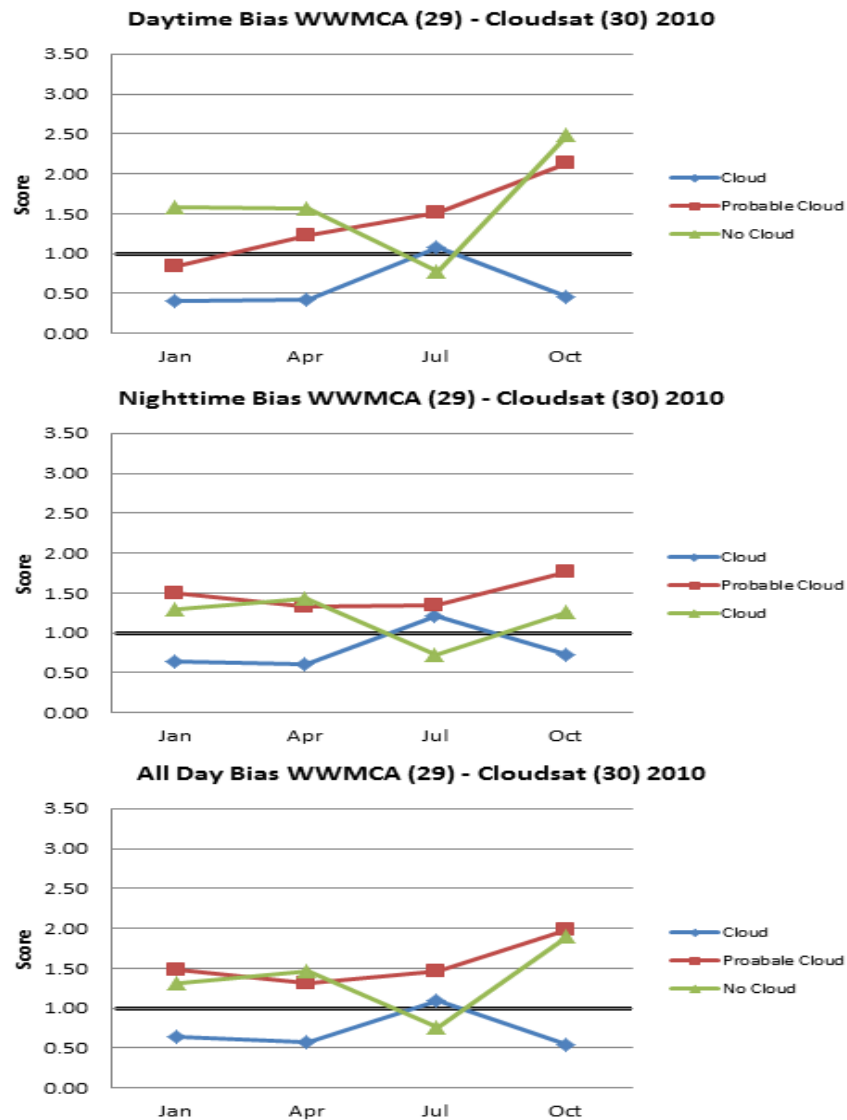

Figure 28. WWMCA bias (B) for WWMCA Box 29 for all three cloud cover events: Definite-Cloud (blue), Probable-Cloud (red), and No-Cloud (green). The top panel shows the results for daytime data, the middle panel for nighttime data, and the bottom panel for both daytime and nighttime data. The heavy dark line at B = 1 indicates an unbiased analysis. Values greater (less) than 1 indicate a cloud cover event that was over (under) analyzed. Results based on using a Cloudsat cloud mask value of 30 for the cloud/no-cloud threshold.

The Heidke skill scores for Box 29 are shown in Figure 29 and are similar for day and night, and for all months. The HSS values are in the 11% to 32% range for Definite-Cloud and No-Cloud, and -4% to 9% range for Probable-Cloud. These relatively low HSS values, compared to Box 22, are consistent with the lower POD, PC, TS and the higher FAR for Box 29 than for Box 22. Note that the Box 29 HSS values show relatively small differences through the year between No-Cloud and Definite-Cloud events, unlike the case, in general, for POD, FAR, and TS. Similar to Box 22, this may be because HSS gives more (less) credit for good performance in analyzing uncommon (common) events (Figure 23).

Positive HSS indicates skill above a random analysis (see Chapter II, Section F.4). However, HSS values that don't exceed 32% for Box 29 (Figure 29) or 65% for Box 22 (Figure 20) are problematic, given that WWMCA is a near real-time analysis (as opposed to a non-zero lead forecast) that is based on many real-time observational data sources. Unfortunately, there do not appear to be any other studies of WWMCA that have reported HSS results or other skill scores that compare WWMCA to a reference, or benchmark, analysis.
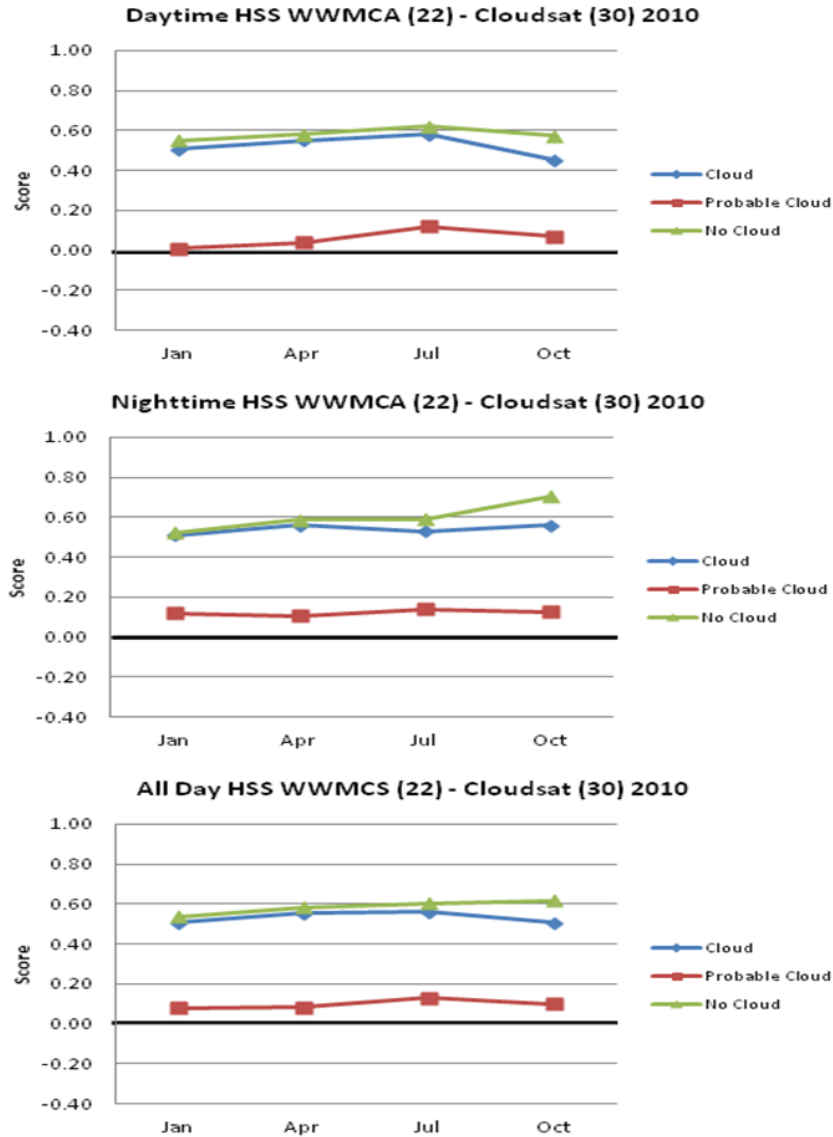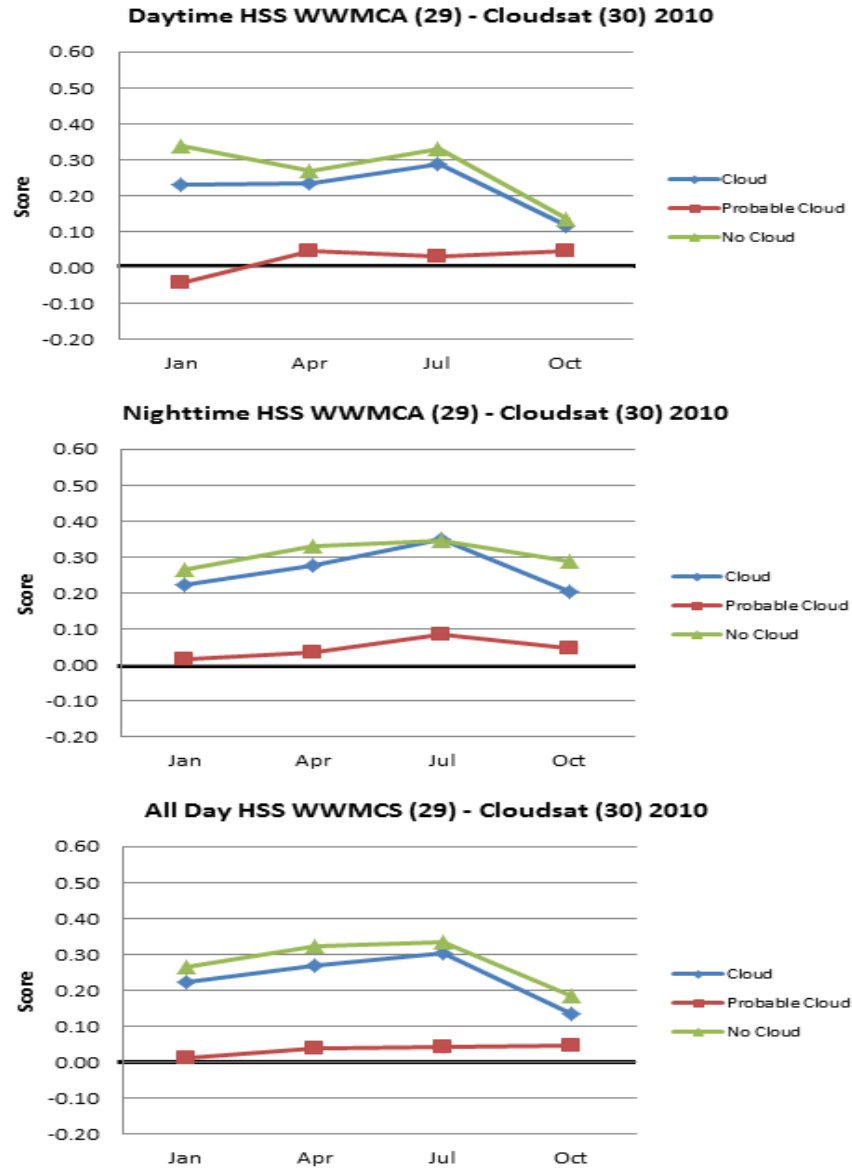
Figure 29. WWMCA Heidke skill score (HSS) for WWMCA Box 29 for all three cloud cover events: Definite-Cloud (blue), Probable-Cloud (red), and No-Cloud (green). The top panel shows the results for daytime data, the middle panel for nighttime data, and the bottom panel for both daytime and nighttime data. The heavy dark line at the zero value indicates that the WWMCA is equivalent to reference analyses (random analyses statistically independent of observations). A perfect WWMCA cloud analysis would have a value of one. Negative values indicate WWMCA performs worse than reference analyses. Results based on using a Cloudsat cloud mask value of 30 for the cloud/no-cloud threshold.

D.   SUMMARY OF RESULTS

The results show that WWMCA performance was: (1) better for the southwest Asia region where there was more persistence in cloud cover events (especially No-Cloud events); and (2) worse for the western Russia – Barents Sea region where there was more variability in cloud cover events. This makes some sense, because persistent conditions tend to be easier to analyze. The marginal distribution and HSS results provide a good summary of how differences in performance were associated with differences in cloud cover event persistence. The relatively good performance for the southwest Asia region may be due to the relatively clear skies that are typical of that region, and that characterized the region during much of 2010, especially in summer and fall. Another factor that may have led to the relatively low performance for the western Russia – Barents Sea region may be the higher pixel ages for the higher latitudes in which polar orbiting satellites are a main source of cloud information for WWMCA (see Chapters II and IV for more on this topic).

There were also notable differences in the results for the different months, and for day and night (e.g., in the All Day POD and HSS results for Box 29, and in the Box 22 bias results for day and night).

Overall, the WWMCA performance results appear to be at least somewhat problematic, since: (1) WWMCA products are near real-time analyses based on many near real-time observational data sources; and (2) WWMCA is used to initialize cloud forecast models that are used in IC planning.

IV. SUMMARY, CONCLUSIONS AND RECOMMENDATIONS

A. SUMMARY

We conducted a verification of the WWMCA cloud analysis product generated by CDFS II that is used in the planning of overhead imagery collection. Our independent verification data source was data from the Cloudsat atmospheric sounder, a satellite-borne radar system designed to sense condensed cloud particles. We looked at the cloud analyses of two WWMCA boxes that are of high interest to the national intelligence community and that differ in their meteorological characteristics. One box was centered in western Russia and the nearby polar region, and the other box was in the mid-latitudes and contained mountain, desert, ocean, and coastal regions. We analyzed one year of data for these two WWMCA boxes to test a system for routinely monitoring WWMCA performance.

Our goal was to analyze the performance of WWMCA for a range of cloud cover events, times, and locations, and using a range of performance metrics. To do so, we had to develop a method to match the data sets and to ensure an adequate amount of ground truth measurements fell within each WWMCA cell to confidently verify that cell's cloud analysis. The WWMCA data set we used was provided by the 16th Weather Squadron. The Cloudsat data was downloaded from the Cloudsat Data Processing Center website. After overcoming the differences in temporal and spatial resolutions of the data, we were able to calculate metrics that provide useful information about the performance of WWMCA.

B. CONCLUSIONS

Our performance metrics showed that WWMCA performed better under persistent cloud cover situations than more variable cloud situations. For instance, WWMCA had a high POD for No-Cloud events when there were persistently few clouds. For mid- and high latitudes, Definite-Cloud events were under analyzed and No-Cloud events were over analyzed, except for the summer when both events were unbiased. The

Heidke skill scores for mid-latitude cloud analyses were considerably higher than those for high latitude cloud analyses—for example, high HSS values in the mid-latitudes of about 60% versus about 30% for the high latitudes. Performance in analyzing Probable-Cloud events was especially poor in both regions. For example: (1) HSS for Probable-Cloud events ranged between -5% and 15% in both mid- and high-latitudes; and (2) the Heidke Skill Scores were less than 14% for Boxes 22 and 29 year round.

The better performance of WWMCA in the mid-latitudes could be accounted for by the higher temporal resolution of the geostationary satellites that provide the majority of the observations at those latitudes (evident in the pixel ages listed in Table 8). The mean pixel ages for Box 22 are 34–36 minutes and have a maximum standard deviation of 11 minutes. Conversely, the low temporal resolution of observational imagery from polar-orbiting satellites could explain why the high latitude cloud analyses had lower skill. The mean pixel ages for Box 29 are on the order of three hours and standard deviations are about two hours (Table 8).

Table 8.   Pixel age information for satellite observations used in the WWMCA development process. Means and standard deviations calculated from the pixel age data in the WWMCA data set. Negative minutes are due to a portion of the satellite imagery coming in after the :00/:30 time hack (Connor 2012, personal communication).

	Box 22				Box 29			
2010	Min Age	Max Age	Mean Age	Std. Dev.	Min Age	Max Age	Mean Age	Std. Dev.
Jan	16	154	34	7.8	24	503	156	109
Apr	12	138	35	9.5	22	626	166	117
Jul	14	138	36	11	21	613	177	115
Oct	-7	153	36	9.3	-3	497	171	121

We determined that WWMCA performance is relatively insensitive to reasonable choices of the Cloudsat cloud masking threshold (values between 20 and 30), as shown by a comparison of our results in Chapter III to those in Appendix C.

The WWMCA performance results that we developed are generally lower than to those reported in the available documentation for prior studies (e.g., UCAR (2008).

However, reports of performance results from prior studies are sparse (see Chapter I, Section C). In addition, we verified WWMCA performance for larger areas and a wider range of months than most prior studies, and we verified WWMCA using a wider range of metrics. The paper that summarized most of the findings of the prior studies, NGIS (2011), disclosed only the POD and not the FAR or other scores that might have been generated in those studies. Of course, determining performance based only on POD or any other single metrics, is very problematic (cf. Wilks 2006).

C.   RECOMMENDATIONS

Future analyses of WWMCA results and its operational impacts on imagery collection are necessary to truly assess its performance. We recommend that future studies expand on the regions, months, and years examined to evaluate the regional-scale, global-scale, and long-term performance of WWMCA. The analysis of many years of data would help address issues raised by unusual events, such as the record high temperatures and extensive wildfires in western Russia in summer 2010 (which may have had an impact on both Cloudsat observations and WWMCA analyses in 2010).

Our results raised the question: Is WWMCA more accurate when pixels ages are small? We recommend an analysis that attempts to answer that question by testing the sensitivity of WWMCA performance to pixel age, especially the performance at high latitudes.

A future study should test the sensitivity of our assumptions, as discussed at the end of Chapter II. For example, we recommend a future study to test the minimum Cloudsat pixels necessary to confidently represent a WWMCA cell. Recall in Chapter II that we assumed that a minimum of six Cloudsat pixels (25% coverage of a WWMCA cell) could adequately represent a WWMCA cell.

Future studies should use a more dynamic method for determining sunrise/ and sunset times method to flag the data as either day or night. Recall in Chapter II that we chose the mean monthly sunrise and sunset times or a point close to the center of a WWMCA box (Table 6) to represent that entire WWMCA box, and that for the polar

region ($\geq 70^{\circ}$ N), we flagged data as either polar night or polar day based on the season. These approximations were used to reduce the data processing time but also introduced some errors in assigning the time of day to the data that should be removed in future studies that focus on distinguishing day and night performance. Applying a sunrise/sunset library to the data matching stage, such as the one used in Selin (2011, personal communication) study, would help remove these errors.

We found that WWMCA performs better in persistent cloud cover situations—as indicated, for example, by our HSS results. We recommended that a future study compare the skill of WWMCA to that of persistent analysis to test the validity of this finding and to better assess WWMCA skill.

Additionally, we recommend an in-depth study that will exploit the methods developed in our study to analyze large amounts of WWMCA data and show the long-term performance of WWMCA. One benefit of such a study is that it would help determine the value added by past and future changes to CDFS II. This study should look at long time periods, various WWMCA boxes from both hemispheres, and a range of climate conditions (e.g., high and low cloud tops; high and low cloud variability; high and low cloud amounts; land, ocean, snow, ice, mountain, and desert surfaces; tropical, mid-latitude, and polar regions; etc.) to measure the overall and specific aspects of WWMCA performance.

The operational impacts of cloud analyses and forecasts are being tested in an ongoing study at NPS by Lieutenant Brian Moore (classified thesis expected to be published in September 2012, Figure 1). We recommend a review of his study when completed to gain insight into the operational significance of WWMCA in imagery collection.

For access to the data sets and computer coding used in this study, contact Dr. Tom Murphree in the Department of Meteorology at the Naval Postgraduate School (murphree@nps.edu).

"Who is wise enough to number all the clouds...?"

—Job 38.37

APPENDIX A. CLOUD DEPICTION FORECAST SYSTEM (CDFS) II PROCESSING LEVELS

Satellite and conventional observations (surface observations and upper air soundings) undergo a four level process to be merged into a global cloud analysis (Figure 30). Level one is data calibration, level two classifies each pixel into cloudy or clear, level three applies cloud layering and typing, and level four consists of merging the separate analyses into one global analysis (HQ AFWA/DNXM 2011).
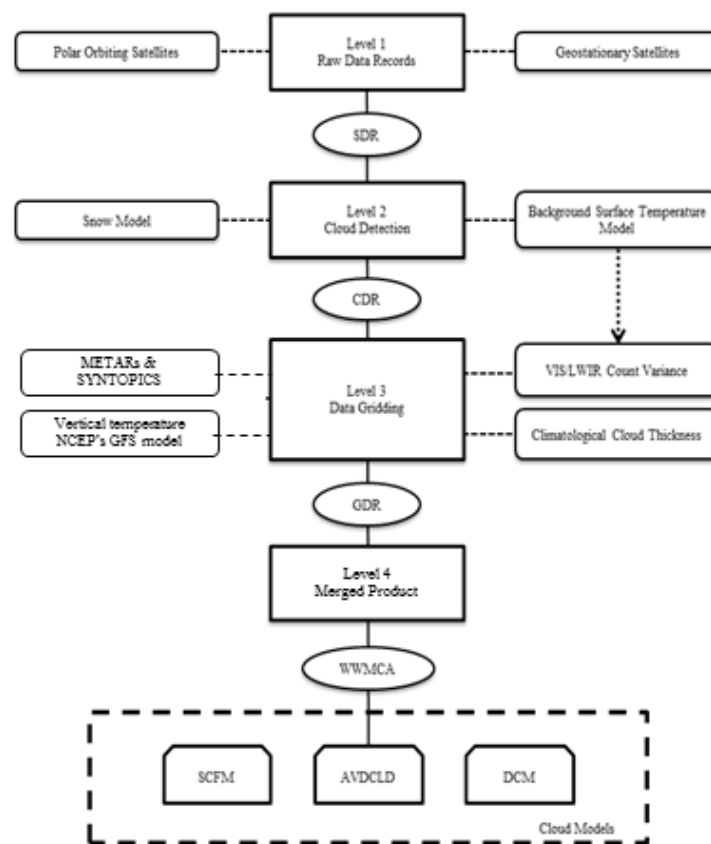
Figure 30.   Illustration of the four processing levels within Cloud Depiction Forecast System II. Observations are received from meteorological satellites, conventional observations, and global analysis from various models. These observations are merged into one global cloud analysis that is used to initiate cloud forecast models. Shapes are defined as: rectangles are processes; rounded rectangles are inputs; ovals are products; and snipe same side corner rectangles are cloud models.

A.   LEVEL 1

Level one processing consists of data ingestion and calibration.   Satellite telemetry transmissions are received by AFWA's Satellite Data Handling System located at Offutt Air Force Base in Nebraska. Downlinked satellite data is encoded and must be decoded.   The decoded data reveal physical parameters for radiance measurements received by the detectors on the sensor's focal plane array and are placed in the Sensor Data Records (SDR).   Satellite imagers' focal plane array consist of detectors that represent the pixels, which measure the radiance received from reflected or emitted energy within Earth's atmosphere. CDFS II use the data from the satellite's visible and infrared channels. A calibration step for the infrared data converts the measured emitted energy into either radiance or brightness temperature. Brightness temperature is the temperature of an object if it was radiating as a black body. The brightness temperature is the parameter required by CDFS II to make the analysis. Reflectance values are measured from the satellite's visible channels are used directly in the algorithms (HQ AFWA/DNXM 2011).

B.   LEVEL 2

Level two is where cloud detection occurs. Each sensor has its own tailored algorithms designed to optimize their instrument's ability to exploit measurements made in different channels in an attempt to distinguish cloud from clear scene. DMSP's Operational Line Scanner (OLS) sensor, has the highest spatial resolution, but only two broadband channels (one visible and one infrared), whereas, NOAA POES' Advanced Very-High Resolution Radiometer (AVHRR), have six narrowband channels (one visible, one near-infrared, and four infrared).   DMSP's OLS cloud detection is accomplished by comparing a pixel's brightness temperature to a cloud-free referenced pixel's brightness temperature.   If the pixel is determined to be cloud free, its brightness temperature is then used as the clear-scene brightness temperature for all other pixels in the frame. To determine a cloud-filled pixel, the observed brightness temperature of the said pixel is compared to the predicted clear-scene brightness temperature.   The difference in magnitude of brightness temperature determines if the pixel is cloud-filled

or cloudfree. A similar method is used for the visible channel when available. Threshold values are used to determine the cutoff between cloudy and clear pixel (HQ AFWA/DNMX 2011).

The algorithm for NOAA's AVHRR exploits the multispectral properties of the sensor to identify cloud or clear scene. The strength of the AVHRR is its six channels designs, which are listed in Table 9 with their respective wavelengths and typical use. Each channel differs in their sensitivity to reflectivity and emissivity properties of clouds and clear terrestrial surfaces. In addition to the sensors data, the algorithm uses clear-scene characterizations of the terrestrial background. The algorithm utilizes various techniques to include straight threshold type algorithms, inter-channel comparisons and spectral comparisons between the terrestrial surface and satellite data. A suite of twelve tests are used to characterize the different spectral characteristics of clouds and background surfaces to determine cloud-filled or clear scene. Each test is based on one or more specific spectral signatures that compare the radiance measurement of one or more channels, and fall into either cloud tests or background tests categories (HQ AFWA/DNXM 2011).

Table 9.   The channels below are from the AVHRR/3 sensor. The AVHRR is a
            radiation-detection imager that can be used for remotely determining cloud
            cover and the surface temperature. Note that the term *surface* can mean the
            surface of the Earth, the upper surfaces of clouds, or the surface of a body of
            water. This scanning radiometer uses 6 detectors that collect different bands
            of radiation wavelengths as shown below. Measuring the same view, this
            array of diverse wavelengths, after processing, permits multi spectral analysis
            for more precisely defining hydrologic, oceanographic, and meteorological
            parameters. Comparison of data from two channels is often used to observe
            features or measure various environmental parameters. The three channels
            operating entirely within the infrared band are used to detect the heat
            radiation from and hence, the temperature of land, water, sea surfaces, and
            the clouds above them. Table based from
                                    NOAASIS (2011).

Channel number	Resolution at nadir (km)	Wavelength (μm)	Typical use
1	1.09	0.58-0.68	Daytime cloud and surface mapping
2	1.09	0.725-1.00	Land-water boundaries
3a	1.09	1.58-1.64	Snow and ice detection
3b	1.09	3.55-3.93	Night cloud mapping, sea surface temperature
4	1.09	10.30-11.30	Night cloud mapping, sea surface temperature
5	1.09	11.50-12.50	Sea surface temperature

There are nine cloud tests and three background tests, which are summarized in Table 10. Different tests are used to identify clouds under different conditions. The low clouds and fog test for solar-illuminated data is used to identify water droplets based low-level cloud when the scene is illuminated by sunlight, and the non-illuminated test is used during nighttime. Since no one test will identify all the clouds in a scene, the cloud tests must be used in combination to accurately identify all cloud-filled pixels.   The background tests are unique to the AVHRR algorithm, which exploits the multispectral characteristics of AVHRR data, to identify snow and ice, desert and sun glint backgrounds. These tests are essential because clouds and surface features often exhibit similar spectral signatures in the visible spectrum, however; a positive result from these tests does not automatic mean a cloudfree pixel. These tests identify suspected visible data; the infrared cloud tests must still be applied to determine a cloud-filled pixel (HQ AFWA/DNXM 2011).

Table 10.   Cloud analysis test for the NOAA AVHRR level 2 algorithm. Table from HQ AFWA/DNXM (2011).

Test Type	Test Name	Major Identifying Class	Visible Data	IR Data
Cloud	Low cloud and fog test for solar-illumination data	Solar-illumination liquid water cloud		X
	Precipitation cloud test	Cumulonimbus	X	X
	Thin cirrus cloud test for solar-illumination data	Solar-illumination ice cloud	X	X
	Visible brightness ratio	Solar-illuminated liquid water cloud	X	
	Single channel visible brightness test	Solar-illuminated liquid water cloud	X	
	Cold cloud test	Mid- to high-level optically thick water and ice cloud		X
	Cirrus cloud test	High-level ice cloud		X
	Fog, low stratus test for non-solar-illuminated data	Non-solar-illuminated liquid water cloud		X
	Thin cirrus cloud for non-solar-illuminated data	Non-solar-illuminated ice cloud		X
Background	Sun glint background test	Water surfaces exhibiting specular reflection	X	X
	Desert background test	Highly reflective non-vegetated land surfaces	X	X
	Snow/ice cover background test	Highly reflective snow or ice covered land and water surfaces	X	X

There are three algorithms used to detection clouds from geostationary satellite data. Geostationary satellites have a high temporal resolution but the spatial resolution is degraded due to its altitude (~36,000 km). The first algorithm takes advantage of the high temporal resolution to identify cloud-filled pixels by testing for rapid changes in brightness temperature and reflectance values in pixels representing the same geolocation. The pixels that exhibit changes in radiance values greater than the amount expected for clear scene from frame to frame are identified as cloud-filled. The second algorithm is a dynamic threshold algorithm that identifies cloud with similar characteristics. Cloud-filled pixels identified through the temporal difference algorithm are processed by the dynamic threshold algorithm. The dynamic threshold algorithm identifies maximum and minimum brightness temperatures or reflectance within a grid cell, which are used to define threshold values for cloud-filled and cloud-free pixels remaining within the grid cell.   The third algorithm uses a series of spectral discrimination tests similar to the OLS and AVHRR spectral tests. Not all geostationary satellite data are the same, so a different set of tests may need to be ran for each satellite system. For instance, METOSAT platforms have different spectral channels than GOES (HQ AFWA/DNXM 2011). Tables 11 and 12 summarize the spectral channels for

METEOSAT and GOES, respectively. The resultant dataset, generated for each satellite data source, is called Cloud Data Records (CDR).

Table 11.   Spectral channels and bandwidth for METEOSAT satellites. Table from EUMETSAT (2011).

Channel	Wavelength (µm)	Spatial Resolution at nadir (km)	Remarks
VIS 0.6	0.56-0.71	3	Similar to AVHRR
VIS 0.8	0.74-0.88	3	Similar to AVHRR
IR 1.6	1.50-1.78	3	Similar to AVHRR
IR 3.9	3.48-4.36	3	Similar to AVHRR
IR 8.7	8.30-9.10	3	New
IR 10.8	9.80-11.80	3	Similar to AVHRR
IR 12.0	11.00-13.00	3	Similar to AVHRR
WV 6.2	5.35-7.15	3	Water vapor channel
WV 7.3	6.85-7.85	3	Water vapor channel
IR 9.7	9.38-9.94	3	Ozone absorption channel as on HIRS
IR 13.4	12.40-14.40	3	CO_2 absorption channel as on GOES-VAS sounder
HRV	0.5-0.9	1	High Resolution Visible (HRV); Broadband visible channel

Table 12.   GOES imager channels. Table from GOES Imager Channel Notation (2011).

Channel number	Resolution at nadir or IFOV* (km)	Wavelength (µm)	Remarks
1	1	0.55-0.75	Visible
2	4	3.80-4.00	Shortwave Infrared
3	8	6.50-7.00	Moisture
4	4	10.20-11.20	Infrared 1
5	4	11.50-12.50	Infrared 2

* Instantaneous Field of View

C.   LEVEL 3

Level three is where the satellite pixels are gridded onto AFWA's standard Polar-stereographic grid at "16th mesh" with a horizontal resolution of 24 km (true at 60° latitude). Pixels are assembled into the 16th mesh grid cells by computing the coordinates that correspond to the latitude and longitude of each pixel (Hoke et al., 1981 Rev. March 1985). A detailed description of the Polar-stereographic grid is provided in Map Projections and Grid System for Meteorological Applications, *AFGWC Technical Notes 79/003* (Hoke et al., 1981 Rev. March 1985). The cloud layers are identified through the

Long Wave Infrared (LWIR) brightness temperature data contained within each grid cell. A clustering algorithm clusters pixels of similar brightness characteristics to identify potential layer separations. Statistical procedures are applied to the grid cell to limit the identified layers to four. Once the layers are identified, cloud top temperatures are compared against vertical temperature information from the Nation Centers for Environmental Prediction (NCEP) Global Forecast System (GFS) model to assign a cloud top height. The cloud top height and temperature information is used with the visible/LWIR-count variance, from the background surface temperature model employed in level two, to assign each layer to one of nine different cloud types listed in Table 13. Along with each derived cloud type is a climatological cloud thickness that is subtracted from the cloud top height to determine the cloud base height (HQ AFWA/DNXM 2011). At the end of level three, each satellite family (e.g., DMSP, NOAA, Geostationary) have a common gridded cloud mask that consists of cloud fraction up to four layers. The cloud masking also includes cloud type, and cloud top/base heights. These datasets are called Gridded Data Records (GDR).

Table 13.   WWMCA default cloud thickness according to height. Cloud thickness is based on climatology. Table from HQ AFWA/DNXM (2011).

Type Code	Cloud Type	Thickness (m)
1	Cumulonimbus (Cb)	6300
2	Strata (St)	600
3	Stratocumulus (Sc)	1800
4	Cumulus (Cu)	1200
5	Altostratus (As)	1200
6	Nimbostratus (Ns)	2100
7	Altocumulus (Ac)	1800
8	Cirrostratus (Cs)	1800
9	Cirrus (Ci)	900

Level three processing also includes hourly global surface and upper air based data, METARS or SYNTOPIC type formats, which contain fractional cloud coverage and cloud base heights from the World Meteorological Organization. These conventional observations are combined with the satellite data to determine the cloud mask, cloud type, and cloud top/base heights.

D.   LEVEL 4

Level four is where the satellite family GDRs and conventional surface observations are merged into a single global analysis of cloud cover information. One problem that arises in level four is that the independent gridded analyses have different valid times because the satellites input their data into CDFS II at different times. Each independent gridded analysis has strengths and weaknesses. For example, the polar-orbiters (DMSP and NOAA satellites) derived analyses have greater accuracy from the spatial resolution (polar satellites are in a lower orbit, ~800 km); however, the temporal resolution is course, usually passing over a particular region one or two times a day. Geostationary satellites analyses have a finer temporal resolution, every 30 minutes, but spatial resolution, or instantaneous field of view (IFOV), varies from 1 to 8 km depending on the channel. See the resolution at nadir column in Table 12 for each channel's IFOV. The timeliness and accuracy of the observations is a major concern when merging the data into a one global analysis (HQ AFWA/DNXM 2011).

Integration of total cloud amounts supersedes integration of layered quantities since total cloud fraction estimates are more accurate than individual layer fraction due to the sample size of total cloud amount is far greater than the layered cloud amounts (HQ AFWA/DNXM 2011). Bartlett (2009) explains how the total cloud amount analysis works:

> Total cloud fraction is then set to either 100 or 0 percent, respectively. If neither analysis is completely cloud-filled or completely cloud-free, then the error for each analysis is estimated. The estimated errors for the analyses are compared to one another to see if the most recent analysis also has the lowest estimated error. Optimum interpolation (OI) occurs when one analysis cannot be chosen as the most accurate. OI maintains a blended estimate of total cloud fraction from multiple input analyses. Weighting functions for the OI are based on the estimated analysis errors which are computed for each individual analysis. Analysis errors are defined as an initial analysis error plus an additional error growth function which grows linearly with time. The error growth function is a tunable parameter that analysts can adjust to correct for inconsistencies.

When total cloud amount is completed the other cloud parameters are merged. Rules applied, to determine which analysis is superior, in the layered analysis are similar

to the total cloud amount; however, if multiple timely analyses have 100% cloud cover or it is determined that an OI technique is necessary. The integration of layered cloud amounts undergoes a more extensive algorithm. Most likely the individual analyses will have varying vertical distributions of cloud and cloud type due to the differences in sensor characteristics for each satellite family. The more complex algorithm determines which analyses is the most accurate and designates that analyses as the master template for which all other timely analyses are merged on. This process impacts discrete values such as the number of cloud layers and cloud types because these when integrated they will assume the values of the master template. The OI procedure is used for varying layered cloud faction and cloud top temperature. The OI process combines layers that closely match in cloud top temperatures and determines the layered cloud fraction. Special cloud algorithms have been designed for certain satellite sensors to enhance detection of low level stratus and cirrus. These special-case clouds are verified against the integrated analysis to be certain that the analysis is accurate, and are effective in showing the persistence of the observations in the subsequent integration analysis (HQ AFWA/DNXM 2011).

All the output variables are placed in a GriB file (a collection of individual self-containing records, and the individual records themselves can stand alone as meaningful data) and is published as the Worldwide Merge Cloud Analysis (WWMCA).

THIS PAGE INTENTIONALLY LEFT BLANK

APPENDIX B. SPREADSHEET STRUCTURE AND FORMULAS USED TO VERIFY WWMCA WITH CLOUDSAT

Sheet	Section	Column	Name	Formula	Remarks
Processed Data		A	WWMCA valid time		Imported from CSV file
		B	Cloudsat time		Imported from CSV file
		C	Cloudsat Lat		Imported from CSV file
		D	Cloudsat Lon		Imported from CSV file
		E	WWMCA Lat		Imported from CSV file
		F	WWMCA Lon		Imported from CSV file
		G	Distance Between WWMCA and Cloudsat Points (m)		Imported from CSV file
		H	Cloudsat Max Mask		Imported from CSV file
		I	Cloudsat Mask Text (20 threshold)		Imported from CSV file
		J	Cloudsat Occurrence Value (20 threshold)		Imported from CSV file
		K	Cloudsat Mask Text (30 threshold)		Imported from CSV file
		L	Cloudsat Occurrence Value (30 threshold)		Imported from CSV file
		M	WWMCA Valid Time		Imported from CSV file
		N	WWMCA i		Imported from CSV file
		O	WWMCA j		Imported from CSV file
		P	Hemisphere		Imported from CSV file
		Q	WWMCA Layer 1 Cloud Cover (%)		Imported from CSV file
		R	WWMCA Layer 1 Cloud Type		Imported from CSV file
		S	WWMCA Layer 1 Height of Cloud Base (m)		Imported from CSV file
		T	WWMCA Layer 1 Height of Cloud Top (m)		Imported from CSV file
		U	WWMCA Layer 2 Cloud Cover (%)		Imported from CSV file
		V	WWMCA Layer 2 Cloud Type		Imported from CSV file

Sheet	Section	Column	Name	Formula	Remarks
Processed Data		W	WWMCA Layer 2 Height of Cloud Base (m)		Imported from CSV file
		X	WWMCA Layer 2 Height of Cloud Top (m)		Imported from CSV file
		Y	WWMCA Layer 3 Cloud Cover (%)		Imported from CSV file
		Z	WWMCA Layer 3 Cloud Type		Imported from CSV file
		AA	WWMCA Layer 3 Height of Cloud Base (m)		Imported from CSV file
		AB	WWMCA Layer 3 Height of Cloud Top (m)		Imported from CSV file
		AC	WWMCA Layer 4 Cloud Cover (%)		Imported from CSV file
		AD	WWMCA Layer 4 Cloud Type		Imported from CSV file
		AE	WWMCA Layer 4 Height of Cloud Base (m)		Imported from CSV file
		AF	WWMCA Layer 4 Height of Cloud Top (m)		Imported from CSV file
		AG	WWMCA Total Cloud Cover (%)		Imported from CSV file
		AH	WWMCA Cloud Cover Bin		Imported from CSV file
		AI	WWMCA Pixel Age (min)		Imported from CSV file
		AJ	Cloudsat Total Cloud Cover (% - 20 threshold)		Imported from CSV file
		AK	Cloudsat Cloud Eventing (20 threshold)		Imported from CSV file
		AL	Cloudsat Total Cloud Cover (% - 30 threshold)		Imported from CSV file
		AM	Cloudsat Cloud Eventing (30 threshold)		Imported from CSV file

Sheet	Section	Column	Name	Formula	Remarks
Filtered Data		A	CSV Line Number		Tracks CSV line numbers in this workbook
	From Processed Data	B	WWMCA valid time	='Processed Data'!A3	From Processed Data sheet Column A
		C	WWMCA latitude	='Processed Data'!E3	From Processed Data sheet Column E
		D	WWMCA longitude	='Processed Data'!F3	From Processed Data sheet Column F
		E	WWMCA i	='Processed Data'!N3	From Processed Data sheet Column N
		F	WWMCA j	='Processed Data'!O3	From Processed Data sheet Column O
		G	Cloudsat time	='Processed Data'!B3	From Processed Data sheet Column B
		H	WWMCA total cloud amount (%)	='Processed Data'!AG3	From Processed Data sheet Column AG
		I	WWMCA cloud cover event	='Processed Data'!AH3	From Processed Data sheet Column AH
		J	Cloudsat-20 total cloud amount (%)	='Processed Data'!AJ3	From Processed Data sheet Column AJ
		K	Cloudsat-30 total cloud amount (%)	='Processed Data'!AL3	From Processed Data sheet Column AL
		L	Cloudsat-20 cloud cover event	='Processed Data'!AK3	From Processed Data sheet Column AK
		M	Cloudsat-30 cloud cover event	='Processed Data'!AM3	From Processed Data sheet Column AM
	Filtered Data	N	Filtered WWMCA cloud cover event (Cloudsat-20)	=IF(J3"n/a (less than 6 close points)", "", I3)	Filtered out WWMCA cloud cover bin values that corresponded to Cloudsat-20 cells that had "n/a (less than 6 close points)" and replace with ""
		O	Filtered WWMCA cloud cover event (Cloudsat-30)	=IF(K3"n/a (less than 6 close points)", "", I3)	Filtered out WWMCA cloud cover bin values that corresponded to Cloudsat-30 cells that had "n/a (less than 6 close points)" and replace with ""
		P	Filtered Cloudsat-20 total cloud amount (%)	=IF(J3"n/a (less than 6 close points)", "", J3)	Filtered out the "n/a (less than 6 close points)" from Cloudsat-20 total cloud amount and replace with ""
		Q	Filtered Cloudsat-30 total cloud amount (%)	=IF(K3"n/a (less than 6 close points)", "",K3)	Filtered out the "n/a (less than 6 close points)" from Cloudsat-30 total cloud amount and replace with ""
		R	Filtered Cloudsat-20 cloud cover event	=IF(L3=-1, "", L3)	Filtered out values of -1 from Cloudsat-20 cloud cover event

Sheet	Section	Column	Name	Formula	Remarks
Filtered Data	Filtered Data	S	Filtered Cloudsat-30 cloud cover event	=IF(M3=-1, "", M3)	Filtered out values of -1 from Cloudsat-30 cloud cover event
		T	WWMCA cloud cover event (Cloudsat-20) w/ values of '2' removed	=IF(N3=2, "", N3)	
		U	WWMCA cloud cover event (Cloudsat-30) w/ values of '2' removed	=IF(O3=2, "", O3)	
		V	Cloudsat-20 cloud cover event w/ values of '2' removed	=IF(R3=2, "", R3)	
		W	Cloudsat-30 cloud coverevent w/ values of '2' removed	=IF(S3=2, "", S3)	
	Percent Difference of Total Cloud Amount	X	% Diff in WWMCA & Cloudsat-20 total cloud amount (%)	=(H3-P3)/H3	
		Y	% Diff in WWMCA & Cloudsat-30 total cloud amount (%)	=(H3-Q3)/H3	
		Z	Filtered % Diff in WWMCA & Cloudsat-20 total cloud amount (%)		Filtered out values of '#DIV/0!' from % diff in WWMCA & Cloudsat-20 total cloud amount with a blank by find/replace function.
		AA	Filtered % Diff in WWMCA & Cloudsat-30 total cloud amount (%)		Filtered out values of '#DIV/0!' from % diff in WWMCA & Cloudsat-30 total cloud amount by find/replace function.
	Time of Day Flags	AZ	Cloudsat time for Flagging	=G3	time in decimal form
		BA	Day/Night Flag	=IF(AND(AZ3>0.625, AZ3<1), "Day", "Night")	see Figure 12 for other daytime ranges
		BB	Polar Night Flag	IF('Processed Data"!C3>=70, "Night", BA3)	Used for Cloudsat latitudes above 70°N. For Polar Day, replace "Night" with "Day."

Sheet	Section	Column	Name	Formula	Remarks
Filtered Data	**Contingency Table Scores of All Day (Cloudsat-20)**	AB	Event 3 (Cloudsat-20) Cell A (Hit)	=IF(AND(N3=3, R3=3), "Hit", "")	
		AC	Event 3 (Cloudsat-20) Cell B (False Alarm)	=IF(AND(N3=3, R3<2), "FA", "")	
		AD	Event (Cloudsat-20) Cell C (Miss)	=IF(AND(N3<2, R3=3), "Miss", "")	
		AE	Event 3 (Cloudsat-20) Cell D (Correct Rejection)	=IF(AND(N3<2, R3<2), "Reject", "")	
	Contingency Table Scores of All Day for Cloudsat-20	AF	Event 2 (Cloudsat-20) Cell A (Hit)	=IF(AND(N3=2, R3=2), "Hit", "")	
		AG	Event 2 (Cloudsat-20) Cell B (False Alarm)	=IF(AND(N3=2, V3<3), "FA", "")	
		AH	Event 2 (Cloudsat-20) Cell C (Miss)	=IF(AND(T3<3, R3=2), "Miss", "")	
		AI	Event 2 (Cloudsat-20) Cell D (Correct Rejection)	=IF(AND(T3<3, V3<3), "Reject", "")	
		AJ	Event 1 (Cloudsat-20) Cell A (Hit)	=IF(AND(N3=1, R3=1), "Hit", "")	
		AK	Event 1 (Cloudsat-20) Cell B (False Alarm)	=IF(AND(N3=1, R3>1), "FA", "")	
		AL	Event 1 (Cloudsat-20) Cell C (Miss)	=IF(AND(N3>1, R3=1), "Miss", "")	
		AM	Event 1(Cloudsat-20) Cell D (Correct Rejection)	=IF(AND(N3>1, R3>1), "Reject", "")	

Sheet	Section	Column	Name	Formula	Remarks
Filtered Data	Contingency Table Scores of All Day for Cloudsat-30	AN	Event 3 (Cloudsat-30) Cell A (Hit)	=IF(AND(P33, S33), "Hit", "")	
		AO	Event 3 (Cloudsat-30) Cell B (False Alarm)	=IF(AND(P33, S3<2), "FA", "")	
		AP	Event (Cloudsat-30) Cell C (Miss)	=IF(AND(P3<2, S33), "Miss", "")	
		AQ	Event 3 (Cloudsat-30) Cell D (Correct Rejection)	=IF(AND(P3<2, S3<2), "Reject", "")	
		AR	Event 2 (Cloudsat-30) Cell A (Hit)	=IF(AND(P32, S32), "Hit", "")	
		AS	Event 2 (Cloudsat-30) Cell B (False Alarm)	=IF(AND(P32, W3<3), "FA", "")	
		AT	Event 2 (Cloudsat-30) Cell C (Miss)	=IF(AND(U3<3, S32), "Miss", "")	
		AU	Event 2 (Cloudsat-30) Cell D (Correct Rejection)	=IF(AND(U3<3, W3<3), "Reject", "")	
		AV	for bin (1 - 30) Cell A (Hit)	=IF(AND(P31, S31), "Hit", "")	
		AW	for bin (1 - 30) Cell B (False Alarm)	=IF(AND(P31, S3>1), "FA", "")	
		AX	for bin (1 - 30) Cell C (Miss)	=IF(AND(P3>1, S31), "Miss", "")	
		AY	for bin (1 - 30) Cell D (Correct Rejection)	=IF(AND(P3>1, S3>1), "Reject", "")	

Sheet	Section	Column	Name	Formula	Remarks
Filtered Data	Contingency Table Scores of Daytime for Cloudsat-20	BC	Event 3 (Cloudsat-20) Cell A (Hit)	=IF($BB3"Day", AB3, "")	
		BD	Event 3 (Cloudsat-20) Cell B (False Alarm)	=IF($BB3"Day", AC3, "")	
		BE	Event (Cloudsat-20) Cell C (Miss)	=IF($BB3"Day", AD3, "")	
		BF	Event 3 (Cloudsat-20) Cell D (Correct Rejection)	=IF($BB3"Day", AE3, "")	
		BG	Event 2 (Cloudsat-20) Cell A (Hit)	=IF($BB3"Day", AF3, "")	
		BH	Event 2 (Cloudsat-20) Cell B (False Alarm)	=IF($BB3"Day", AG3, "")	
		BI	Event 2 (Cloudsat-20) Cell C (Miss)	=IF($BB3"Day", AH3, "")	
		BJ	Event 2 (Cloudsat-20) Cell D (Correct Rejection)	=IF($BB3"Day", AI3, "")	
		BK	Event 1 (Cloudsat-20) Cell A (Hit)	=IF($BB3"Day", AJ3, "")	
		BL	Event 1 (Cloudsat-20) Cell B (False Alarm)	=IF($BB3"Day", AK3, "")	
		BM	Event (Cloudsat-20) Cell C (Miss)	=IF($BB3"Day", AL3, "")	
		BN	Event 1 (Cloudsat-20) Cell D (Correct Rejection)	=IF($BB3"Day", AM3, "")	

Sheet	Section	Column	Name	Formula	Remarks
Filtered Data	**Contingency Table Scores of Daytime for Cloudsat-30**	BO	Event 3 (Cloudsat-30) Cell A (Hit)	=IF($BB3"Day", AN3, "")	
		BP	Event 3 (Cloudsat-30) Cell B (False Alarm)	=IF($BB3"Day", AO3, "")	
		BQ	Event (Cloudsat-30) Cell C (Miss)	=IF($BB3"Day", AP3, "")	
		BR	Event 3 (Cloudsat-30) Cell D (Correct Rejection)	=IF($BB3"Day", AQ3, "")	
		BS	Event 2 (Cloudsat-30) Cell A (Hit)	=IF($BB3"Day", AR3, "")	
		BT	Event 2 (Cloudsat-30) Cell B (False Alarm)	=IF($BB3"Day", AS3, "")	
		BU	Event 2 (Cloudsat-30) Cell C (Miss)	=IF($BB3"Day", AT3, "")	
		BV	Event 2 (Cloudsat-30) Cell D (Correct Rejection)	=IF($BB3"Day", AU3, "")	
		BW	Event 1 (Cloudsat-30) Cell A (Hit)	=IF($BB3"Day", AV3, "")	
		BX	Event 1 (Cloudsat-30) Cell B (False Alarm)	=IF($BB3"Day", AW3, "")	
		BY	Event 1 (Cloudsat-30) Cell C (Miss)	=IF($BB3"Day", AX3, "")	
		BZ	Event 1(Cloudsat-30) Cell D (Correct Rejection)	=IF($BB3"Day", AY3, "")	

Sheet	Section	Column	Name	Formula	Remarks
Filtered Data	**Contingency Table Scores of Nighttime for Cloudsat-20**	CA	Event 3 (Cloudsat-20) Cell A (Hit)	=IF($BB3"Night", AB3, "")	
		CB	Event 3 (Cloudsat-20) Cell B (False Alarm)	=IF($BB3"Night", AC3, "")	
		CC	Event (Cloudsat-20) Cell C (Miss)	=IF($BB3"Night", AD3, "")	
		CD	Event 3 (Cloudsat-20) Cell D (Correct Rejection)	=IF($BB3"Night", AE3, "")	
		CE	Event 2 (Cloudsat-20) Cell A (Hit)	=IF($BB3"Night", AF3, "")	
		CF	Event 2 (Cloudsat-20) Cell B (False Alarm)	=IF($BB3"Night", AG3, "")	
		CG	Event 2 (Cloudsat-20) Cell C (Miss)	=IF($BB3"Night", AH3, "")	
		CH	Event 2 (Cloudsat-20) Cell D (Correct Rejection)	=IF($BB3"Night", AI3, "")	
		CI	Event 1 (Cloudsat-20) Cell A (Hit)	=IF($BB3"Night", AJ3, "")	
		CJ	Event 1 (Cloudsat-20) Cell B (False Alarm)	=IF($BB3"Night", AK3, "")	
		CK	Event 1 (Cloudsat-20) Cell C (Miss)	=IF($BB3"Night", AL3, "")	
		CL	Event 1(Cloudsat-20) Cell D (Correct Rejection)	=IF($BB3"Night", AM3, "")	

Sheet	Section	Column	Name	Formula	Remarks
Filtered Data	Contingency Table Scores of Nighttime for Cloudsat-30	CM	Event 3 (Cloudsat-30) Cell A (Hit)	=IF($BB3"Night", AN3, "")	
		CN	Event 3 (Cloudsat-30) Cell B (False Alarm)	=IF($BB3"Night", AO3, "")	
		CO	Event (Cloudsat-30) Cell C (Miss)	=IF($BB3"Night", AP3, "")	
		CP	Event 3 (Cloudsat-30) Cell D (Correct Rejection)	=IF($BB3"Night", AQ3, "")	
		CQ	Event 2 (Cloudsat-30) Cell A (Hit)	=IF($BB3"Night", AR3, "")	
		CR	Event 2 (Cloudsat-30) Cell B (False Alarm)	=IF($BB3"Night", AS3, "")	
		CS	Event 2 (Cloudsat-30) Cell C (Miss)	=IF($BB3"Night", AT3, "")	
		CT	Event 2 (Cloudsat-30) Cell D (Correct Rejection)	=IF($BB3"Night", AU3, "")	
		CU	Event 1 (Cloudsat-30) Cell A (Hit)	=IF($BB3"Night", AV3, "")	
		CV	Event 1 (Cloudsat-30) Cell B (False Alarm)	=IF($BB3"Night", AW3, "")	
		CW	Event 1 (Cloudsat-30) Cell C (Miss)	=IF($BB3"Night", AX3, "")	
		CX	Event 1(Cloudsat-30) Cell D (Correct Rejection)	=IF($BB3"Night", AY3, "")	

APPENDIX C. RESULTS FOR WWMCA BOXES 22 AND 29 FOR CLOUDSAT CLOUD MASK VALUE OF 20 USED FOR CLOUD/NO-CLOUD THRESHOLD
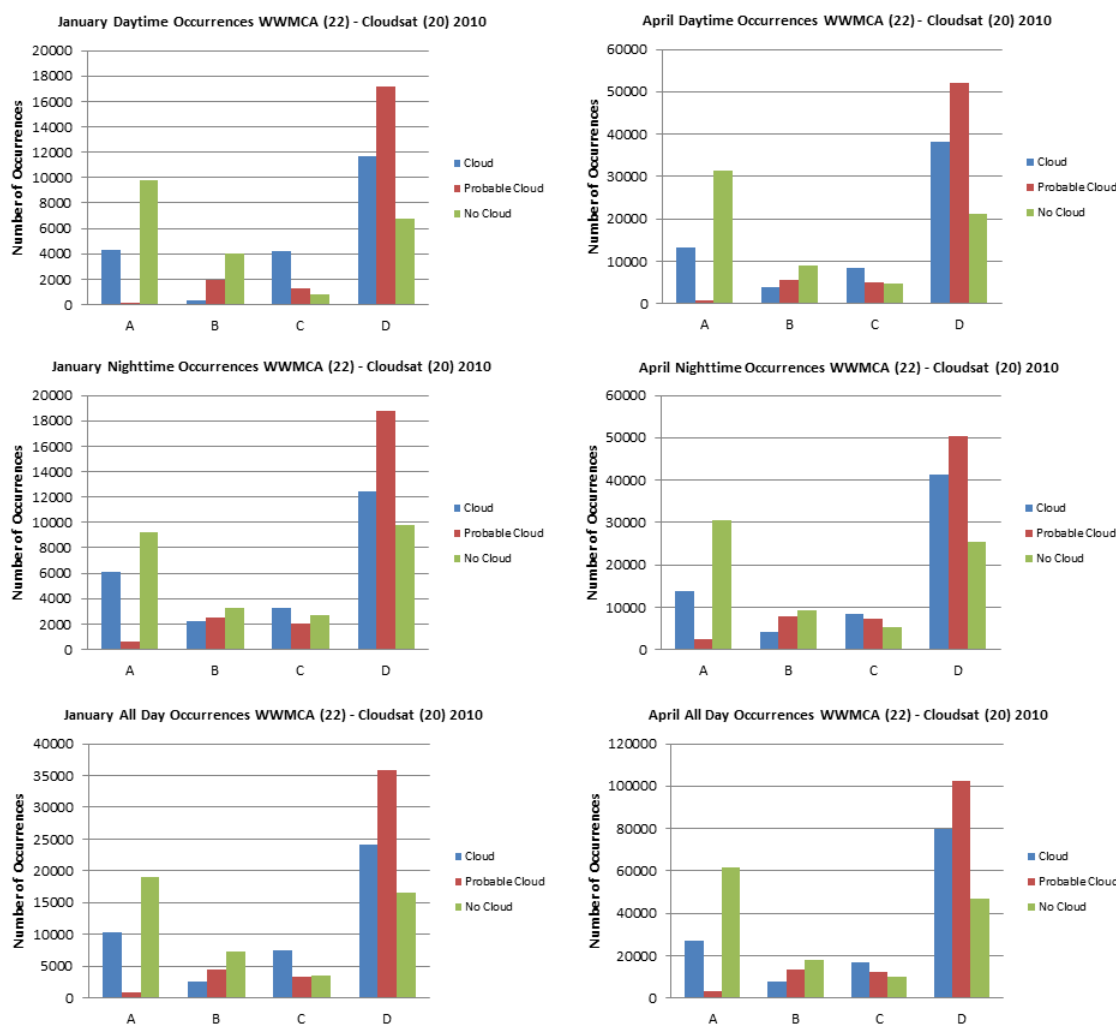
A.   WWMCA BOX 22

Figure 31.   Number of occurrences in January and April 2010 for WWMCA Box 22 for all three cloud cover events (cloud, probable cloud, and no-cloud) using a Cloudsat cloud mask value of 20 for cloud/no-cloud threshold. The "cloud" event (blue) represents the "definite cloud" event. The horizontal axes are the occurrence categories: A—Hits; B—False Alarms; C—Misses; and D—Correct Rejections. The top panels are the occurrences for daytime, the middle panels are nighttime occurrences, and the bottom panels are the combined results of both daytime and nighttime occurrences.
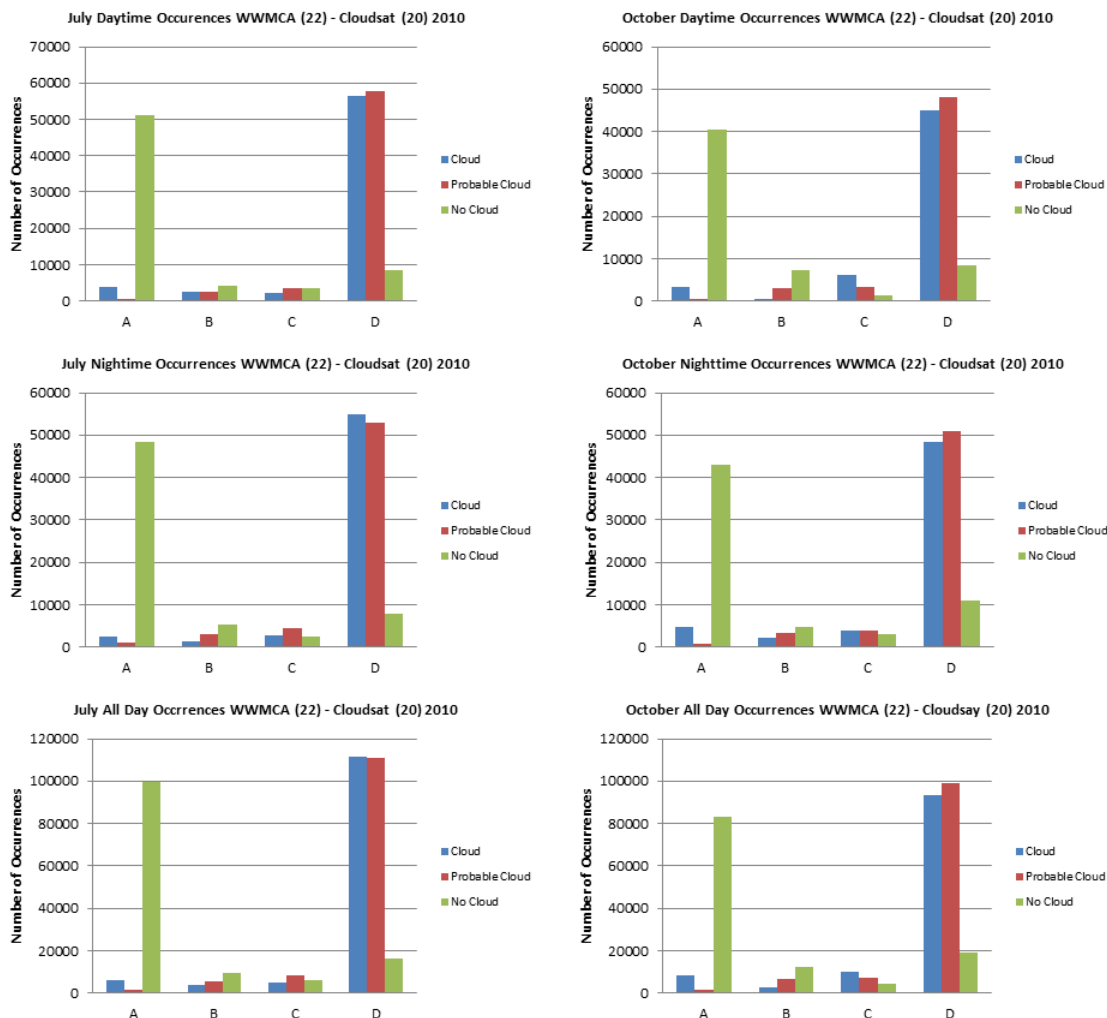
Figure 32.   Number of 2 x 2 contingency table occurrences in July and October 2010 for WWMCA Box 22 for all three cloud cover events: Definite-Cloud (blue), Probable-Cloud (red), and No-Cloud (green). On the horizontal axes: A indicates Hits, B indicates False Alarms, C indicates Misses, and D indicates Correct Rejections. The top panels shows the daytime occurrences, the middle panels shows the nighttime occurrences, and the bottom panels show the results for both daytime and nighttime occurrences. Results based on using a Cloudsat cloud mask value of 20 for the cloud/no-cloud threshold.
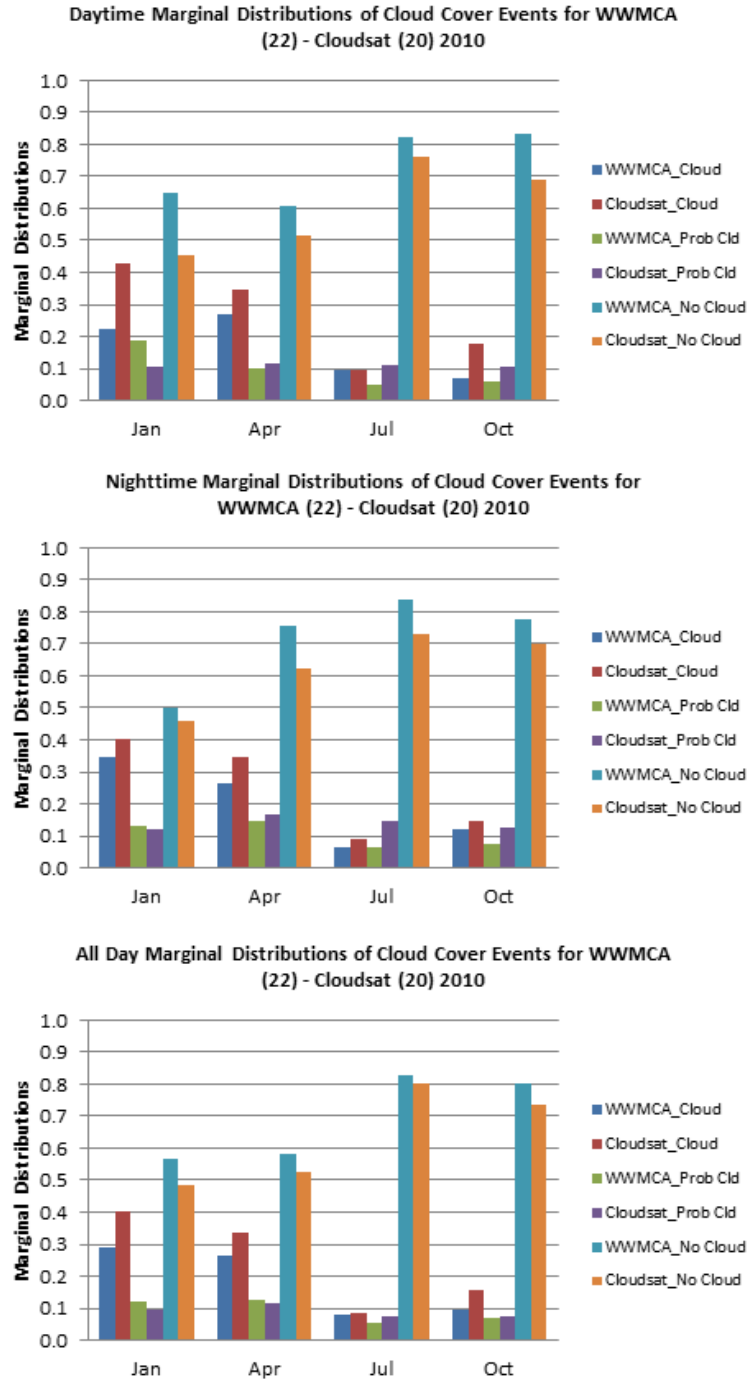
Figure 33.   Marginal distributions of cloud cover events for WWMCA and Cloudsat for
WWMCA Box 22: Definite-Cloud, Probable-Cloud, and No-Cloud). The
calculation of the marginal distributions is shown in Table 7. The top panel
shows the results for daytime data, the middle panel for nighttime data, and
the bottom panel for both daytime and nighttime data. Results based on using
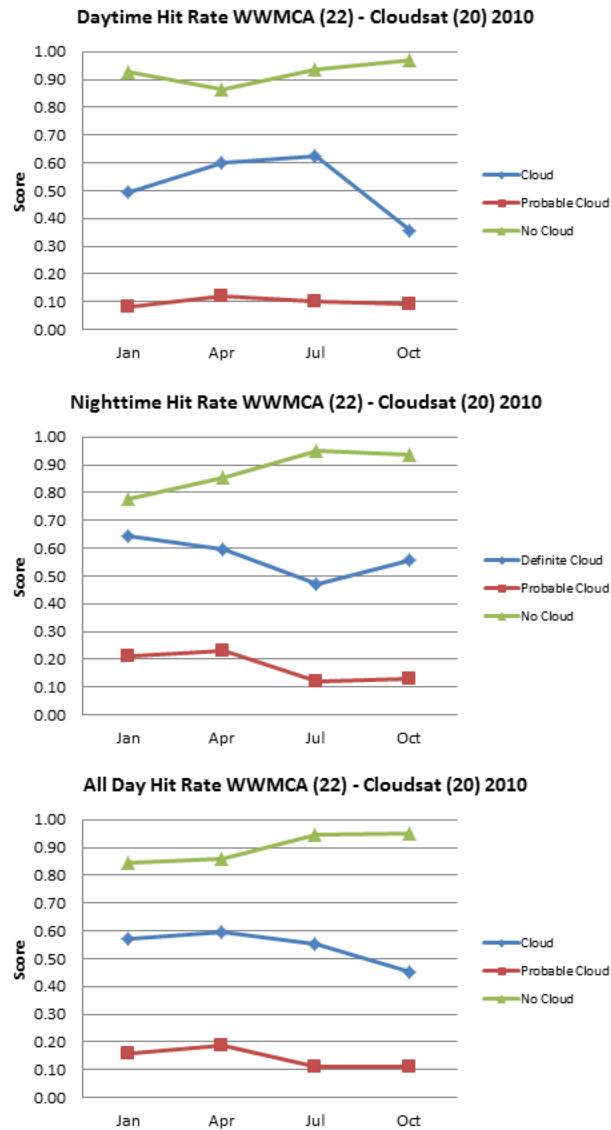a Cloudsat cloud mask value of 20 for the cloud/no-cloud threshold.

Figure 34.   WWMCA probability of detection (POD), or hit rate (H), for WWMCA Box
22 for all three cloud cover events: Definite-Cloud (blue), Probable-Cloud
(red), and No-Cloud (green). The top panel shows the results for daytime
data, the middle panel for nighttime data, and the bottom panel for both
daytime and nighttime data. Results based on using a Cloudsat cloud mask
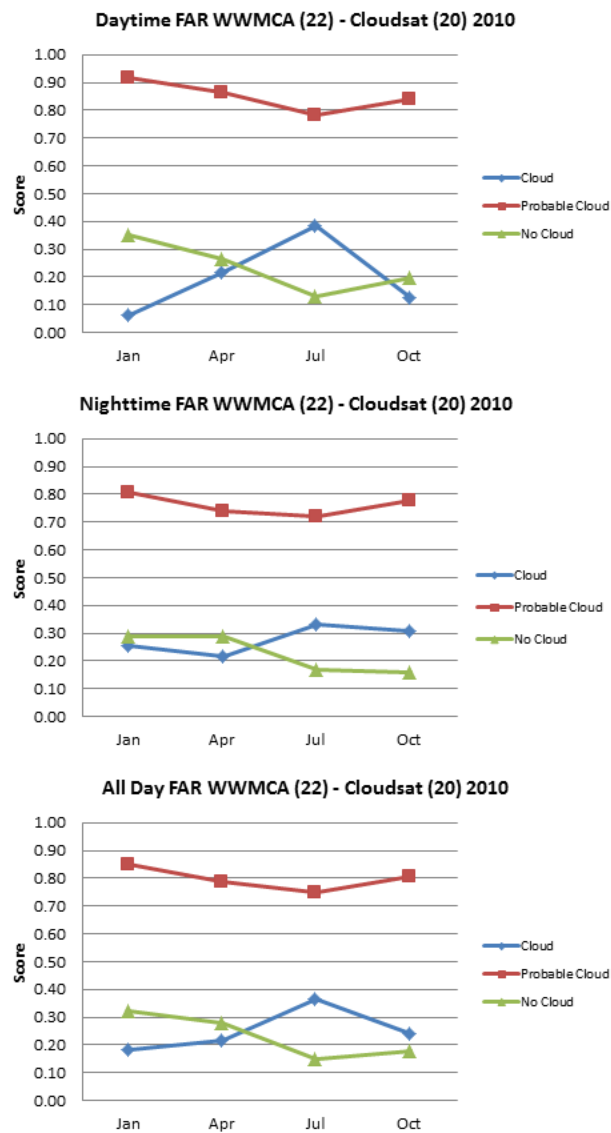value of 20 for the cloud/no-cloud threshold.

Figure 35.   WWMCA false alarm ratios for WWMCA Box 22 for all three cloud cover
events: Definite-Cloud (blue), Probable-Cloud (red), and No-Cloud (green).
The top panel shows the results for daytime data, the middle panel for
nighttime data, and the bottom panel for both daytime and nighttime data.
Results based on using a Cloudsat cloud mask value of 20 for the cloud/no-
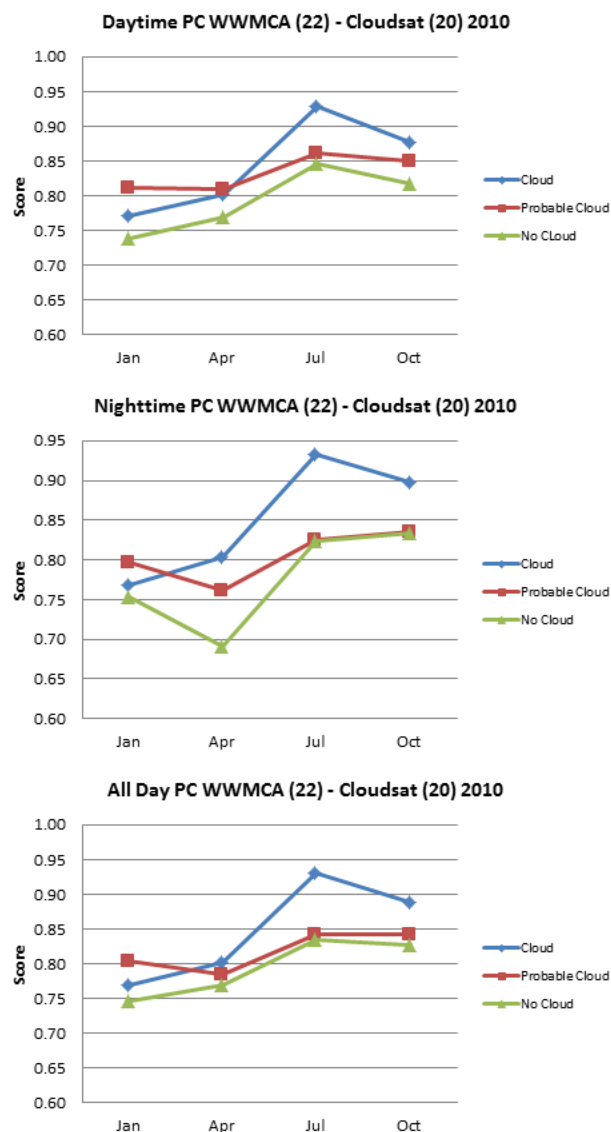cloud threshold.

Figure 36.   WWMCA proportion correct (PC) for WWMCA Box 22 for all three cloud cover events: Definite-Cloud (blue), Probable-Cloud (red), and No-Cloud (green). The top panel shows the results for daytime data, the middle panel for nighttime data, and the bottom panel for both daytime and nighttime data. Results based on using a Cloudsat cloud mask value of 20 for the cloud/no-cloud threshold.
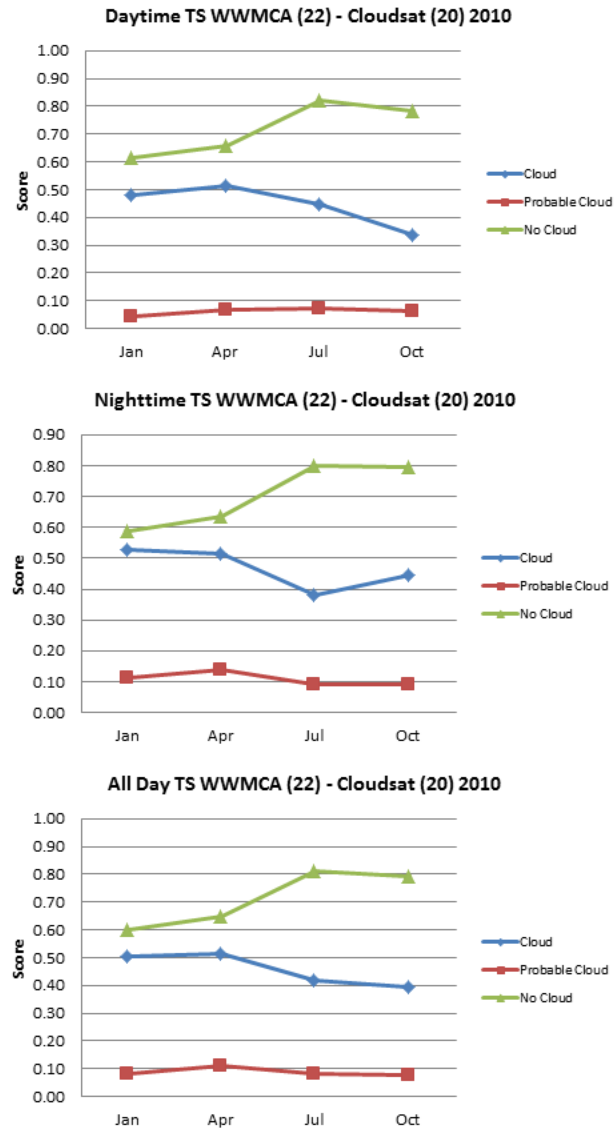
Figure 37. WWMCA threat scores (TS) for WWMCA Box 22 for all three cloud cover events: Definite-Cloud (blue), Probable-Cloud (red), and No-Cloud (green). The top panel shows the results for daytime data, the middle panel for nighttime data, and the bottom panel for both daytime and nighttime data. Results based on using a Cloudsat cloud mask value of 20 for the cloud/no-cloud threshold.
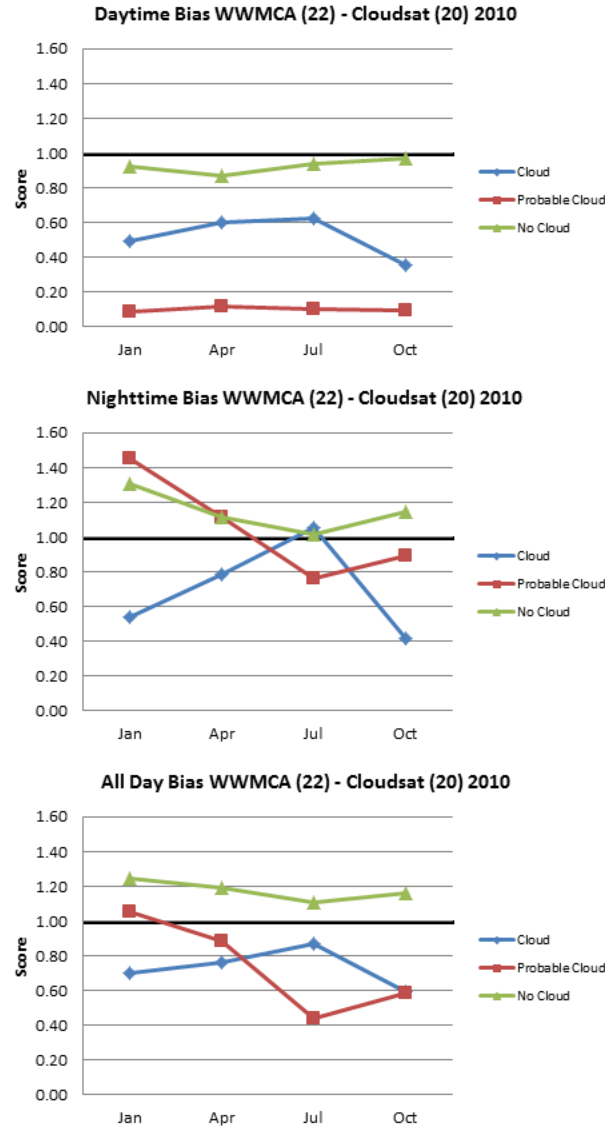
Figure 38.   WWMCA bias (B) for WWMCA Box 22 for all three cloud cover events: Definite-Cloud (blue), Probable-Cloud (red), and No-Cloud (green). The top panel shows the results for daytime data, the middle panel for nighttime data, and the bottom panel for both daytime and nighttime data. The heavy dark line at B = 1 indicates an unbiased analysis. Values greater (less) than 1 indicate a cloud cover event that was over (under) analyzed. Results based on using a Cloudsat cloud mask value of 20 for the cloud/no-cloud threshold.
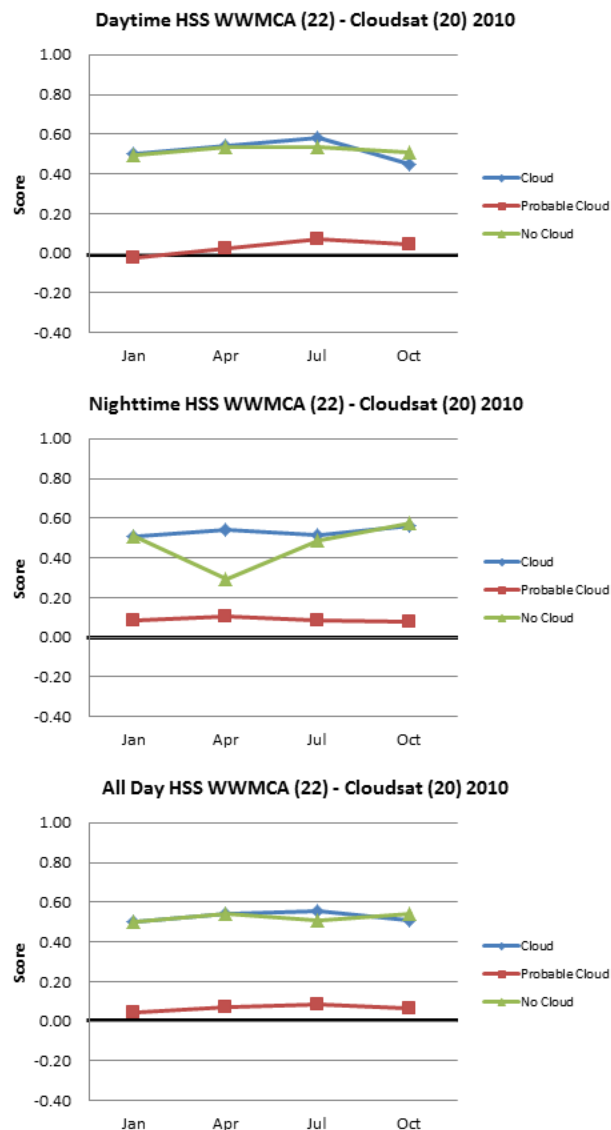
Figure 39.   WWMCA Heidke skill score (HSS) for WWMCA Box 22 for all three cloud cover events: Definite-Cloud (blue), Probable-Cloud (red), and No-Cloud (green). The top panel shows the results for daytime data, the middle panel for nighttime data, and the bottom panel for both daytime and nighttime data. The heavy dark line at the zero value indicates that the WWMCA is equivalent to reference analyses (random analyses statistically independent of observations). A perfect WWMCA cloud analysis would have a value of one. Negative values indicate WWMCA performs worse than reference analyses. Results based on using a Cloudsat cloud mask value of 20 for the cloud/no-cloud threshold.
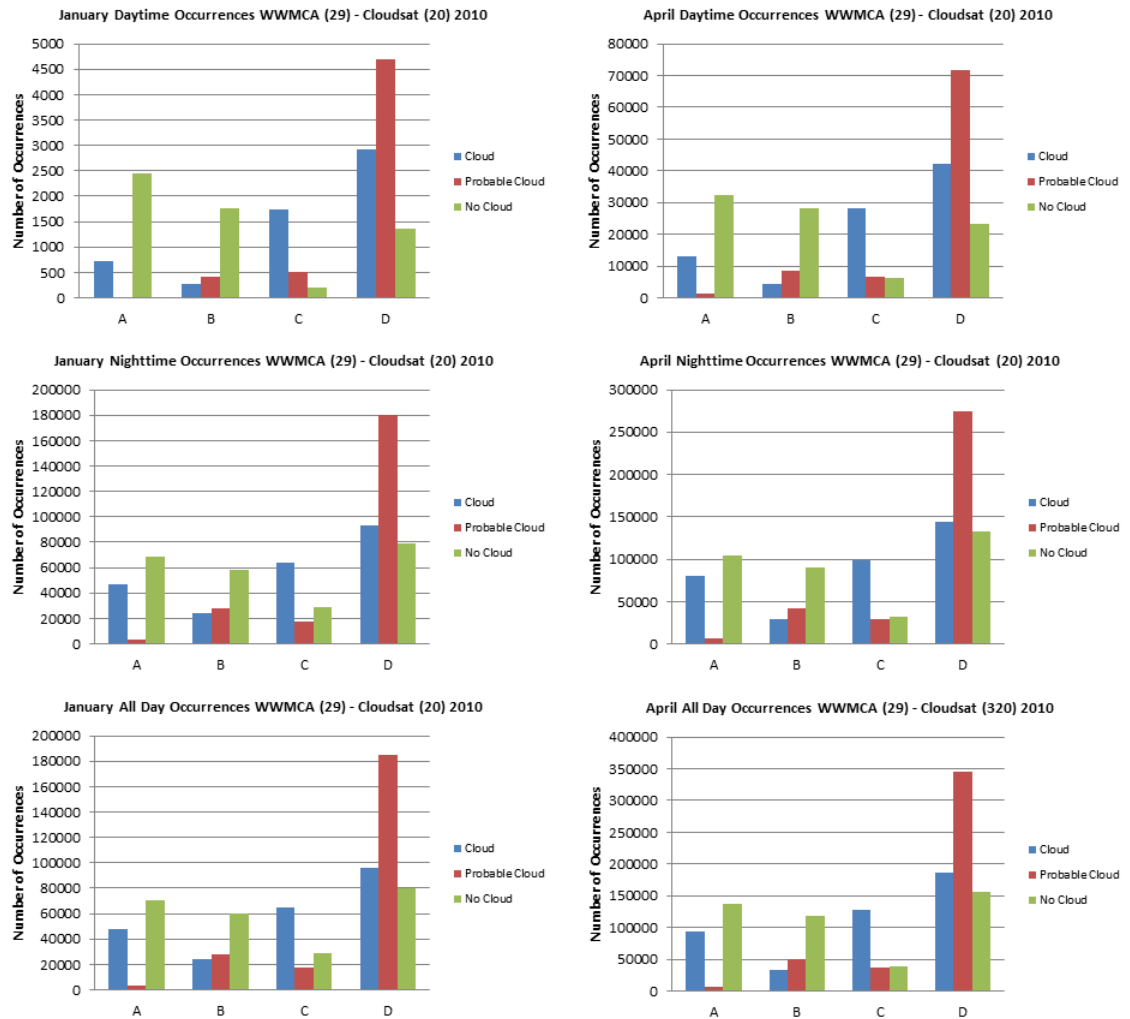
Figure 40.   Number of 2 x 2 contingency table occurrences in January and April 2010 for WWMCA Box 29 for all three cloud cover events: Definite-Cloud (blue), Probable-Cloud (red), and No-Cloud (green). On the horizontal axes: A indicates Hits, B indicates False Alarms, C indicates Misses, and D indicates Correct Rejections. The top panels shows the daytime occurrences, the middle panels shows the nighttime occurrences, and the bottom panels show the results for both daytime and nighttime occurrences. Results based on using a Cloudsat cloud mask value of 20 for the cloud/no-cloud threshold.
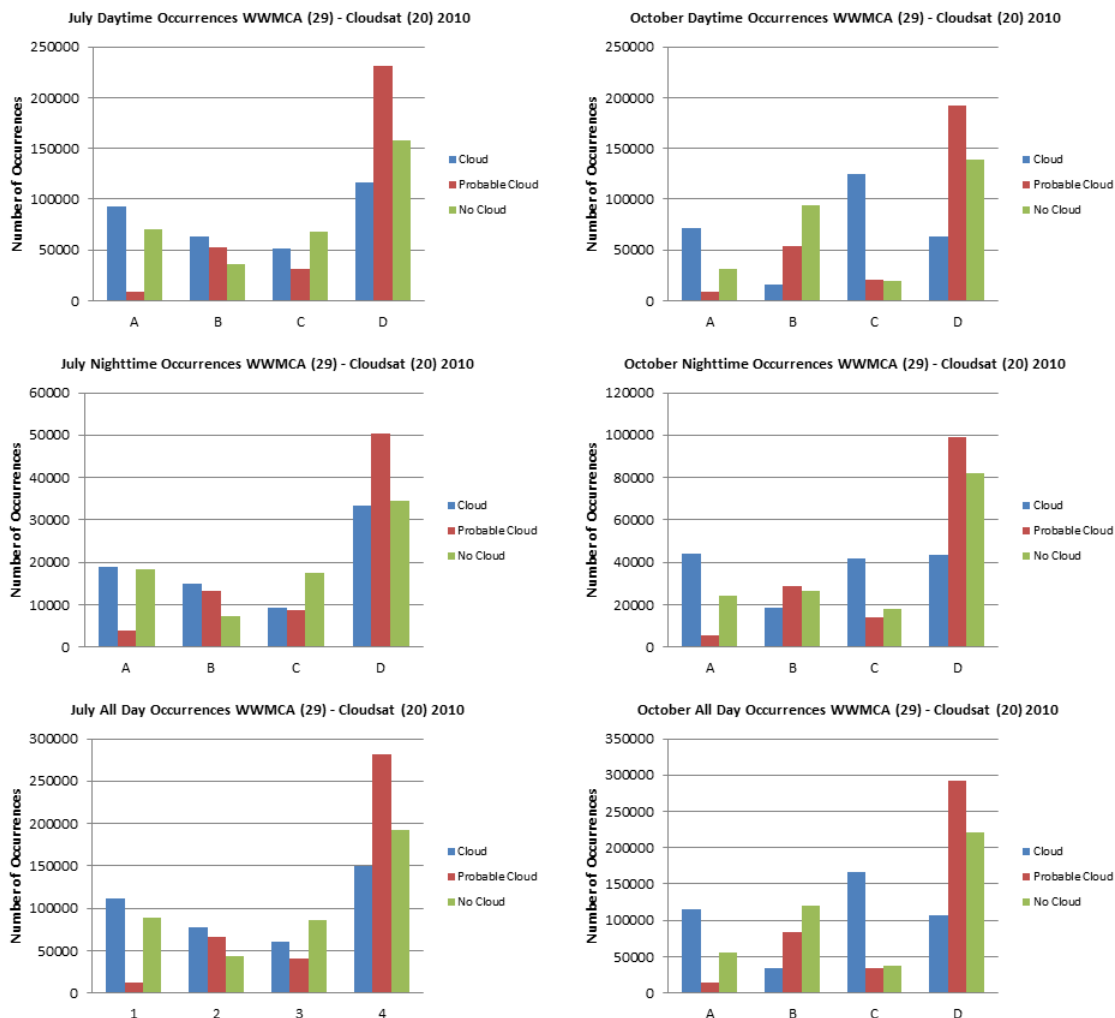
Figure 41.   Number of 2 x 2 contingency table occurrences in July and October 2010 for
WWMCA Box 29 for all three cloud cover events: Definite-Cloud (blue),
Probable-Cloud (red), and No-Cloud (green). On the horizontal axes: A
indicates Hits, B indicates False Alarms, C indicates Misses, and D indicates
Correct Rejections. The top panels shows the daytime occurrences, the
middle panels shows the nighttime occurrences, and the bottom panels show
the results for both daytime and nighttime occurrences. Results based on
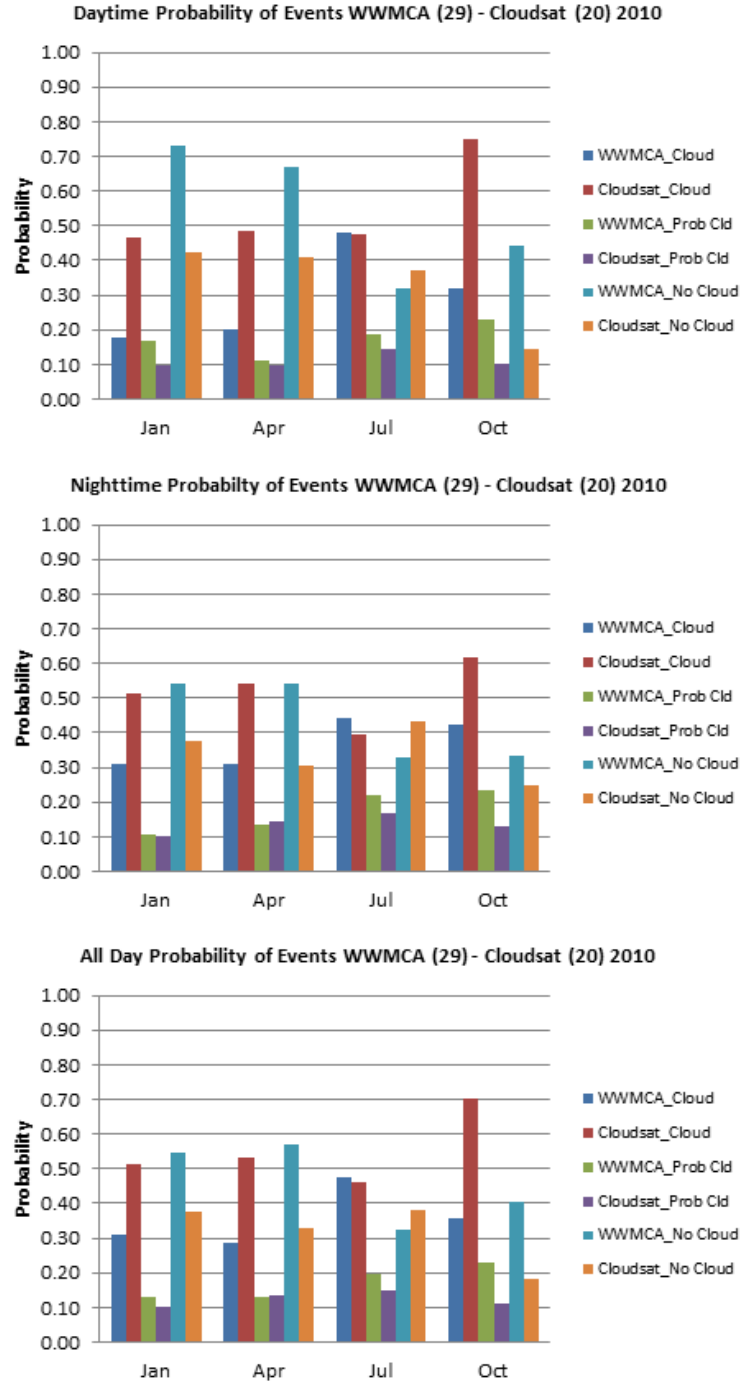using a Cloudsat cloud mask value of 20 for the cloud/no-cloud threshold.

Figure 42.   Marginal distributions of cloud cover events for WWMCA and Cloudsat for
WWMCA Box 29: Definite-Cloud, Probable-Cloud, and No-Cloud). The
calculation of the marginal distributions is shown in Table 7. The top panel
shows the results for daytime data, the middle panel for nighttime data, and
the bottom panel for both daytime and nighttime data. Results based on using
a Cloudsat cloud mask value of 20 for the cloud/no-cloud threshold.

Figure 43.   WWMCA probability of detection (POD), or hit rate (H), for WWMCA Box
29 for all three cloud cover events: Definite-Cloud (blue), Probable-Cloud
(red), and No-Cloud (green). The top panel shows the results for daytime
data, the middle panel for nighttime data, and the bottom panel for both
daytime and nighttime data. Results based on using a Cloudsat cloud mask
value of 20 for the cloud/no-cloud threshold.

Figure 44.   WWMCA false alarm ratios for WWMCA Box 29 for all three cloud cover events: Definite-Cloud (blue), Probable-Cloud (red), and No-Cloud (green). The top panel shows the results for daytime data, the middle panel for nighttime data, and the bottom panel for both daytime and nighttime data. Results based on using a Cloudsat cloud mask value of 20 for the cloud/no-cloud threshold.
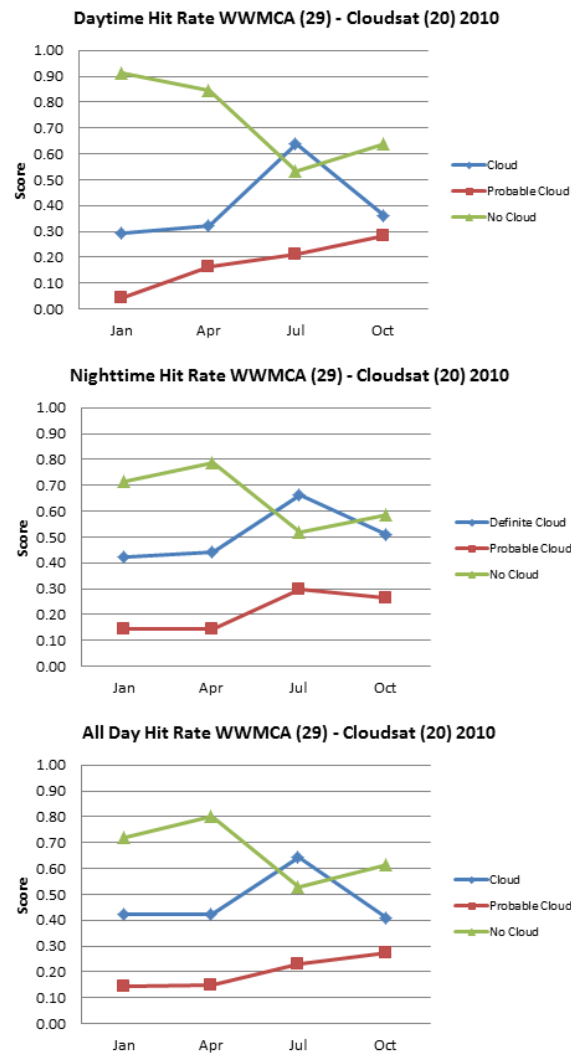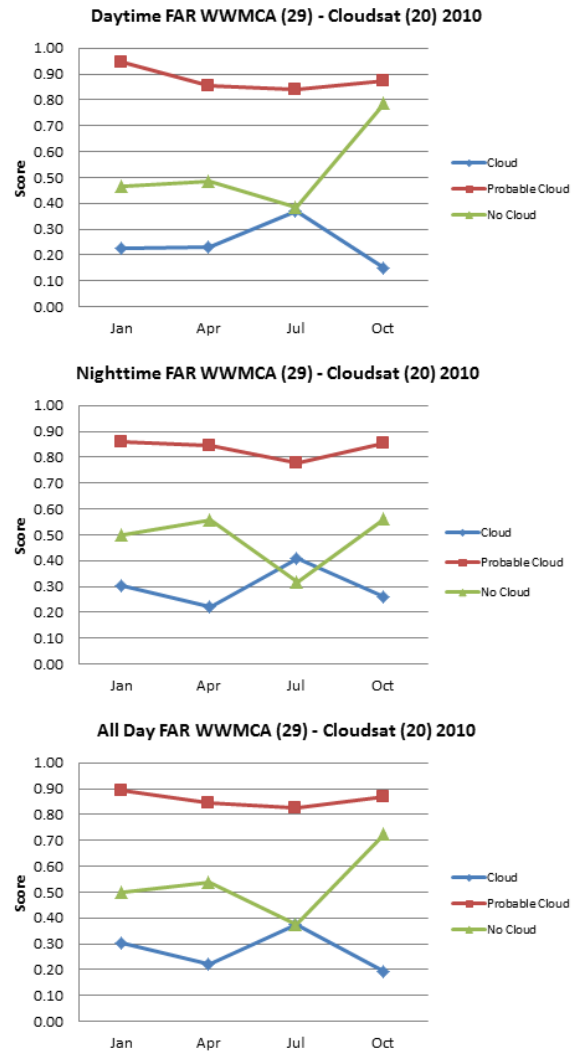
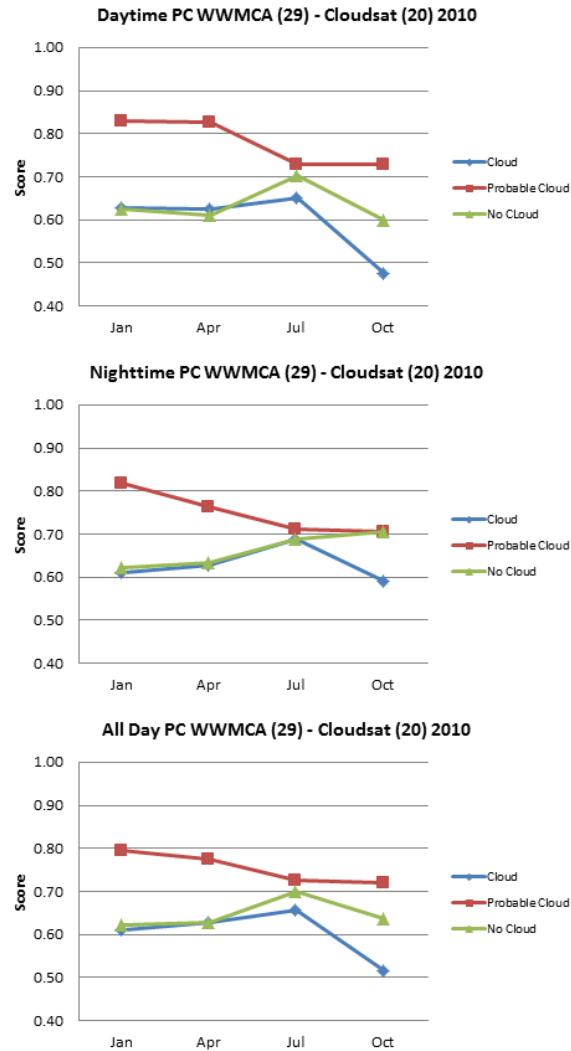Figure 45.   WWMCA proportion correct (PC) for WWMCA Box 29 for all three cloud cover events: Definite-Cloud (blue), Probable-Cloud (red), and No-Cloud (green). The top panel shows the results for daytime data, the middle panel for nighttime data, and the bottom panel for both daytime and nighttime data. Results based on using a Cloudsat cloud mask value of 20 for the cloud/no-cloud threshold.
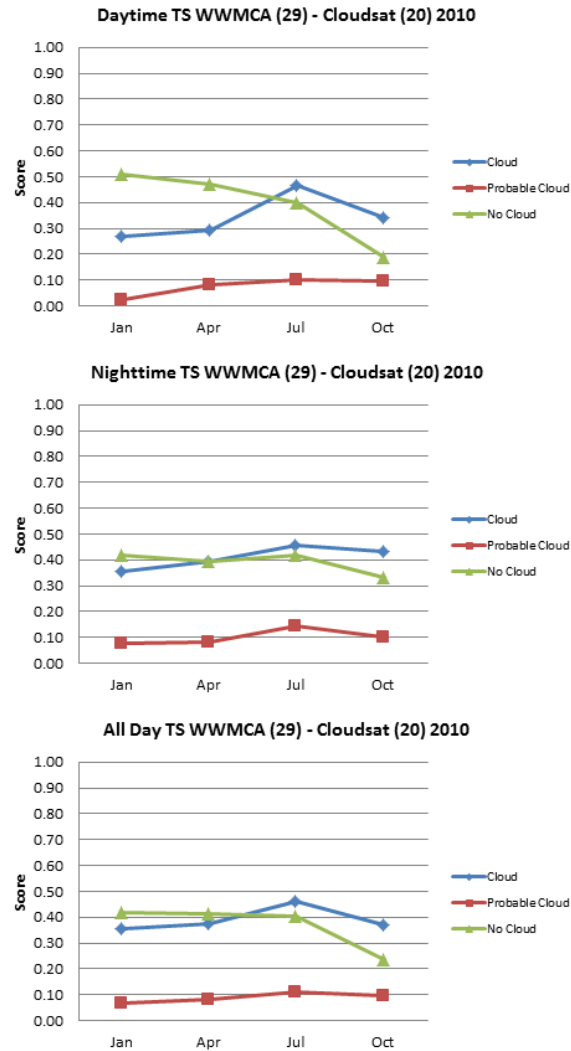
Figure 46.   WWMCA threat scores (TS) for WWMCA Box 29 for all three cloud cover events: Definite-Cloud (blue), Probable-Cloud (red), and No-Cloud (green). The top panel shows the results for daytime data, the middle panel for nighttime data, and the bottom panel for both daytime and nighttime data. Results based on using a Cloudsat cloud mask value of 20 for the cloud/no-cloud threshold.

Figure 47.   WWMCA bias (B) for WWMCA Box 29 for all three cloud cover events:
Definite-Cloud (blue), Probable-Cloud (red), and No-Cloud (green). The top
panel shows the results for daytime data, the middle panel for nighttime data,
and the bottom panel for both daytime and nighttime data. The heavy dark
line at B = 1 indicates an unbiased analysis. Values greater (less) than 1
indicate a cloud cover event that was over (under) analyzed. Results based on
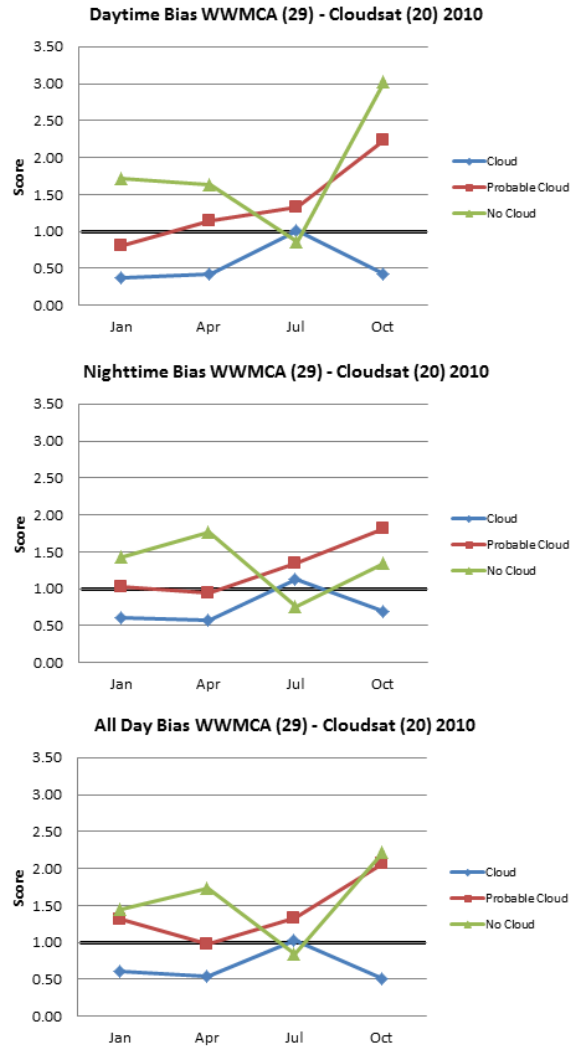using a Cloudsat cloud mask value of 20 for the cloud/no-cloud threshold.
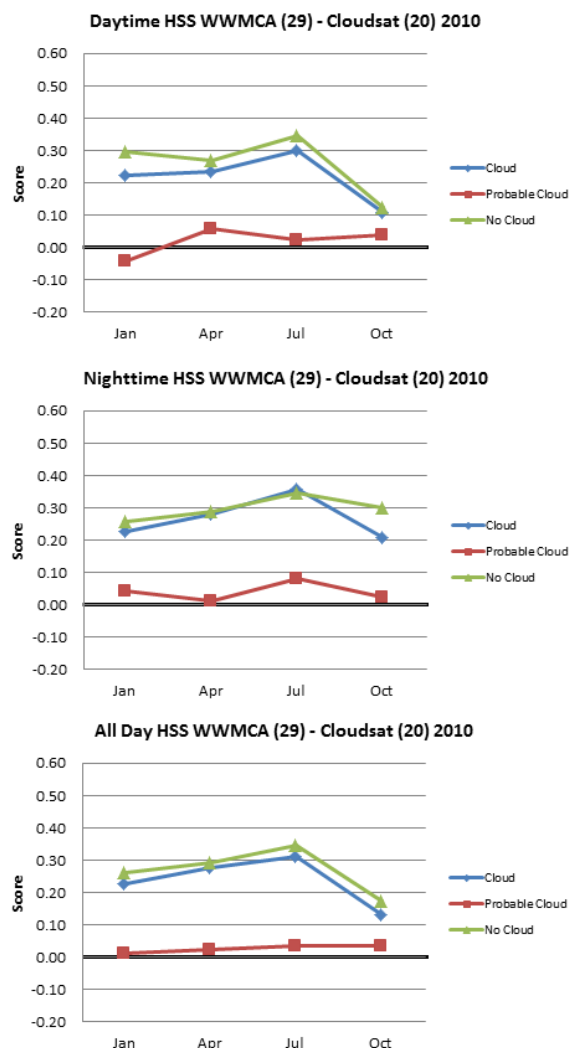
Figure 48.   WWMCA Heidke skill score (HSS) for WWMCA Box 29 for all three cloud
cover events: Definite-Cloud (blue), Probable-Cloud (red), and No-Cloud
(green). The top panel shows the results for daytime data, the middle panel
for nighttime data, and the bottom panel for both daytime and nighttime data.
The heavy dark line at the zero value indicates that the WWMCA is
equivalent to reference analyses (random analyses statistically independent of
observations). A perfect WWMCA cloud analysis would have a value of one.
Negative values indicate WWMCA performs worse than reference analyses.
Results based on using a Cloudsat cloud mask value of 20 for the cloud/no-
cloud threshold.

LIST OF REFERENCES

Bartlett, M.J., 2009: An Evaluation of Methods for Verifying Cloud Distribution in the Worldwide Merged Cloud Analysis. M.S. Thesis. Dept. of Meteorology, Naval Postgraduate School, 68 pp.

Cloudsat Standard Data Products Handbook, 2008. [Available online http://www.cloudsat.cira.colostate.edu/cloudsat_documentation/CloudSat_Data_Users_Handbook.pdf]

Cloudsat—Education: FAQ , 2011. [Available online at http://cloudsat.atmos.colostate.edu/education/faq]

Cloudsat Data Processing Center, 2011. [Available at http://www.cloudsat.cira.colostate.edu/dataSpecs.php?prodid=9]

Cloudsat 2B GEOPROF Quality Statement: May 2007 (Version R04). [Available online at http://www.cloudsat.cira.colostate.edu/dataICDlist.php?go=list&path=/2B-GEOPROF]

EUMETSAT—Channel Spectral bands, 2011. [Available online at http://www.eumetsat.int/groups/ops/documents/document/pdf_ten_052561_msg1_spctrbnds.pdf]

Goes Imager Channel Notation, 2011. [Available online at http://www.comet.ucar.edu/class/satmet/goeschan.html]

Gustafson, G. B. et al., 2011: Cloud Optical Properties (COP) Integration/Cloud, Dust, Wind Performance Requirements, *Interim Report*, Presented at Air Force Weather Agency, Bellevue, NE, 6 July 2011.

HQ AFWA/DNXM, 2011: Algorithm Description for the Cloud Depiction and Forecast System II. Offutt AFB, NE 68113.

Hoke, J.E., J.L. Hayes, and L.G. Renniger, 1981 (Rev. March 1985): *Map Projections and Grid Systems for Meteorological Applications*, AFGWC Technical Notes 79/003, USAF AFGWC, Offutt AFB NE 86 pp.

Horsman, S. J., 2007: An Assessment of the World Wide Merged Cloud Analysis Using Interactive Graphics. M.S. Thesis. Dept. of Meteorology, Naval Postgraduate School, 59 pp.

Kiess, R. B. and W. M. Cox, 1988: The Air Force Global Weather Central, Air Weather Service: The Automatic Real-time Analysis Model. AFGWC/TN-88-001, Offutt AFB, NE 68113.

Level 2 GEOPROF Product Process Description and Interface Control Document
Algorithm: June 2007, (Version 5.3). [Available online at
http://www.cloudsat.cira.colostate.edu/dataICDlist.php?go=list&path=/2B-
GEOPROF]

Mace, G. G., R. Marchand, Q. Zhang, and G. Stephens, 2007: Global hydrometeor
occurrence as observed by CloudSat; initial observations from summer 2006.
Geophys. Res. Lett., 34, L09808, doi: 10.1029/2006GL029017.

NASA Facts—A-Train, 2003: Formation Flying: The Afternoon "A-Train" Satellite
Constellation. NASA Facts. [Available online at
http://aqua.nasa.gov/doc/pubs/A-Train_Fact_sheet.pdf]

NGIS, 2011: Verification & Validation (V & V) of the World Wide Merged Cloud
Analysis (WWMCA): A Review. Technical Note Prepared for the Air Force
Weather Agency, Bellevue, NE. SEMSD.1553715944.

NOAASIS—NOAA Satellite Information System for NOAA Meteorological / Weather
Satellites, 2011. [Available online
http://noaasis.noaa.gov/NOAASIS/ml/avhrr.html]

Norquist, D. C., 2007: World-Wide Merged Cloud Analysis Verification and
Improvement Task 1. Technical Note Prepared for the Air Force Weather
Agency, Bellevue, NE.

Ruggiero, F. H., 2000: A Comparison of Cloud-Top Height Estimates from Satellite and
NWP Analysis Data. Pre-Prints, Battlespace Atmospheric and Clouds Impacts to
Military Operations (BACIMO) conference, 24–27 Apr, Fort Collins, CO.

Sassen, K., and V. I. Khvorostyanov, 2007: Microphysical and radiative properties of
mixed phase altocumulus: A model evaluation of glaciation effects, *Atmos. Res.,
84*, 390– 398, doi:10.1016/j.atmosres.2005.08.017.

Stephens, G. L., Vane, D. G., Tanelli, S., Im, E., Durden, S., Rokey, M., Reinke, D.,
Partain, P., Mace, G. G., Austin, R., L'cuyer, T., Haynes, J., Lebsock, M., Suzuki,
K., Waliser, D., Wu, D., Kay, J., Gettelman, A., Wang, Z., and Marchand, R.,
2008, CloudSat mission: Performance and early science after the first year of
operation, *J. Geophys. Res., 113*, D00A18, doi:10.1029/2008JD009982.

Wilks, D. S., 2006: *Statistical Methods in the Atmospheric Sciences*. 2nd ed.
International Geophysics Series, Academic Press, 627 pp.

INITIAL DISTRIBUTION LIST

1. Defense Technical Information Center
   Ft. Belvoir, Virginia

2. Dudley Knox Library
   Naval Postgraduate School
   Monterey, California

3. AS&T
   National Reconnaissance Office
   Chantilly, Virginia

4. 16th Weather Squadron (16WS/WXE)
   2d Weather Group (Air Force Weather Agency)
   Offutt AFB

5. 2nd Weather Squadron
   2d Weather Group (Air Force Weather Agency)
   Offutt AFB

6. The Aerospace Corporation
   Chantilly, Virginia

7. Clear Science, Inc.
   Jacksonville, Florida

8. Tom Murphree
   Naval Postgraduate School
   Monterey, California

9. Karl D. Pfeiffer
   TASC, Inc.
   Charlottesville, Virginia

10. Brian Moore
    Naval Postgraduate School
    Monterey, California